UNIVERSIDADE FEDERAL DO CEARÁ
CENTRO DE TECNOLOGIA
DEPARTAMENTO DE ENGENHARIA HIDRÁULICA E AMBIENTAL
PROGRAMA DE PÓS-GRADUAÇÃO EM ENGENHARIA CIVIL

JOÃO DEHON DE ARAÚJO PONTES FILHO

MULTIVARIATE ANALYSIS OF SPATIO-TEMPORAL DROUGHTS: A WAY TO ADVANCE DROUGHT PLANNING AND MANAGEMENT

FORTALEZA
2023

JOÃO DEHON DE ARAÚJO PONTES FILHO

MULTIVARIATE ANALYSIS OF SPATIO-TEMPORAL DROUGHTS: A WAY TO ADVANCE DROUGHT PLANNING AND MANAGEMENT

PhD Thesis submitted at the Water Resources and Environmental Sanitation Post-Graduate Program of the Technology Center at the Federal University of Ceará, as partial requirement to obtain the doctor degree in Civil Engineering. Concentration Area: Water Resources.

Advisor: Prof. Dr. Francisco de Assis de Souza Filho
Co-Advisor: Profa. Dra. Ticiana Marinho de Carvalho Studart.

FORTALEZA

2023

Dados Internacionais de Catalogação na Publicação
Universidade Federal do Ceará
Sistema de Bibliotecas
Gerada automaticamente pelo módulo Catalog, mediante os dados fornecidos pelo(a) autor(a)

P858m Pontes Filho, João Dehon de Araújo.
Multivariate analysis of spatio-temporal droughts : a way to advance drought planning and management / João Dehon de Araújo Pontes Filho. – 2023.
121 f. : il. color.

Tese (doutorado) – Universidade Federal do Ceará, Centro de Tecnologia, Programa de Pós-Graduação em Engenharia Civil: Recursos Hídricos, Fortaleza, 2023.
Orientação: Prof. Dr. Francisco de Assis de Souza Filho.
Coorientação: Profa. Dra. Ticiana Marinho de Carvalho Studart.

1. Seca. 2. Análise multivariada. 3. Análise espaço-temporal. 4. Extremos hidrológicos. I. Título.
CDD 627

JOÃO DEHON DE ARAÚJO PONTES FILHO

MULTIVARIATE ANALYSIS OF SPATIO-TEMPORAL DROUGHTS: A WAY TO ADVANCE DROUGHT PLANNING AND MANAGEMENT

PhD thesis defended at the Water Resources and Environmental Sanitation Post-Graduate Program of the Technology Center at the Federal University of Ceará, as a partial requirement to obtain the doctorate degree in Civil Engineering. Concentration Area: Water Resources.

Approved on 14/04/2023

EXAMINING COMMITTEE

_____
Prof. Dr. Francisco de Assis de Souza Filho (Advisor)
Universidade Federal do Ceará (UFC)

_____
Profa. Dra. Ticiana Marinho de Carvalho Studart (Co-Advisor)
Universidade Federal do Ceará (UFC)

_____
Prof. Dr. Eduardo Sávio Passos Rodrigues Martins
Universidade Federal do Ceará (UFC)

_____
Prof. Dr. Carlos de Oliveira Galvão
Universidade Federal de Campina Grande (UFCG)

_____
Profa. Dra. Rosa Maria Formiga Johnsson
Universidade do Estado do Rio de Janeiro (UERJ)

_____
Prof. Dr. Dirceu Silveira Reis Júnior
Universidade de Brasília (UnB)

ACKNOWLEDGMENTS

I would like to express my sincere gratitude to my thesis supervisor, Professor Dr. Francisco de Assis de Souza Filho, for his invaluable guidance, support, and patience throughout the entire research process. Assis is an example not only in the academic field, but mainly in the human field, where he demonstrated several times his empathy and leadership during the whole process. In addition, he gave us lessons on how to face the most important challenges in life, always with a positive attitude and a lot of willingness to do more.

I am also thankful to my co-supervisor, Profa. Dra. Ticiana Marinho de Carvalho Studart, for her contributions to this work. I learned from her how to make ideas clearer and how to tell stories that can make our works impact readers more deeply. Furthermore, because of her, I had the opportunity to collaborate with Profa. Dra. Manuela Portela, during a period of time at the Instituto Superior Técnico of the University of Lisbon. With Profa. Manuela, I learned that hard work pays off.

I would also like to thank the thesis committee members, Prof. Dr. Eduardo Sávio Passos Rodrigues Martins, Prof. Dr. Carlos de Oliveira Galvão, Profa. Dra. Rosa Maria Formiga Johnsson, Prof. Dr. Dirceu Silveira Reis Júnior, for their time and valuable contributons on this thesis work.

I would like to extend my heartfelt thanks to my family for their unwavering support, encouragement, and understanding throughout my academic journey. Especially my wife, companion and best friend Quévia Camboim, for all the support during the comings and goings from João Pessoa to Fortaleza. I would like to thank my mother Ana Maria and my grandmother Iracema for dreaming this dream together with me. Also, to thank my sister Gabriella Coutinho Gomes Pontes Teixeira for always stimulating me to go further. I would also like to thank my nephews Giovanna and Pedro for the moments of joy that recharged my energy on the way home.

I would also like to thank the friends I have made during this journey, especially Dr. Francisco Gleson dos Santos Moreira, with whom I have shared joys since my UFCG days, my friends from the Climate Risk Management Group (GRC), especially Victor Costa Porto and Dr. Renan Vieira Rocha, who have been present at decisive moments of my life, and my new friends from FUNCEME, with whom I have had the pleasure of sharing the last moments involved in this research.

I would like to acknowledge the financial support provided by Coordenação de Aperfeiçoamento de Pessoal de Nível Superior—Brasil (CAPES), which made this research

possible. Also to the Ceará Meteorology and Water Resources Foundation (FUNCEME), for the opportunity to continue my activities as a researcher, now in this renowned research institution.

This thesis represents the end of my formal education, but it is far from being the end of my learning process.

"Simplicity is the ultimate sophistication." –
Leonardo da Vinci

ABSTRACT

Drought is a complex, multifaceted phenomenon that crosses political and geographical borders. However, it is usually studied using one-dimensional time series of drought variables, ignoring the multivariate characteristics of droughts and their interdependence. On the other hand, increasing the complexity of drought analysis by considering multiple variables can be difficult to incorporate into management. Impediments to using multivariate analysis in this context may include high entrance barriers for analysts to perform multivariate analysis and difficulty presenting the results to decision-makers. This gap prevents us from adequately forecasting, planning, and managing to cope with the adverse effects of droughts. Therefore, finding a balance between complexity and simplicity is something that must be sought. In this thesis, I argue that the shift to understanding drought as a multivariate event provides enough gain of information to justify its use in drought planning and management if it is possible to make a link between science and management. To do so, I study droughts' compounding relationships in three different dimensions of drought risk: monitoring and early warning, multivariate frequency analysis, and spatio-temporal characterization. (i) Droughts can be anticipated and mitigated using a Continuous Drought Probability Monitoring System (CDPMS). This system uses the conditional probability theory to monitor the occurrence probability of drought during the rainy season, as the rainy season advances. The likelihood that the rainy season is defined as drought is updated every month inside this period. The concept of precipitation thresholds is used in CDPMS to simplify the drought analysis for decision-makers. The model was assessed in mainland Portugal and demonstrated the capacity to anticipate drought by modeling the complex dependence structures between total and given precipitation. The proposed framework can be used to quantify the risk of drought and mitigate its impacts; (ii) Traditional drought frequency analysis uses only one characteristic of drought (e.g., the duration), which is an incomplete representation of the event and ignores mutual dependence. Also, it frequently ignores the spatial extent of droughts or considers it without a relationship with drought management. A framework to perform multivariate frequency analysis at a spatial level that can be related to socioeconomic impacts was proposed. The 2012-2018 drought in northeast Brazil was studied using this framework. Improved risk assessment was achieved by simultaneously considering drought duration and severity at the hydrographic region level. This framework is already being used as a planning instrument in new proactive drought plans that are being constructed in the studied region. (iii) The multivariate characterization of droughts can present the following dilemma: to oversimplify and ignores other sides of the problem or to increase

complexity and make it difficult for decision-makers to have a clear view of the event. To improve our understanding of the compounding effects of spatio-temporal relationships it is proposed a simple way to analyze the drought dynamics over time and space. Intra-event analysis of drought dynamics and searching for patterns and relationship between mean drought characteristics are presented. The first part proposes the use of growth curve, growth rate and acceleration to understand how drought evolves in time and space inside the drought event. The second analyses the mean characteristics of all drought events in search for patterns and relationships that can be helpful for decision-makers in drought monitoring and early warning. It was found that central part of the Northeast region developed longer, more severe, and more widespread droughts than any other area. This result is important for preparing for upcoming events that presents its centroid's onset at this region. This thesis presents strategies and frameworks that can increase our knowledge of drought events by considering multiple characteristics but still making them simple and straightforward for decision-makers. This way we can link science and management, advancing our understanding of drought events and improving our ability to cope with future droughts.

Key-words: drought; multivariate analysis; spatio-temporal analysis; hydrological extremes.

RESUMO

A seca é um fenómeno complexo e multifacetado que atravessa fronteiras políticas e geográficas. Contudo, é normalmente estudado utilizando séries temporais unidimensionais de variáveis de seca, ignorando as características multivariadas das secas e a sua interdependência. Por outro lado, aumentar a complexidade da análise da seca, considerando múltiplas variáveis, pode ser difícil de incorporar na gestão. Os impedimentos à utilização da análise multivariada neste contexto podem incluir altas barreiras de entrada para os analistas efetuarem análises multivariadas e dificuldade em apresentar os resultados aos decisores. Esta lacuna impede-nos de prever, planear e conseguir lidar adequadamente com os efeitos adversos das secas. Por conseguinte, encontrar um equilíbrio entre complexidade e simplicidade é algo que deve ser procurado. Nesta tese, defendo que a mudança para compreender a seca como um evento multivariado proporciona ganhos de informação suficientes para justificar a sua utilização no planeamento e gestão da seca, se for possível estabelecer uma ligação entre ciência e gestão. Para tal, estudo as relações de composição das secas em três dimensões diferentes do risco de seca: monitorização e alerta precoce, análise multivariada de frequência, e caracterização espaço-temporal. (i) As secas podem ser antecipadas e mitigadas utilizando um Sistema de Monitorização da Probabilidade de Seca Contínua (CDPMS). Este sistema utiliza a teoria da probabilidade condicional para monitorizar a probabilidade de ocorrência de seca durante a estação chuvosa, à medida que a estação chuvosa avança. A probabilidade de que a estação chuvosa seja definida como seca é atualizada todos os meses dentro deste período. O conceito de limiares de precipitação é utilizado no CDPMS para simplificar a análise da seca para os decisores. O modelo foi avaliado em Portugal Continental e demonstrou a capacidade de antecipar a seca, modelando as complexas estruturas de dependência entre a precipitação total e a precipitação dada. O quadro proposto pode ser utilizado para quantificar o risco de seca e mitigar os seus impactos; (ii) A análise tradicional da frequência da seca utiliza apenas uma característica da seca (por exemplo, a sua duração), que é uma representação incompleta do evento e ignora a dependência mútua. Além disso, ignora frequentemente a extensão espacial das secas ou considera-a sem uma relação com a gestão da seca. Foi proposto um quadro para realizar uma análise multivariada da frequência a nível espacial que pode ser relacionada com os impactos socioeconómicos. A seca de 2012-2018 no nordeste do Brasil foi estudada utilizando este quadro. Foi conseguida uma melhor avaliação do risco, considerando simultaneamente a duração e gravidade da seca a nível da região hidrográfica. Este quadro já está a ser utilizado como um instrumento de planeamento em novos planos de seca proativos

que estão a ser construídos na região estudada. (iii) A caracterização multivariada das secas pode apresentar o seguinte dilema: simplificar excessivamente e ignorar outros lados do problema ou aumentar a complexidade e tornar difícil para os decisores ter uma visão clara do evento. Para melhorar a nossa compreensão dos efeitos compostos das relações espaço-temporais, propõe-se uma forma simples de analisar a dinâmica da seca no tempo e no espaço. São apresentadas análises intra-evento da dinâmica da seca e procura de padrões e relações entre as características da seca média. A primeira parte propõe a utilização da curva de crescimento, taxa de crescimento e aceleração para compreender como a seca evolui no tempo e no espaço dentro do evento da seca. A segunda analisa as características médias de todos os eventos de seca em busca de padrões e relações que possam ser úteis para os decisores no monitoramento e alerta precoce da seca. Verificou-se que a parte central da região nordeste desenvolveu secas mais longas, mais severa e mais generalizada no espaço do que qualquer outra área. Este resultado é importante para a preparação dos próximos eventos em que o centroide da seca se iniciar nesta região. Esta tese apresenta estratégias e quadros que podem aumentar os nossos conhecimentos sobre eventos de seca, considerando múltiplas características, mas ainda assim tornando-as simples e diretas para os decisores. Desta forma, podemos ligar a ciência e a gestão, fazendo avançar a nossa compreensão dos eventos de seca e melhorando a nossa capacidade de lidar com futuras secas.

Palavras-chave: seca; análise multivariada; análise espaço-temporal; extremos hidrológicos.

LIST OF FIGURES

LIST OF TABLES

LIST OF CHARTS

SUMMARY

1 INTRODUCTION

Droughts are recognized as the world's deadliest and one of the costliest natural hazards (PIEPER, 2020). According to the International Emergency Events Database (EM-DAT) (EM-DAT, 2023), droughts account for 5% of natural disasters globally while causing more than 36% of the fatalities linked to natural disasters since 1900. Drought is an extensive and slow-onset natural disaster, which means the drought events manifest over a widespread area and its impacts are manifested over months or years. Drought can occur at different spatial and temporal scales, from local to global and from short-term to long-term (Wilhite & Svoboda, 2000).

Droughts are complex and multifaceted natural phenomena that do not respect political or geographical borders. A key aspect of drought planning and management is to recognize its main characteristics: duration, severity, and spatial extent (ANDREADIS *et al.*, 2005; LIU *et al.*, 2020; SHEFFIELD; WOOD, 2007; ZHU *et al.*, 2019). Drought impacts can vary depending on those three characteristics. A shorter drought can affect vast areas and have an intense severity, causing effects on the environment, economy, and society. Also, long-lasting droughts, even with lower severity, can decrease water availability to a point where few measures can be taken to reduce impacts. Widespread droughts lessen the ability to cope with drought once the surrounding areas also suffer similar impacts. So, recognizing those characteristics and their relationship is a critical step in better understanding the phenomenon.

However, droughts are traditionally studied using one-dimensional time series of drought variables, and methods usually consider station-based, areal average-based or grid-based information (SONG *et al.*, 2021). Generalizing drought information simplifies its interpretation at the cost of loss of information as the hazard presents multiple correlated characteristics variables in space and time (HAO *et al.*, 2017; STAHL *et al.*, 2016). Numerous studies have shown that the risk of compound events may be underestimated if the dependence between variables are not considered (BEVACQUA *et al.*, 2017; HAO *et al.*, 2019; HAO; SINGH; ASCE, 2020; RIBEIRO *et al.*, 2020; WU *et al.*, 2019). By reducing the problem's dimensionality, we ignore the dependence structure among those aspects, resulting in a poorer representation of the phenomenon (ALIDOOST; SU; STEIN, 2019; XU *et al.*, 2015a).

The scientific community has recently begun using multivariate analysis to better understand droughts (ANDREADIS *et al.*, 2005; HAO; SINGH; HAO, 2018; SHIAU, 2006). This has been possible due to computational advances, increased hydroclimatic variables

monitored, and the popularization of statistical techniques. However, little of this advance can be seen in drought planning and management. Impediments to using multivariate analysis in this context may include high entrance barriers for drought analysts to perform multivariate analysis and difficulty in presenting more complex results to decision-makers.

This gap prevents us from properly forecasting, planning, and managing to cope with the adverse effects of droughts. For instance, investigating the spatiotemporal characteristics of droughts and their mutual dependence would provide decision-makers of drought-prone areas with reliable information on what kind of measures can be taken to cope with future droughts (LIU *et al.*, 2020). We could also increase forecast skills by exploring the propagation and dependence between different random variables.

On the other hand, we need to care about the enhanced complexity created by increasing the number of random variables to observe. Drought analysis is already difficult to understand because it has different classifications and various forms of political interference. Therefore, we need to shift from the paradigm of analyzing drought as a univariate event to understanding it as a multivariate event, however seeking for simple results presentation.

1.1 Hypothesis

Multivariate drought analysis provides enough gain of information to justify its use in drought planning and management.

1.2 Objectives

The main objective of this thesis is to advance the understanding of droughts by providing multivariate analysis frameworks that can be used to cope with the adverse effects of droughts.

Specifically, it aims to:

- Develop a monitoring and early warning system based on the persistence of droughts using conditional probability theory.
- Provide a framework to include multivariate frequency analysis into drought planning and management.
- Develop a spatial-temporal drought analysis searching for patterns that can help early warning and decision making.

1.3 Scientific Contributions

The specific objectives of this thesis are answered through three scientific papers. Each of them focuses on answering a single specific objective.

The first paper presents an innovative solution that applies the copula functions to predict the occurrence of drought. The second presents a technological contribution by establishing a framework on how to use multivariate information in drought planning. The third paper presents an innovative solution to monitor the space-time dynamics of droughts and finds patterns that can help monitoring and early warning for droughts in Northeast Brazil.

The next chapter situates the reader in the theme in which the present thesis is located and introduces how the articles are structured, what are the main results and how they are related to each other.

2 SCIENTIFIC BACKGROUND

There is no unique definition of drought as its perception varies according to users' specific interests (PALMER, 1965). However, all definitions are somehow related to below-average precipitation. If the event persists long enough, it can progressively affect soil moisture, water resources, and economic and social development. For example, for a farmer who only cultivates rain feed cultures, drought impacts can be perceived earlier than a water supply company that uses stored water from reservoirs. Therefore, a classical classification of droughts according to their impacts are: meteorological, agricultural, hydrological, and socioeconomic (Heim, 2002; Wilhite & Glantz, 1985).

In addition to the perception of drought being different according to the type of water use, the analysis of drought should also seek to understand the different variables that are linked to the definition of drought. The most common characteristics used to characterize a drought event are duration, severity, and area. (Andreadis et al., 2005; Liu et al., 2020; Sheffield & Wood, 2007; Zhu et al., 2019). To analyze drought characteristics, first one must extract them from a drought index time series. Many different indices have been proposed in the last decades. For example, the first drought index to gain relevance was the Palmer Drought Severity Index (PDSI) (PALMER, 1965). Recently, the World Meteorological Organization (WMO) recommended the Standardized Precipitation Index (SPI) (MCKEE; DOESKEN; KLEIST, 1993) to monitor meteorological drought conditions since it relies only in precipitation variable, the most available hydroclimatic variable in the world.

To use SPI, a long-term precipitation time-series is required (MISHRA; SINGH, 2010). This time-series is fitted to a probability distribution, usually Gamma or Pearson type III (GUTTMAN, 1999; MCKEE; DOESKEN; KLEIST, 1993; SANTOS *et al.*, 2013; VICENTE-SERRANO, 2006), which is then transformed to a normal distribution. The result of this mathematical transformation is that the mean precipitation value is transformed into zero SPI value for the location and desired period. This transformation allows SPI values to be compared in any region of the world.

Despite the drought index used, drought characteristics can be identified from historical time series data based on the run theory (Yevjevich, 1967). Using run theory, each drought event can be analyzed separately from the original time series. This technique gained popularity in drought analysis as it allows univariate and multivariate frequency analysis and comparisons between different drought variables (ESPINOSA *et al.*, 2021; RIBEIRO *et al.*, 2020; SHIAU, 2006; WU *et al.*, 2018).

As introduced earlier, the definition of drought depends on the user's perception and type of water use. This consideration can be incorporated into the drought characterization by changing the threshold by which the separation of drought events will occur from run theory. Less extreme thresholds allow the event to start earlier and take longer to exit. More extreme thresholds define more extreme events, that is, they take longer to start and are less likely to occur. This makes the definition of drought sensitive to the choice of threshold. The decision on what threshold to choose is up to the drought analyst and the intent of his analysis (DRACUP; LEE; PAULSON, 1980).

Another way to influence the characterization of drought is the time aggregate used in the analysis. Standardized drought indices such as SPI can accumulate information over several months. The time aggregate, also known as timescale, is used to study the influence of a larger number of months within the definition of the event. For example, smaller timescales, such as 1 or 3 months, are used to characterize short-term events, generally associated with impacts on agriculture. Longer timescales are used to study drought associated with long-term impacts, such as using 12 or 24 months to study hydrological and/or socio-economic droughts.

A discussion that arises in drought definition due to the impact of parameters in drought definition is the difficulty to stablish when a drought event starts or ends. Each timescale used will provide a different date to be marked as the drought onset. Therefore, instead of focusing on determining exactly when did the drought started or ended, we recommend the use of reference periods. This reference periods can be seasons or years when the drought event begins. Less attention should be given to the proper definition of exactly month when the drought has its onset. The focus should shift to the reference period itself. Therefore, making easier to analyze drought events using different time-scales. In addition to the complexity of defining droughts according to users' perceptions, understanding that there is dependence between the variables and that this dependence can be used to improve understanding of the drought event is fundamental.

Factors that lead to the dependence of the variables can be linked to the following: external factors, system feedback and conditional dependence (HAO; SINGH; ASCE, 2020). External factors are related to general atmospheric circulation, such as natural cycles (e.g., El Niño–Southern Oscillation, ENSO) or circulation patterns (e.g., low-pressure, or high-pressure systems). These external factors can influence persistence over time in a given area and/or co-occurrence in different areas at the same time. If these areas become connected, they form a contiguous drought affected area. The land-atmosphere feedback is another cause of compound events. The lower precipitation can reduce evapotranspiration, creating even more favorable

conditions for drought to occur. This feedback can influence the migrations of droughts across continents (HERRERA-ESTRADA; DIFFENBAUGH, 2020; HERRERA-ESTRADA; SATOH; SHEFFIELD, 2017). Conditional dependence happens when the occurrence of one variable determines, to some extent, the occurrence of another variable. For example, the propagation of drought through the water cycle is a well-known behavior. The lack of precipitation influences the dryness of the soil, later reducing the amount of water available in the river and subsequently reducing groundwater levels (VAN LOON, 2015). Therefore, understanding how different variables are related can improve drought planning and management capacity.

Best practices for drought planning requires information about the two different components of drought risk: hazard and impacts (TIJDEMAN *et al.*, 2022). The drought hazard does not imply the impact as the exposed system needs to be vulnerable to the impact really occurs. For example, previously taken measures can increase the capacity to cope with drought, reducing the vulnerability, and consequently, the impact. From a hazard perspective, it is essential to understand meteorological drought better, as it can be used as an early sign of further impacts during drought propagation through the terrestrial part of the hydrological cycle (VAN LOON, 2013).

Therefore, from a risk analysis perspective, the study of droughts can be divided into two major dimensions, hazard, and impact, each one having its relevance. In the perspective of hazard, some dimensions deserve to be highlighted, such as monitoring and early warning and frequency analysis and spatio-temporal characterization. In this sense, this thesis presents three different papers that use multivariate analyses, and each present a framework to improve understanding of droughts by using multivariate analysis (Figure 1). Each framework is independent and was built to achieve specific purposes to consider multiple variables and simplify the results for decision makers. These frameworks are easily replicable in other regions and this thesis did not seek to apply them to the same region. Next, each framework will be explained in greater detail and the main results will be presented.

Figure 1: Drought study area, from a risk assessment perspective. The bigger circle indicates the state-of-the-art knowledge in drought area. The orange lines indicate where this thesis expands the current knowledge.

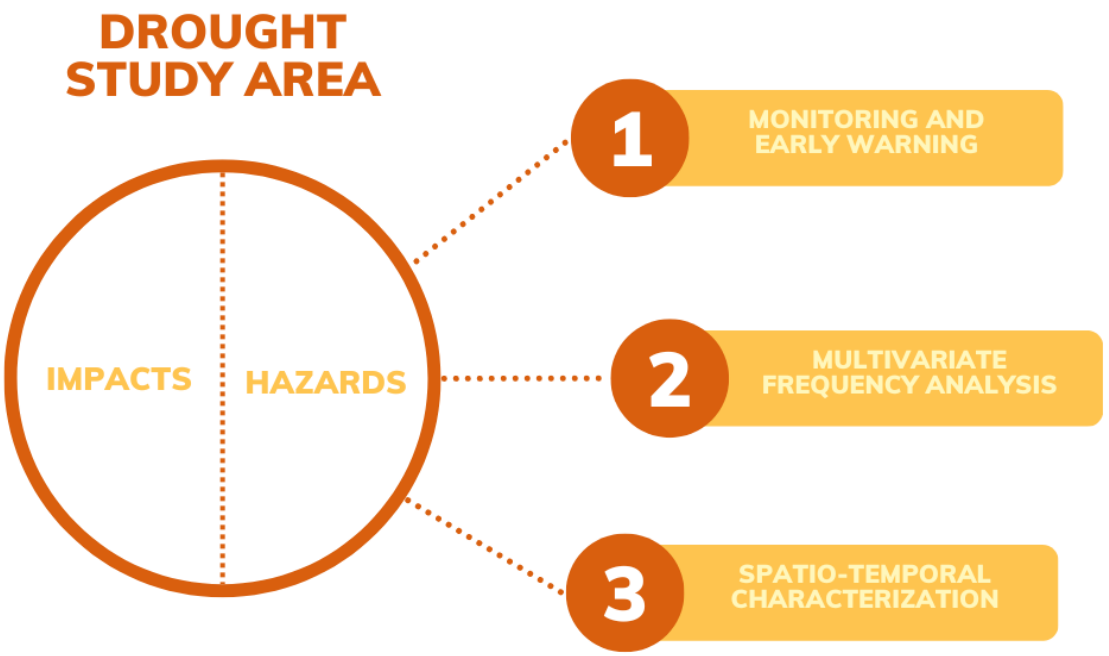

Source: Prepared by the author

The first paper is related to monitoring and early warning which forms the basis for proactively dealing with droughts (Wilhite, 2012; Wilhite et al., 2005; Wilhite & Svoboda, 2000). Dynamic and statistical modeling are the most common approaches to early warning systems (YANG; LIU, 2020). Dynamic modeling uses General Circulation Models (GCMs) to predict rainfall based on the temperature conditions of the ocean's surface (DELGADO *et al.*, 2018; PORTELE *et al.*, 2021). Statistical modeling uses regressions, stochastic, probabilistic, and artificial intelligence modeling to understand the persistence of environmental variables (KRISHNAMURTHY R *et al.*, 2020).

To model the persistence of drought over time, it is important to incorporate the complex relationship between what has already happened and what is about to happen. In this study we created an innovative framework that uses the conditional probability theory using copula functions to model this complex structure using the advantages of copula functions that allow flexibility in the choice of marginal distribution and split between dependency and marginal structure analysis. Therefore, a copula-based Continuous Drought Probability Monitoring System (CDPMS) was developed. The compounding effect of monthly rainfall during the rainy season was used to calculate the likelihood that drought is onset by the end of

the season. To facilitate understanding by decision makers, the concept of drought thresholds was used. This concept translates information from the drought index to absolute precipitation values.

The proposed framework intends to answer the following question: will there be a drought in the rainy season this year, knowing what has happened so far? To answer this question, first delimit the location, then the rainy season. Throughout the selected rainy season, the probability of a drought will be updated as each month's precipitation occurs. For example, knowing that the threshold for the occurrence of a moderate drought in a location is 200 mm in the period from January to June and knowing that it rained 100 mm between January and March, ask: What is the probability of the accumulated Jan-Jun being less than 200mm given that it rained 100mm from Jan-Mar? This response is given and updated month by month by the CDPMS as more information is generated.

This framework was assessed in mainland Portugal and demonstrated the capacity to anticipate drought by modeling the complex dependence structures between precipitations at different time intervals. Results demonstrate the capacity to anticipate drought by modeling the complex dependence structures between total precipitation and the given precipitation for the period. Since the first month, the forecast using the CDPMS has beaten the climatology. In addition, the model improves performance as it gains more information over the months. Therefore, CDPMS has proven to be a valuable tool for monitoring and early warning of droughts with information that is simple for decision makers to understand. This innovative approach was applied in Pakistan (Niaz, Almazah, Hussain, and Pontes Filho 2022; Niaz, Almazah, Hussain, Pontes Filho, et al. 2022).

The second paper refers to multivariate frequency analysis. Drought memory has great relevance in mitigating future events and should be preserved in proactive drought plans. Frequency analysis allows the identification of the exceptionality of each event and can serve as a marker of the memory of that event. It gives insights into how often a drought event occurs. Traditionally only one variable is used to perform the frequency analysis, which ignores the dependence structure with other variables and performs an incomplete representation of the phenomenon. Also, most previous studies on frequency analysis have only focused on station-based assessment or considered mathematical regionalization that do not correspond to social-political organization. Thus, these simplifications ignore widespread impacts and how mitigation actions are organized. This indicates a need to provide a framework that can incorporate multivariate frequency analysis at a territory scale that is linked to drought planning and management.

This paper attempts to show that analyzing an extreme event such as the 2012-2018 drought in northeast Brazil by simultaneously considering drought duration and severity at the hydrographic region scale can improve risk assessment. The results indicate that the 2012-2018 drought event presented the highest bivariate return period ever recorded, 240 years. Events with similar duration but less severe than the 2012-2018 were also found, enhancing the importance of considering the dependence between both characteristics. The proposed framework has shown institutional relevance for the region and is being used as a tool within the proactive drought plans being produced for the region.

The regionalized analysis of droughts considering the spatial territory of hydrographic regions proposed in the second paper's framework proved to be relevant for drought planning, as it easily relates to drought management practices. However, droughts do not respect political or geographic borders and another way to monitor and assess drought risk is to understand how it moves, connects, and splits over time and space.

Thus, the third paper explores the dynamics of spatio-temporal relationship between drought events. Spatio-temporal analysis of droughts can fall into the following dilemma: oversimplify and ignore other faces of the problem or increase the complexity making it difficult for decision makers to understand. A simple framework to visualize drought evolution over time and space is proposed. To do so, we first need to consider the spatio-temporal aspect in a 3D analysis (lat, long, and time). Then, the article provides two different analyses: intra-event analysis of drought dynamics and searching for patterns and relationship between mean drought characteristics. The first part proposes the use of growth curve, growth rate and acceleration to understand how drought evolves in time and space inside the drought event. The second analyses the mean characteristics of all drought events in a search for patterns and relationships that can be helpful for decision-makers in drought monitoring and early warning. It was found that central part of the Northeast region developed longer, more severe and more widespread droughts than any other area. This result is important for preparing for upcoming events that its centroid's is onset on this region.

The three proposed frameworks present possible implementations that help gain insight into drought phenomena by considering multiple variables together, while simplifying analysis and decision making for managers. The proposed frameworks can serve as tools to be considered in proactive drought plans according to the needs of each location, with no need for all three to be incorporated in the same region at the same time. Since the frameworks were created oriented to decision makers, their application becomes simple to be implement. With these tools, it is believed that we can advance drought planning and management.

3 A CONTINUOUS DROUGHT PROBABILITY MONITORING SYSTEM, CDPMS, BASED ON COPULAS[1]

3.1 Introduction

Drought is a natural phenomenon without a clear onset which makes it difficult to recognize identify. It is the world's costliest natural disaster and can provide impacts in a global perspective, not restricted to places with low average precipitation amounts (KEYANTASH; DRACUP, 2002; MISHRA; SINGH, 2010; WILHITE; GLANTZ, 1985). In Europe, the total cost of drought damages recorded from 1976 to 2006 amounted to 100 billion € (COMMISSION, 2012). Therefore, the continuous monitoring of the probability of drought events is crucial to deploy short term emergency measures and to mitigate the social, environmental, and economic costs and losses associated with those events.

Considerable disagreement exists about the definition of drought. However, all the definitions relate the event to below-average precipitation over a period of time. If the event persists long enough, it can progressively affect soil moisture, water resources, and, consequently, economic and social development. According to its impacts, the droughts can be classified into four categories: meteorological, agricultural, hydrological, and socioeconomic (HEIM, 2002; WILHITE; GLANTZ, 1985).

Drought indices are the most suitable tool for drought monitoring and evaluation. Many different indices have been proposed in the last decades. Among the hydrological variables adopted to detect and characterize drought occurrences, precipitation is the most widely used, not only due to its intrinsic link with the phenomenon and its consequences but also because precipitation is widely monitored and there are relatively long historical records.

In 2009, the World Meteorological Organization (WMO) recommended the standardized precipitation index (SPI) (MCKEE; DOESKEN; KLEIST, 1993) to monitor meteorological drought conditions. Since then, the SPI is used worldwide to detect anomalous precipitation over different time scales. The SPI has the advantage of being independent of the magnitude of the mean precipitation, because it is a standardized index, and hence, able to compare droughts in different climatic zones.

---

[1]The paper can be cited as: Pontes Filho, J. D., Portela, M. M., Marinho de Carvalho Studart, T., & Souza Filho, F. D. A. (2019). A continuous drought probability monitoring system, CDPMS, based on copulas. *Water*, *11*(9), 1925.

However, because it provides a standardized numerical value, it is difficult to connect it expeditiously to precipitation deficits, and, consequently, to use it to recognize or to predict drought events.

The droughts have traditionally been studied in a univariate context, mostly aiming at identifying and describing their occurrences. However, as many of the hydrological phenomena, they are characterized by multiple aspects some of them expectably correlated. Since a univariate approach ignores the dependence structure among those aspects, it may result in a poorer representation of the phenomenon.

Before copulas approach, some multivariate techniques were introduced in hydrological studies, such as in the case of the analysis of floods, droughts, and storms. Those techniques contribute to improving the accuracy of the estimates and provide information about the dependence structure among the characteristics. Most of them used bivariate probability distributions, such as bivariate gaussian, exponential, gamma, and extreme value distributions. The disadvantage of such approaches is that the marginals must have the same probability distribution and extensions to more than the bivariate case are not clear (GENEST; FAVRE, 2007; SINGH; ZHANG, 2007). However, copulas can overcome such difficulties (CHEN *et al.*, 2013). The advantages of using copulas to model complex relationships among variables are (1) flexibility in choosing arbitrary marginals and structures of dependence, (2) capability to model more than two variables, and (3) splitting of marginal and dependence structure analysis (GENEST; FAVRE, 2007; HAO; SINGH, 2016; LAZOGLOU; ANAGNOSTOPOULOU, 2018; SINGH; ZHANG, 2007).

Multiple dependent random variables need more advanced and complex copulas than the common ones that are applied to the bivariate case. An example is the vine-copulas which are able of coupling multiple variables into a pair-to-pair manner (AAS; CZADO; FRIGESSI, 2009).

The application of copulas in hydrology has gained some relevance in the last decades. Regarding drought analysis, one of the main uses of copulas is to model the frequency analysis, combining different characteristics of the drought events (e.g. intensity, duration, magnitude, and spatial distribution) (AYANTOBO *et al.*, 2018; CHEN *et al.*, 2019; MONTASERI; AMIRATAEE; REZAIE, 2018; SHIAU, 2006; XU *et al.*, 2015a). Another important use of copulas is to integrate the drought index to a couple of different drought categories, such as meteorological, hydrological and agricultural (CHANG *et al.*, 2016; KAO; GOVINDARAJU, 2010a; LIU *et al.*, 2019b).

In climatic regions like Mainland Portugal, insufficient precipitation during the short-duration and well-defined rainy season is the main trigger of the drought events. An innovative use of copulas could be its application in a multivariate context to monitor the evolution of the drought probability during that season, based on the continuous updating of precipitation that already occurred and the one that needs to occur, so that there is (or not) a drought by the end of the rainy season (a typical conditional probability problem). The conditional probability theory coupled with copulas is frequently used in hydrological applications to analyze multivariate dependence (MONTASERI; AMIRATAEE; REZAIE, 2018; SHIN *et al.*, 2018; TOSUNOGLU; CAN, 2016) and will be applied in this study.

Aiming at exploring copula's forecasting capabilities in a drought monitoring context, the concept of a precipitation threshold for drought recognition developed by (PORTELA *et al.*, 2012; SANTOS, 2012; SANTOS *et al.*, 2013) was used. In each rain gauge, if the cumulative precipitation in a given timespan falls below the precipitation threshold for that timespan, a drought with a severity (from moderate to extreme), defined by the threshold, will occur. Figure 2 exemplifies the application to Mainland Portugal of the precipitation surface threshold concept applied to recognize moderate to extreme droughts from October to March (the rainy season). If in a certain location the precipitation registered falls below the value given by one of the maps, then the location experienced a drought, with the intensity given by the threshold to which the map relates.

Figure 2: Mainland Portugal. Surfaces of precipitation thresholds, R_N^*, for the 6-month period from October to March (SPI6), from the right to the left, for moderate (−0.84), severe (−1.28), and extreme (−1.65) droughts.

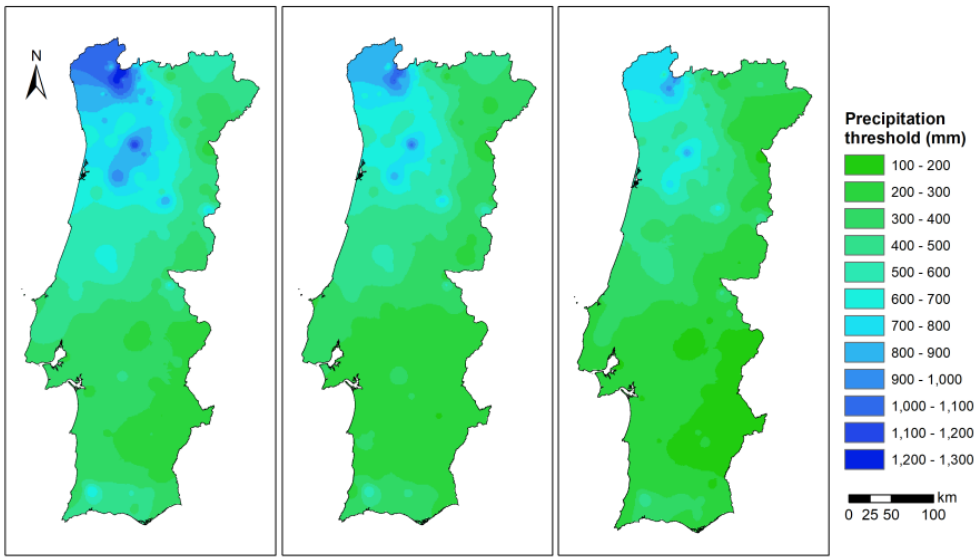

Source: Adapted from (Portela et al. 2012)

The application of the precipitation threshold concept in the scope of the present study can be formulated as follows: for a season of N months to which the time scale of the SPI and the precipitation threshold, R_N^*, refer, let R_n denote the observed precipitation in the first n months ($1 \leq n \leq N$) and R_N the total seasonal precipitation.

A drought will occur by the end of the N-month period if R_n added to the (unknown) precipitation in the remaining $(N-n)$ months, $R_{(N-n)}$, is not enough to meet the threshold, R_N^*, i.e.,:

$$R_n + R_{(N-n)} \leq R_N^* \quad \Leftrightarrow \quad R_N \leq R_N^* \tag{1}$$

Consider, for example, the six-month season, $N = 6$, from October to March (during which most of the precipitation in Portugal falls) and, that at the end of December of a given year, an estimate of the probability of a moderate, severe or extreme drought occurrence is envisaged. Given the observed precipitation from October to December (R_n with $n = 3$), the problem to be addressed for each drought intensity can be stated as what is the probability the precipitation from January to March (still unknown) added to the precipitation from October to December being below the drought threshold? The solution is the drought probability given by the following equation:

$$P\ (R_N \leq\ R_N^*|R_n) \quad \Leftrightarrow \quad P\ (R_6 \leq\ R_6^*|R_3) \tag{2}$$

By coupling a copulas approach with the precipitation threshold concept, the main objectives of this study were as follow: 1) to develop a methodology for a Continuous Drought Probability Monitoring System, CDPMS, 2) to evaluate the performance of CDPMS, and 3) to apply the CDPMS to a study area. To demonstrate the methodology, Mainland Portugal and its rainy season (from October to March) were selected. In Portugal, the precipitation regime is characterized by very pronounced seasonality, in average with 80% of the precipitation occurring from October to March, which makes it relevant to be able to anticipate if drought conditions are expected by the end of that period.

3.2 Materials and Methods

The development of the CDPMS was based on the stepwise approach described in Sections 2.1.1 to 2.1.3 and shown in Figure 3, steps (a) to (c). First, the drought threshold for a given time span or scale of the SPI, N, and drought severity is defined. After that, the copula candidates aiming at modeling the precipitation correlation structure are evaluated and those with best-fit are selected. Finally, the drought probability given by Equation (2) is computed. Having in mind that the goal of the CDPMS is to continuously monitor the probability of drought by the end of a N-month period, steps (b) and (c) are repeated from $n = 1$ to $n = N-1$. The Leave-One-Out Cross-Validation (LOOCV) methodology (steps (b) and (c) repeated from x = 1 until the length x of time series) was used to evaluate the model performance using the Brier and the Brier Skill scores (d).

The CDPMS was applied to Mainland Portugal based on precipitation records at 45 rain gauges (described later in Section 3).

Figure 3: Development of the CDPMS and evaluation of its performance

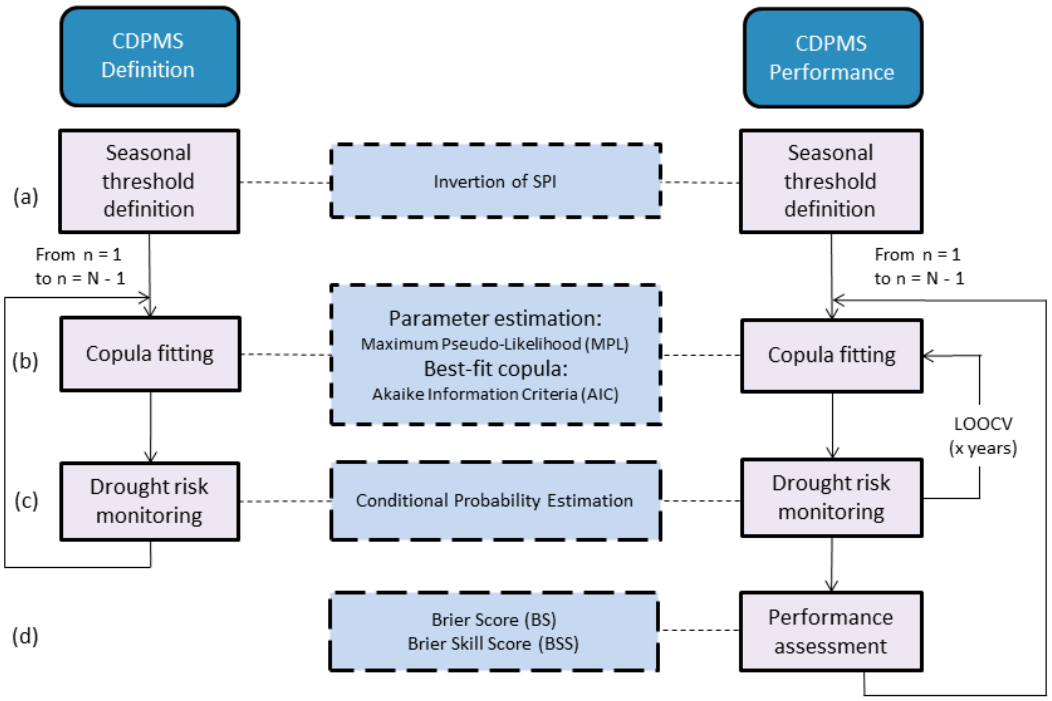

Source: Prepared by the author

3.2.1 CDPMS Definition

3.2.1.1 Seasonal Threshold Definition

The precipitation in Mainland Portugal falls mainly from October (beginning of the hydrological year) to March, representing, on average, almost 70% and 85% of the annual precipitation in the North and South, respectively. Therefore, it was considered relevant to estimate the probability of drought occurrence by the end of the rainy season. The corresponding precipitation thresholds were obtained by inverting the SPI from October to March, SPI6, for each of the drought intensities proposed by Agnew [26] and presented in Table 1. For a given rain gauge and drought severity, the precipitation threshold, R_N^*, give the SPI value back to the precipitation field (PORTELA *et al.*, 2012; SANTOS, 2012; SANTOS *et al.*, 2013).

Table 1: Classes of drought intensity, associated probability, and SPI value

Drought Class	Probability	SPI Value
Moderate Drought	0.20	Less than −0.84
Severe Drought	0.10	Less than −1.28
Extreme Drought	0.05	Less than −1.65

Adapted from (AGNEW, 2000).

3.2.1.2 Copula Fitting

The analysis of the dependency structure between two or more random variables can be used to indicate predictive relationships among them. The most common method is to measure the linear relationship using the Pearson correlation coefficient. One of the main weaknesses of linear correlation is that it tends to detect only the degree of dependence despite its dependence structure.

The consideration of non-linear dependence is possible by applying a rank correlation coefficient such as Spearman rank correlation and Kendall's Tau. The last coefficient is more used because its value directly indicates the probability of observing concordant or discordant pairs. There exists a relationship between the rank correlation coefficient and copula function that allows the use of copulas to study non-linear dependences.

According to Sklar's theorem (NELSEN, 2006), if the random variables x_1, …, x_m follow a marginal probability distribution function $F_1(x_1)$, …, $F_m(x_m)$, respectively, there exists a copula, C, that can join these marginal distribution functions in the form of a joint distribution function (Equation (3)),

$$H(x_1, x_2 \dots, x_m) = C[(F_1(x_1), F_2(x_2), \dots, F_m(x_m) = C(u_1, u_2, \dots, u_m) \quad (3)$$

where, $F_k(x_k) = u_k$ for k = 1, ..., m, with $u_k \sim u(0,1)$ and C(u_1, ..., u_m) being the copula function.

Although copulas may be implemented in multiple dimensions only bivariate copulas were considered in the present study.

Different families of copulas have been described by Nelsen (NELSEN, 2006), the families are commonly classified in four main groups: Meta-elliptical copulas (Gaussian and t Student), Archimedean copulas (Clayton, Gumbel, Frank, and Joe), Extreme value type (Gumbel, Husler-Reiss, Galambos, Tawn, and t-EV), and miscellaneous type (Plackett and Farlie–Gumbel–Morgenstern).

The Archimedean copulas are very popular for hydrological analyses as they allow modeling a great diversity of dependence structures, especially for dependent tail structures, and because of its accessible generation properties (AYANTOBO; LI; SONG, 2019; SINGH; ZHANG, 2007; XU *et al.*, 2015a). At higher orders, the use of Archimedean copulas is limited because their structure imposes restrictions related to dependence characteristics that are extremely difficult to satisfy for more than two variables (KAO; GOVINDARAJU, 2010b).

Meta-Elliptical copulas, on the other hand, can model higher-order due to their simple structure that can better fit the complex dependence of multi-dimensional problems (CHEN *et al.*, 2013; SHARIFI; SAGHAFIAN; STEINACKER, 2019).

The parameters for the copulas families can be estimated either by the method of moments, inversion of Kendall's Tau or by maximum likelihood estimation (MLE). The first method has the disadvantage of being applicable only to one-parameter copulas. As for the MLE method, two possibilities exist the inference functions from margins (IFM) (JOE, 1997) or the maximum pseudo-likelihood method (MPL) (GENEST; GHOUDI; RIVEST, 1995). How the transformation to [0,1] interval was made will dictate which is the best method, parametric for IFM and MPL for rank-based (BRECHMANN; SCHEPSMEIER, 2013).

To model the dependence structure between the precipitation in a given sub-period of the rainy season and the seasonal precipitation itself, as is the case of the current application, the most popular Meta-Elliptical copulas (Gaussian and t Student), and Archimedean copulas (Clayton, Gumbel, and Frank) were tested as candidates. The copula formulation for each candidate family and its parameters' interval are presented in Table 2. For each month of the rainy season, the bivariate model was constructed based on the two variables: precipitation in its initial n months (R_n) and the total seasonal precipitation (R_N).

Table 2: Copula candidate family formulation and parameter range.

Class	Family	$C(u_1, u_2)$	Parameter Range
Archimedean	Gumbel	$\exp\{-[(-\ln u_1)^{\theta} + (-\ln u_2)^{\theta}]^{\frac{1}{\theta}}$	$\theta \in [1, +\infty)$
Archimedean	Frank	$\frac{1}{\theta}\log\left(1 + \frac{(e^{\theta u_1} - 1)(e^{\theta u_2} - 1)}{(e^{\theta} - 1)}\right)$	$\theta \in (-\infty, +\infty)$
Archimedean	Clayton	$(u_1^{-\theta} + u_2^{-\theta} - 1)^{\frac{-1}{\theta}})$	$\theta \in (0, +\infty)$
Meta-Elliptical	Gaussian	$\phi_{\rho}(\phi^{-1}(u_1), \phi^{-1}(u_2))$	$\rho \in (-1,1)$
Meta-Elliptical	t Student	$T_{\rho,v}(T_v^{-1}(u_1), T_v^{-1}(u_2))$	$\rho \in (-1,1), v > 2$

Source: Prepared by the author

The parameters θ for Archimedean copulas and ρ and v for Meta-Elliptical copulas, with v standing for the degrees of freedom (only needed for t Student copulas), were estimated for the candidate copulas. This method was chosen because it can estimate both one and two parameters of the copula without requiring the establishment of the marginal distributions.

The Akaike Information Criterion (AIC) was applied to compare the bivariate copula models for the candidate families. The AIC method penalizes the models with the

highest number of parameters, allowing to find the model with maximum explanatory power and fewer parameters, according to the parsimony principle.

3.2.1.3 Copula Probability

The conditional probability theory associated with copulas is highly used in hydrological applications to analyze multivariate dependence (MONTASERI; AMIRATAEE; REZAIE, 2018; SHIN *et al.*, 2018; TOSUNOGLU; CAN, 2016) and can be expressed by Equation (5). Let two random variables X and Y with $U_1 = F_x(x)$, $U_2 = F_y(y)$ and u_1 and u_2 being specific values. The conditional distribution of X given $Y = y$ is given by:

$$H(X \leq x \,|Y = y) = C_\theta(U_1|U_2 = u_2) = \quad (5)$$
$$= \frac{\partial}{\partial u_2} C_\theta(u_1, u_2)$$

3.2.2 CDPMS Performance Assessment

The CDPMS performance was measured by the Brier Score based on the previous computation of the probability of the coupled precipitation events for all the years with data but one ($x-1$), according to the LOOCV. The validity of the probabilistic prediction was evaluated by the Brier Skill Score. In the LOOCV method, each of the x observed years is evaluated by removing one year of the time series, by fitting the model to the remaining $x-1$ years, and by estimating the removed data (WILKS, 2011). The process is repeated x times to exclude any bias in performance verification. It is important to note that LOOCV is not part of CDPMS, as it was used only to assess the model's performance, as shown in Figure 2. The model performance is compared against a random reference forecast.

3.2.2.1 Brier Score (BS)

The drought probability provided by the proposed copula-based model for each month can be analyzed using the Brier Score (*BS*), a verification measure of binary events (yes/no) that is used in multivariate models (HAO *et al.*, 2019; KLEIN *et al.*, 2016). *BS* can mainly be regarded as the mean squared error between the probability of the drought prediction (p_i), and a value of a binary variable associated with the observations (o_i) by assigning 1, if the event occurs, and 0, if it does not, where x is the length of the time series. The BS takes values in the range 0 to 1, with 0 being a perfect prediction, according to (WILKS, 2011):

$$BS = \frac{1}{x}\sum_{i=1}^{x}(p_i - o_i)^2 \quad (6)$$

3.2.2.2 Brier Skill Score (BSS)

The Brier Skill Score (*BSS*) was used to evaluate the reliability of the probabilistic prediction (or skill). The score is calculated from the BS for the CDPMS (BS_{CDPMS}) and from the BS for a reference forecast (BS_{REF}) according to Equation (7), whose results range from $-\infty$ to 1. $BSS = 0$ means no skill in comparison to the reference, and $BSS = 1$, perfect skill.

$$BSS = 1 - \frac{BS_{CDPMS}}{BS_{REF}} \quad (7)$$

In the application carried out, the reference forecast selected for the evaluation of the prediction performance is the random probability of occurrence of a drought with a given intensity. Since this score was only applied to moderate droughts ($SPI < -0.84$, corresponding to the 20th percentile (AGNEW, 2000) the p_i for the BS_{REF} was set equal to 0.20.

3.2.3 Precipitation Data

To construct a reliable bivariate statistical model for concurrent precipitation distributions, long historical continuous observations are needed. In the application presented herein, 45 rain gauges evenly distributed over mainland Portugal were selected (Figure 4, Chart 1).

Figure 4: Location of the 45 rain gauges used in the study.

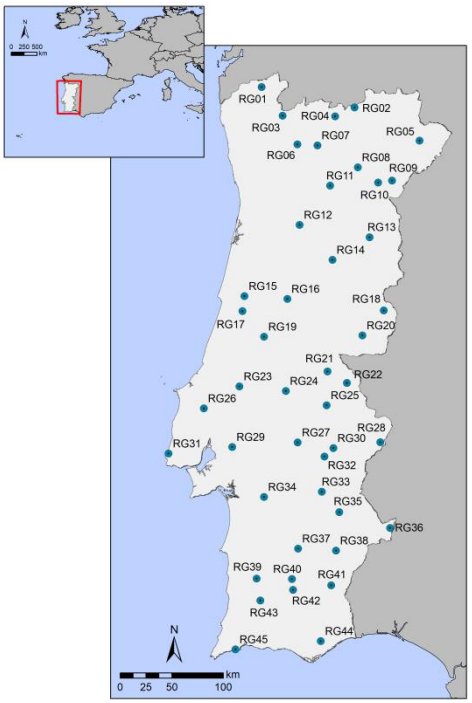

Source: Prepared by the author

Chart 1: Name, code, identification (ID), and geographic coordinates (WGS84 system) of the 45 rain gauges of Figure 3.

Name	Code	ID	Lat (°)	Long (°)	Name	Code	ID	Lat (°)	Long (°)
Merufe	01G03UG	RG01	42.0180	-8.3890	Bemposta	17I02UG	RG24	39.3490	-8.1410
Travancas	03N01G	RG02	41.8280	-7.3056	Alter do Chão	18L01UG	RG25	39.2182	-7.6844
Leonte	03I03UG	RG03	41.7650	-8.1470	Pragança	18C01G	RG26	39.1990	-9.0640
Soutelo (Chaves)	03L02UG	RG04	41.7530	-7.5348	Pavia	20I01G	RG27	38.8965	-8.0136
Campo de Víboras	04R03UG	RG05	41.5240	-6.5580	Caia (Monte Caldeiras)	20O02UG	RG28	38.8873	-7.0898
Cabeceiras de Basto	04J06UG	RG06	41.5127	-7.9792	Santo Estevão	20E02UG	RG29	38.8600	-8.7460
Santa Marta da Montanha	04K02G	RG07	41.5008	-7.7460	Estremoz	20L01G	RG30	38.8416	-7.6159
Folgares	06N01C	RG08	41.3032	-7.2828	Colares (Sarrazola)	21A01C	RG31	38.8020	-9.4570
Carviçais	06P02UG	RG09	41.1790	-6.8900	Évora-Monte	21K02UG	RG32	38.7690	-7.7161
Moncorvo	06O04UG	RG10	41.1650	-7.0510	São Manços	23K01UG	RG33	38.4605	-7.7505
Adorigo	07L01U	RG11	41.1460	-7.6070	Barragem de Pego do Altar	23G01C	RG34	38.4196	-8.3952
Pindelo dos Milagres	09J02U	RG12	40.8060	-7.9630	Amieira	24L01C	RG35	38.2793	-7.5605
Freixedas	09O02U	RG13	40.6880	-7.1630	Barrancos	25P01UG	RG36	38.1321	-7.0013
Gouveia	11L01UG	RG14	40.4940	-7.5930	Santa Vitória	26I01UG	RG37	37.9645	-8.0227
Santo Varão	12F02C	RG15	40.1840	-8.6020	Serpa	26L01UG	RG38	37.9426	-7.6038
Góis	13I01G	RG16	40.1568	-8.1133	Relíquias	27G01G	RG39	37.7030	-8.4825
Soure	13F01G	RG17	40.0521	-8.6250	Castro Verde	27I01G	RG40	37.6976	-8.0933
Penha Garcia	13O01UG	RG18	40.0420	-7.0180	Mértola	28L01UG	RG41	37.6371	-7.6619
Alvaiázere	15G01UG	RG19	39.8270	-8.3810	Rosário (Almodôvar)	28I02U	RG42	37.6020	-8.0810
Ladoeiro	14N02UG	RG20	39.8269	-7.2660	Barragem de Mira	28G01C	RG43	37.5101	-8.4433
Nisa	16L03UG	RG21	39.5160	-7.6690	Santa Catarina (Tavira)	31K01UG	RG44	37.1487	-7.7847
Castelo de Vide	17M01G	RG22	39.4116	-7.4525	Valverde	31E03C	RG45	37.0820	-8.7180
Pernes	17F01UG	RG23	39.3910	-8.6630					

Source: Prepared by the author

The monthly precipitation records were acquired by the Portuguese Environmental Agency, APA, and made available via the SNIRH database (Sistema Nacional de Informacão de Recursos Hídricos, http://snirh.pt), which has high data quality standards. The SNIRH is the

main source of Portuguese hydrological and hydrometeorological data used by researchers and practitioners of water resources engineering and science.

Some of the precipitation series had missing values that were filled by applying an approach based on a linear regression analysis (PORTELA *et al.*, 2015b). For each monthly gap in a given rain gauge, the approach identifies the candidate rain gauges that can be used for filling it. These gauges are next ranked according to the correlation coefficient between paired series for that month at the rain gauge with the gap and at each of the candidate rain gauges. The candidate rain gauge with higher correlation coefficient is next selected and used to fill the gap based on a linear regression model that is specific for each gap (PORTELA *et al.*, 2015b). The length of the series after filling the missing values was x = 100 hydrological years, from 1918/19 to 2017/18.

3.3 CDPMS for Mainland Portugal: Definition and Performance

The following items describe the stepwise development and the performance assessment of the CDPMS developed to continuously monitor the drought probability over Mainland Portugal during the rainy season, based on the precipitation records at the 45 rain gauges of Figure 3. The application to a specific site is presented in Section 5.

3.3.1 Precipitation Thresholds for Drought Recognition

Chart 2 presents the precipitation thresholds, R_N^*, in the 45 rain gauges obtained by inverting the SPI for the time span of 6 months (SPI6), from October to March, for the different drought intensities (moderate, severe, and extreme). By the end of March, a drought with a given intensity occurs in a given rain gauge whenever the precipitation for the period is smaller than the precipitation threshold for that intensity.

Chart 2: Precipitation thresholds, R_N*, (mm) for the six-month period, from October to March,

for the different drought intensities.

Rain gauge ID	Drought intensity			Rain gauge ID	Drought intensity		
	Moderate	Severe	Extreme		Moderate	Severe	Extreme
RG01	745.2	550.6	411.7	RG24	307.4	226.9	165.0
RG02	429.9	351.9	297.6	RG25	269.9	190.0	126.2
RG03	1250.0	933.9	701.4	RG26	442.1	357.1	294.9
RG04	338.9	272.4	228.7	RG27	245.4	181.4	132.1
RG05	252.7	212.2	189.9	RG28	228.6	169.4	122.5
RG06	624.0	467.6	350.5	RG29	272.3	208.9	160.4
RG07	774.4	614.7	500.8	RG30	281.6	208.1	151.8
RG08	250.9	197.3	158.8	RG31	371.7	309.3	263.1
RG09	290.0	221.5	172.2	RG32	265.6	201.5	152.4
RG10	225.0	175.0	137.3	RG33	238.9	178.1	130.7
RG11	280.2	223.0	182.2	RG34	269.6	214.9	174.6
RG12	601.4	479.3	393.2	RG35	256.2	202.4	162.6
RG13	311.6	232.8	170.6	RG36	260.6	204.4	160.0
RG14	517.3	419.1	345.1	RG37	251.9	197.7	155.9
RG15	446.4	361.0	294.2	RG38	237.9	182.4	140.6
RG16	557.5	449.0	364.9	RG39	311.3	242.3	191.1
RG17	415.4	320.1	246.6	RG40	267.9	215.7	175.7
RG18	383.7	310.8	255.6	RG41	184.5	146.8	120.9
RG19	586.6	468.6	378.5	RG42	284.4	223.2	176.3
RG20	288.6	234.7	194.2	RG43	292.3	225.8	173.2
RG21	331.5	256.7	199.4	RG44	318.5	239.5	180.3
RG22	370.7	284.5	221.8	RG45	289.5	229.0	182.3
RG23	379.6	288.8	218.2				

Source: Prepared by the author

3.3.2 Copula Fitting

In each rain gauge, the bivariate model was constructed by coupling the precipitation in the rainy season, R_N for $N = 6$, with the precipitation in the initial n months of that season, R_n (i.e., the precipitation in October, for $n = 1$, from October and November, for $n = 2$ and so on until $n = 5$, from October to February). The length of each coupled (R_N, R_n) series is equal to the length of the recording period (x = 100 years). The parameters were estimated by the MPL method, and the candidate copula families were selected based on the AIC.

For the 45 rain gauges, the frequency of the copula families chosen for each value of n is presented in Figure 5. Considering, for example, $n = 1$, the percentage of rain gauges where the different types of families where selected is as follows: 31% copula Frank, a symmetric Archimedean copula, 38% Clayton copula, an asymmetric copula with lower tail dependence, 4% Survival Clayton copula, a 180 degrees rotated Clayton with upper tail dependence, 18% Gumbel copula, an asymmetric copula with upper tail dependence, and 9% Gaussian copula, a symmetric Meta-Elliptical copula.

As n increases, the percentage of rain gauges where Frank copula is selected decreases from 31 (n = 1) to 7% (n = 5). This is explained by the increase of the linear dependence between variables as the precipitation in additional months of the rainy season is progressively known and provided to the model. The same applies to the Meta-Elliptical copulas, Gaussian and t Student: less than 10% of the rain gauges for n = 1 to approximately 60% of the rain gauges for n from 3 to 5.

Figure 5: Distribution (in percentage) of the selected copulas by the 45 rain gauges as a function of the number of initial months of the rainy season.

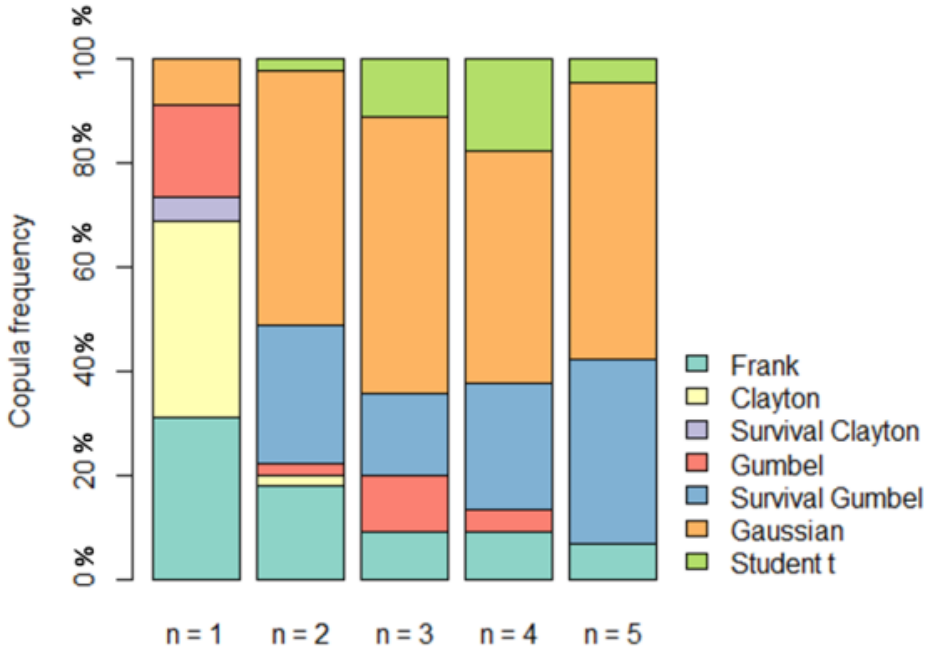

Source: Prepared by the author

3.3.3 Drought Risk Monitoring

After the bivariate model has been set up for each rain gauge, the CDPMS was applied to estimate the drought probability, i.e., the temporal evolution of the conditional probability of drought occurrence as new precipitation records are progressively acquired (Equation (2)).

Figure 6 shows the spatial distribution of the moderated drought probability thus achieved for the rainy season of October 2012 to February 2013, chosen as an example. The probability surfaces were obtained by averaging the results at the 45 rain gauges according to the inverse distance weighting (IDW) method with exponent 2.

Figure 6: Example of the application of the CDPMS to the continuous monitoring of the

likelihood of moderate drought at the end of the six months period from October 2012 to February 2013. Drought probability from the end of October to the end of February

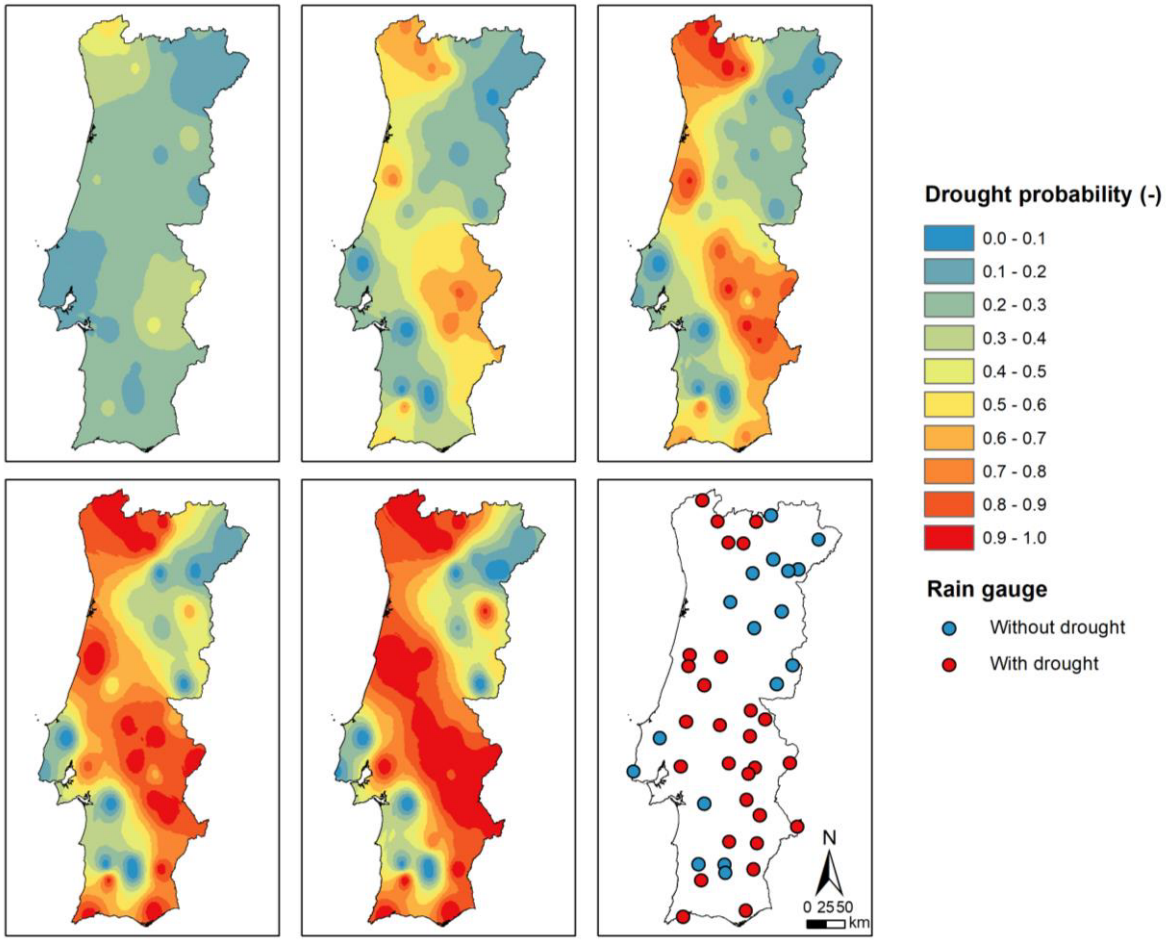

Source: Prepared by the author

It is possible to see that, for n = 1 (that is, by the end of October), two regions presented a higher probability of drought occurrence: northwest and southeast regions. For n = 3 (end of December), the probability of drought in those regions increased and even expanded into some of the central areas. As the precipitation in the following months is progressively known, only a few regions of the country have a drought risk smaller than 50%. This could justify issuing an alert regarding a possible drought at the end of March–with caution in December (n = 3), for sure in January (n = 4) and definitely in February (n = 5). Such an early warning could raise the awareness of water resources managers and of civil protection authorities, urging the implementation of some anticipatory measures aiming at mitigating the consequences of a possible scenario of drought and water scarcity.

The last map of Figure 5 shows what happened by the end of March. The almost perfect match between the areas where the drought probability progressively increased with n (areas shaded from blue to orange and red) and those that in fact experienced drought by the

end of March (red circles) clearly indicates the ability of the model to identify areas of increasing drought probability.

3.3.4 CDPMS Performance Assessment

The performance of the CDPMS was assessed based on the BSS computed for each one of the 45 rain gauges and values of *n*, according to the LOOCV methodology (Section 2.2).

The results achieved for predicted moderate droughts are presented in Chart 3. The values closer to 1 indicate better model performance, and the negative values indicate that the reference forecast outperformed the CDPMS. The ability of the CDPMS to predict the drought probability increases as the number of months, *n*, with known precipitation increases: for $n = 1$ the average performance for the complete set of rain gauges is 0.03 while for $n = 5$ is 0.70.

Chart 3: Moderate droughts. BSS values for n = 1 to n = 5.

Rain gauge ID	n = 1	n = 2	n = 3	n = 4	n = 5	Average	Rain gauge ID	n = 1	n = 2	n = 3	n = 4	n = 5	Average
RG01	0.15	0.27	0.46	0.57	0.69	0.43	RG24	0.03	0.23	0.38	0.56	0.81	0.40
RG02	-0.02	0.10	0.13	0.37	0.55	0.23	RG25	0.02	0.15	0.30	0.57	0.73	0.35
RG03	0.05	0.19	0.47	0.63	0.83	0.44	RG26	-0.05	0.12	0.25	0.60	0.78	0.34
RG04	0.04	0.10	0.25	0.44	0.65	0.30	RG27	0.03	0.17	0.30	0.41	0.67	0.32
RG05	0.00	0.18	0.35	0.51	0.65	0.34	RG28	0.03	0.18	0.29	0.47	0.72	0.34
RG06	0.15	0.27	0.44	0.55	0.77	0.44	RG29	0.02	0.10	0.14	0.41	0.55	0.24
RG07	0.06	0.18	0.35	0.52	0.66	0.35	RG30	-0.04	0.11	0.27	0.40	0.54	0.25
RG08	0.04	0.11	0.23	0.41	0.56	0.27	RG31	0.03	0.07	0.24	0.51	0.73	0.32
RG09	-0.03	0.25	0.27	0.53	0.62	0.33	RG32	0.05	0.15	0.25	0.49	0.62	0.31
RG10	0.01	0.16	0.22	0.41	0.52	0.27	RG33	0.08	0.21	0.37	0.48	0.67	0.36
RG11	0.02	0.14	0.22	0.53	0.64	0.31	RG34	0.01	0.13	0.27	0.41	0.68	0.30
RG12	0.01	0.13	0.28	0.44	0.59	0.29	RG35	0.01	0.11	0.32	0.57	0.71	0.34
RG13	-0.03	0.14	0.39	0.71	0.79	0.40	RG36	0.04	0.19	0.29	0.54	0.68	0.35
RG14	0.00	0.11	0.23	0.52	0.66	0.30	RG37	-0.01	0.14	0.29	0.57	0.84	0.36
RG15	0.02	0.19	0.32	0.44	0.70	0.33	RG38	0.07	0.24	0.31	0.48	0.57	0.33
RG16	0.01	0.11	0.23	0.50	0.73	0.32	RG39	0.04	0.17	0.15	0.54	0.71	0.32
RG17	0.02	0.13	0.31	0.54	0.81	0.36	RG40	0.03	0.13	0.31	0.61	0.80	0.37
RG18	0.00	0.12	0.23	0.44	0.58	0.27	RG41	0.10	0.28	0.47	0.70	0.81	0.47
RG19	-0.02	0.09	0.21	0.50	0.70	0.29	RG42	0.07	0.16	0.42	0.66	0.78	0.42
RG20	0.01	0.07	0.21	0.33	0.65	0.25	RG43	0.08	0.20	0.37	0.54	0.70	0.38
RG21	0.01	0.10	0.29	0.42	0.74	0.31	RG44	0.03	0.08	0.35	0.66	0.82	0.39
RG22	0.00	0.13	0.31	0.47	0.69	0.32	RG45	0.01	0.14	0.19	0.47	0.76	0.32
RG23	0.01	0.31	0.44	0.74	0.83	0.47	Average	0.03	0.16	0.30	0.51	0.70	0.34

Source: Prepared by the author

The rain gauges where CDPMS had a better performance for $n = 1$ were RG01, RG06, RG33, RG38, RG41, RG42, and RG43 indicating a higher correlation between the precipitation in October and from October to March (BBS ≥ 0.07). Only for n = 1 and for seven rain gauges (RG02, RG09, RG13, RG19, RG26, RG30, and RG37) did the CDPMS perform

worse than the reference forecast (BBS < 0). This means that for these rain gauges the knowledge of the precipitation in October does not allow accurate forecasts of the probability of having or not having drought by the end of March. However, the CDPMS performance increases every month, indicating sustained improvement in the monitoring capabilities as new precipitation data is being collected and provided to the model.

Figure 7 shows the spatial distribution and the evolution of the BSS values for moderate droughts as a function of n, allowing to identify the areas where the CDPMS has better monitoring capabilities (higher values of BSS). The spatial interpolation technique used was also the inverse distance weighting (IDW) with exponent 2.

Figure 7: Moderate droughts. BSS values for n = 1 to n = 5. The closer to 1, the better the CDRMS performance

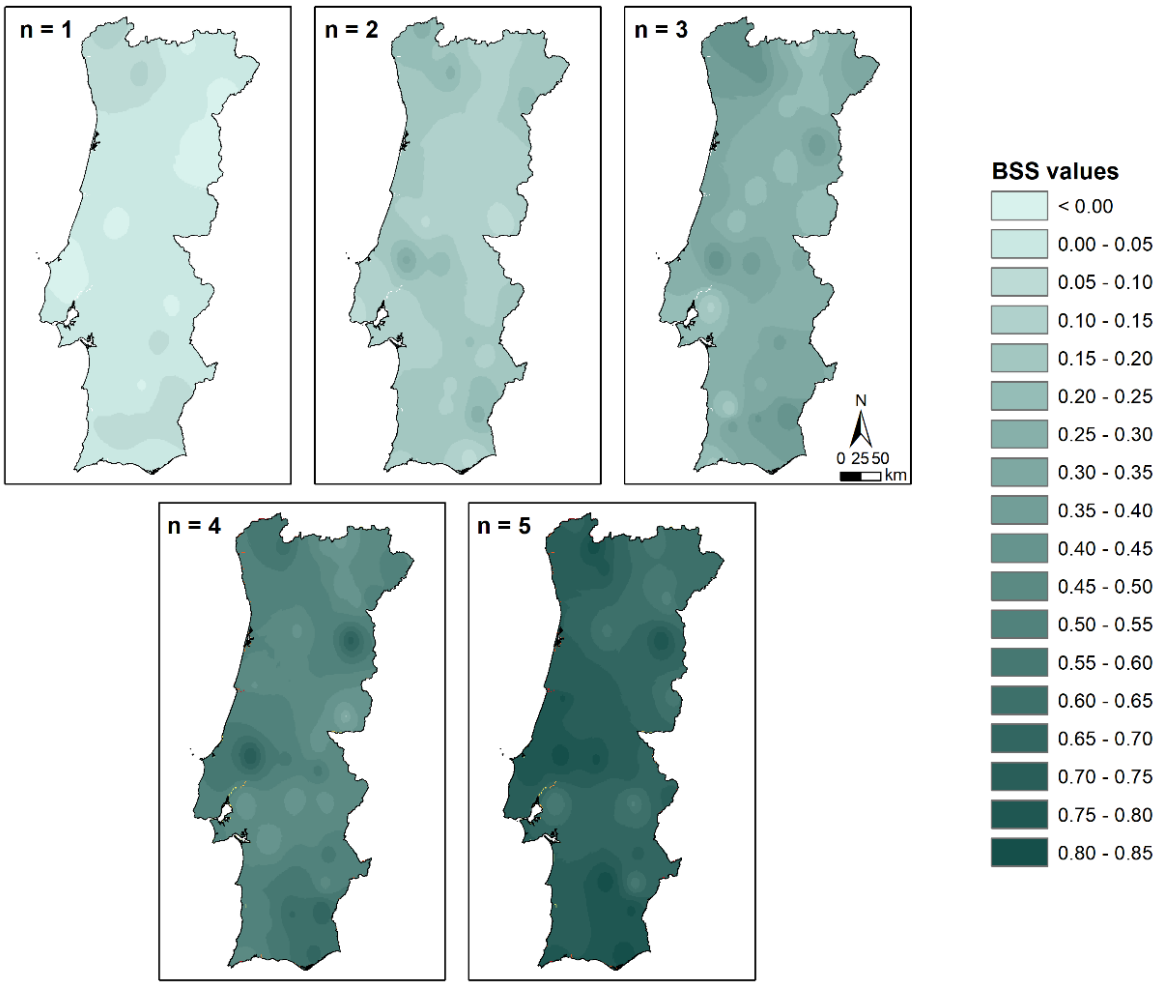

Source: Prepared by the author

To further analyze the variance of the CDPMS performance, box plots were drawn based on the values of BSS for all rain gauges (Figure 7). The whiskers have a maximum length of 1.5 × IQR (interquartile range), and the values outside the whiskers are outliers.

Figure 8 shows that the variance of the performance measure, BSS, increases in the last two months (n = 4 and n = 5) indicating that, in some rain gauges, a high probability may not result in a drought event as there is still precipitation to fall. The opposite is also true, low risk does not mean drought cannot happen, because the above threshold precipitation tendency presented in the initial months of the rainy season may not be enough to counterbalance the deficits during the last months. However, both specific cases are less likely to occur.

Figure 8: Moderate droughts. BSS values for all the rain gauges as a function of the number of initial months of the rainy season with known precipitation (n).

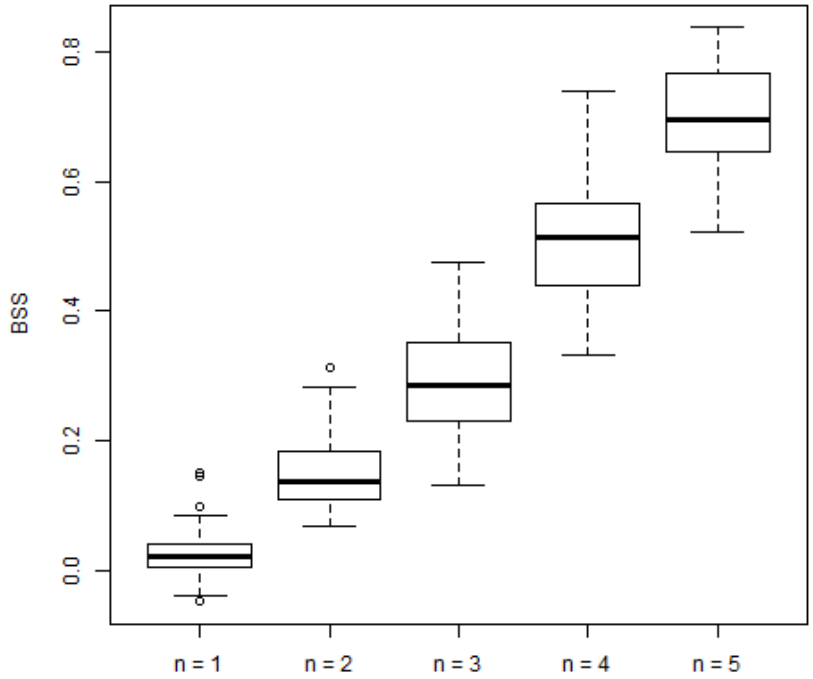

Source: Prepared by the author

Drought occurrence in mainland Portugal is associated with a substantial interannual and decadal variability, strongly linked to precipitation shortage during the rainy season (RUSSO *et al.*, 2015; TRIGO; DACAMARA, 2000). The dynamic interactions among weather types associated with mainland Portugal due to its location between the Atlantic Ocean and the Mediterranean Sea, strong orographic influence and small size contribute to explain high spatial variability and relative disconnection from general circulation (CORTESI *et al.*, 2014; TRIGO *et al.*, 2004, 2008; TRIGO; DACAMARA, 2000). The complex interactions between different weather types during the rainy season, also because of the different geographic conditions, might explain the variability between the model performances.

Overall, due to copula's high flexibility, a great variety of copula families can be chosen to model the temporal dependence structure of the precipitation in each specific rain gauge, and, by this way, to represent its spatial variability.

The increasing performance of the CDPMS over time means that it consistently learns with the addition of the precipitation in the following months. It also consistently outperforms the reference forecasts, indicating that it can be a valuable source for assessing drought probability.

The application of the LOOCV excluded any bias in the performance verification by not choosing specific years that could best fit the expected performance, such as very dry or very wet years. Therefore, the CDPMS proved to be a valuable tool for drought probability monitoring. However, its application to Mainland Portugal to monitor under real-time conditions the probability of drought by the end of the rainy season requires a continuous updating of the precipitation records at the rain gauges of Figure 2, which may not be an easy task. Alternatively, the CDPMS can be applied to a specific site, as exemplified in the next item.

3.4 CDPMS Applied to a Single Site

This item refers to the CDPMS development and application to a single site in Mainland Portugal aiming at exemplifying how the system can be operated as a drought monitoring, but also forecasting tool. For this purpose, the rainy season of the hydrological year of 2017/2018 (October 2017 to March 2018) at the rain gauge of Santa Marta da Montanha (RG07) was selected. It was assumed that the precipitation was progressively recorded and provided to the model until February 2018 aiming at estimating the drought probability by the end of the rainy season. As already said, such knowledge is extremely important to develop anticipatory actions and to mitigate impacts related to water scarcity.

3.4.1 CDPMS Development for Santa Marta da Montanha

The dependence structure for each coupled (R_N, R_n) precipitation series in RG07 rain gauge was modeled by the Archimedean (Frank) and Meta-Elliptical copulas (Gaussian and t Student). Table 3 presents the bivariate models selected for each *n*, from October (n = 1) to February (n = 5). The parameters θ (for the Archimedean copulas) and ρ and v (for the Meta-Elliptical copulas) were estimated using MPL, and the copula families were selected based on the AIC, as described in Section 2.1.2. The Kendall's Tau was applied to verify the non-linear dependence between R_N and R_n modeled by the copulas. A hypothesis test was applied to determine whether R_N and R_n presented a relevant dependence structure, a small p-value provides strong evidence against the null hypothesis that they are independent, for the 95% confidence level.

Table 3: Santa Marta da Montanha (RG07) rain gauge. Bivariate models for each coupled (R_N, R_n) series, their parameters, Kendall Tau correlation (according to the model and empirical), AIC, and p values.

R_n	Family	Parameters		Kendall's Tau		AIC	p-value
		θ or ρ	v	Model	Empirical		
$n = 1$	Frank	1.75	-	0.19	0.19	−6.16	<0.05
$n = 2$	Gaussian	0.60	-	0.41	0.40	−37.86	<0.05
$n = 3$	t Student	0.76	30.00	0.55	0.53	−75.34	<0.05
$n = 4$	Gaussian	0.91	-	0.72	0.72	−161.84	<0.05
$n = 5$	Gaussian	0.96	-	0.83	0.83	−251.14	<0.05

Source: Prepared by the author

The values of the empirical Kendall Tau correlation coefficient presented in Table 3 indicate that as the precipitation in the rainy season is progressively recorded and introduced in the model, the dependence between R_N and R_n becomes stronger. In fact, for n = 1 the precipitation in October explains only 19% of the precipitation of the rainy season, while for n = 2 it explains 40%, and for n = 5, 83%. The small differences between model and empirical Kendall's Tau values show that the dependence between R_N and, R_n was properly modeled by the copulas.

The bivariate model adopted for each coupled (R_N, R_n) series in Santa Marta da Montanha rain gauge is presented in Figure 9. The axes in the figure were graduated in terms of the standard normal deviates that correspond to the non-exceedance probability given by the marginal distributions. The figure shows that as n increases the copulas become narrower due to stronger correlations between R_N and R_n.

Figure 9: Santa Marta da Montanha (RG07) rain gauge. Bivariate models for each coupled (R_N, R_n) series along the rainy season of 2017/2018, from n = 1 to 5.

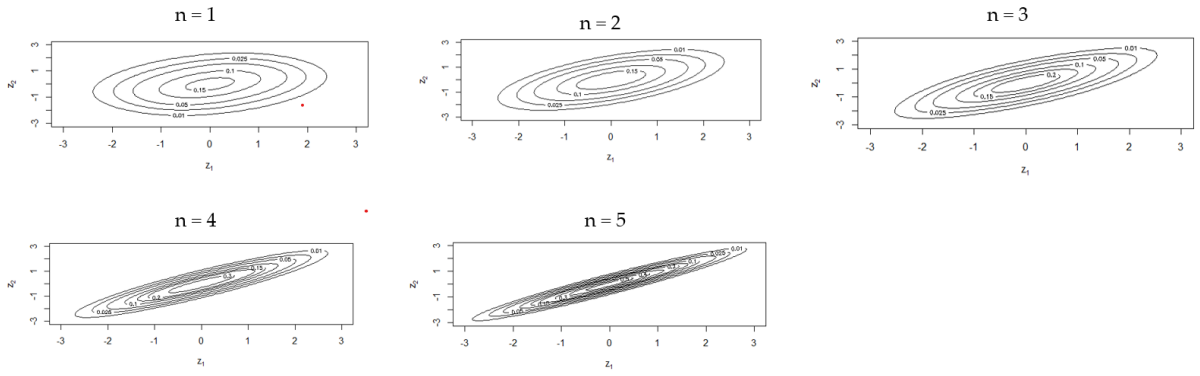

Source: Prepared by the author

3.4.2 CDPMS Application – Drought Risk Monitoring

After the bivariate model has been established, the CDPMS was applied to monitor the drought probability in Santa Marta da Montanha rain gauge during the rainy season of 2017/2018. The results obtained are exemplified in Chart 4 for the three categories of droughts, moderate, severe, and extreme droughts. The table includes the precipitation thresholds, R_N^*, for the different droughts categories, the precipitation that fell along the season (monthly and cumulative precipitations) and the historical average monthly precipitations.

Chart 4: Santa Marta da Montanha (RG07) rain gauge. Probability of moderate, severe, and extreme drought events along the rainy season of 2017/2018 according to the CDPMS (dashed cells).

		Oct	Nov	Dec	Jan	Feb	Mar
Mean monthly precipitation (mm)		133.3	160.9	190.1	197.5	135.2	161.7
Observed precipitation (mm)	Monthly	43.1	40.4	173.0	109.0	58.6	273.5
	Acumulated	43.1	83.5	256.5	365.5	424.1	697.6
Drought category (Threshold)		Drought risk					
Moderate (779.93 mm)		0.31	0.57	0.56	0.71	0.97	Drought
Severe (618.83 mm)		0.16	0.36	0.30	0.31	0.61	No Drought
Extreme (503.49 mm)		0.08	0.21	0.13	0.09	0.14	No Drought

Source: Prepared by the author

From October 2017 to March 2018, the total precipitation was 697.6 mm, i.e., below the threshold for moderate drought and above the thresholds for the other drought categories, meaning that a moderate drought event really occurred by the end of March.

In what concerns the moderate droughts, the CDPMS proved to the able to detect the increasing probability of drought: 31% (October 2017), 57% (November 2017), 56% (December 2017), 71% (January 2018), and 97% (February 2018) which could justify issuing a drought alert, at least in January and for sure in February. Despite the considerable above-the-average precipitation that occurred in March, there was a moderate drought, confirming the prediction of CDPMS.

The CDPMS also identified an increased risk of severe drought by the end of March, though with much smaller probability, only 31% in January and 61% in February. However, there was not a severe drought event, which suggests a poorer performance of the CDPMS. This circumstance can be explained by the anomalous and unforeseeable precipitation that took place in March that dampened the expectations of a severe drought.

The last row of Chart 4 indicates very small probabilities of having an extreme drought by the end of March, which was confirmed.

This example shows the capability of CDPMS in detecting moderate droughts. However, the model was not able to distinguish the intensity of the event, once severe and extreme droughts are very sensitive to an individual precipitation event. Precipitation thresholds for the droughts with higher intensity are lower and can be easily exceeded by a few millimeters of precipitation.

3.5 Discussion and Conclusion

Drought is a harsh natural disaster with onsets difficult to perceive. Therefore, it is relevant and challenging to develop a trustful tool able to recognize its occurrences and to initiate actions aiming at mitigating its impacts. This study developed such a tool, based on copulas applied to the continuous monitoring of the drought probability, using only precipitation data, the CDPMS.

Such a model uses a kind of stepwise procedure applied to each specific location where the drought probability evaluation is required. It starts with the computation of drought-triggering precipitation thresholds, which enable assigning precipitations to the drought categories given by the SPI (PORTELA *et al.*, 2012). The next step refers to the setting up of the copula-based bivariate model that, by using historical monthly precipitation data, "couples" the seasonal precipitation of rainy season (R_N) with the precipitation until the last but one month of such season (R_n), according to the dependence structure between R_N and R_n.

The last step relates to the application of the CDPMS under current conditions to monitor the drought probability during the rainy season aiming to answer the following question: will there be drought by the end of the rainy season? Once the precipitation in each month of the current rainy season is progressively known and incorporated into the CDPMS, the model returns the drought probability, that is, the probability of the precipitation being smaller than the one required to avoid drought conditions by the end of the season. Based on that probability, drought warnings can be issued, and anticipatory drought mitigation and adaptation measures implemented. The application based on a single rain gauge was exemplified for the rainy season from October 2017 to March 2018.

The CDPMS can also be applied to monitor the evolution of the drought probability during the rainy season in a region, instead of a single site, based on the continuous updating of the precipitation deficits or surplus in the region. Such an innovative application was demonstrated by the application of the CDPMS to Mainland Portugal to monitor the drought probability during the rainy season from October 2012 to March 2013, based on 100-year of

precipitation data at 45 rain gauges evenly distributed over the country. The application demonstrated that the CDPMS can anticipate the regions that later experienced, in fact, drought conditions.

The study showed that the continuous drought probability monitoring system can detect drought events simply based on precipitation data. However, it has lower confidence in distinguishing among the drought intensities, probably because the differences among precipitation thresholds for the different intensities are too small and can be easily exceeded by also small, but unforeseeable, amounts of precipitation during the rainy season. The dynamic interactions among weather types associated with Mainland Portugal due to its location between the Atlantic Ocean and the Mediterranean Sea, the strong orographic influence in the precipitation spatial and temporal patterns and its small area may result in the CDPMS performing better in some regions than in others.

Notwithstanding, the CDPMS can help decision-makers to anticipate actions and strategies to decrease potential negative impacts, based on the assignment of a quantitative measure (the probability) to the imminence of a drought event. It also contributes to a systematic warning for water managers and civil protection authorities, allowing them to gradually adjust the public awareness as the threat of a possible drought event becomes more reliable.

The marked seasonality of the rainfall regime in Mainland Portugal makes the precipitation shortages during the rainy season a fundamental trigger of droughts, which explains the good performance of CDPMS despite only based on precipitation data. However, previous studies suggest that, due to the location of the country, the addition of other variables linked to climate, such as teleconnection indexes (North Atlantic Oscillation and sea surface temperature), may improve the drought forecasting capabilities (OJEDA, 2018; SANTOS; PORTELA; PULIDO-CALVO, 2014). In addition, other climatic and hydrological variables such as temperature and runoff could also be incorporated into the model. Further studies could also try to implement a time-varying copula model for bivariate modeling precipitation (R_N and R_n) designed to address the nonstationary behavior of some of the hydrological variables that are expected to result from climate change.

4 COPULA-BASED MULTIVARIATE FREQUENCY ANALYSIS OF THE 2012 - 2018 DROUGHT IN NORTHEAST BRAZIL[1]

4.1 Introduction

The Northeast of Brazil (NEB) has experienced one of its worst droughts ever recorded, from 2012 to 2018, leading to devastating widespread impacts on water storages, agriculture, livestock, and industry (BRITO *et al.*, 2018; CUNHA *et al.*, 2015, 2018; DE AZEVEDO *et al.*, 2018; GUTIÉRREZ *et al.*, 2014; MARENGO *et al.*, 2017; MARENGO; CUNHA; ALVES, 2016; MARTINS; MAGALHÃES; FONTENELE, 2017; VIEIRA *et al.*, 2015). Solely in Ceará State, 39 out of 153 monitored reservoirs completely collapsed, another 42 reservoirs reached their minimum operating water level, and 52% of the State's municipalities experienced water supply interruptions by the end of 2016 (MARTINS *et al.*, 2018).

Droughts are reported in NEB since the colonial period (CAMPOS, 2015; MARENGO; TORRES; ALVES, 2017; MARTINS; MAGALHÃES; FONTENELE, 2017). Historically, the States of Ceará, Rio Grande do Norte, Paraiba, and Pernambuco concentrate drought hotspots (SILVA *et al.*, 2019). Drought hazard caused massive migration and significant population death, such as the drought of 1877 – 1879, with human drought-related deaths estimated around 500,000 persons in Ceará State alone (CAMPOS, 2015). The population had no warning alert, and countless citizens chose to endure with minimal provisions before migrating to less impacted areas. Many did perish in the process.

The inherent characteristics of the semi-arid region (strong seasonality coupled with high rainfall and discharges variability of its), shallow soils (most above crystalline rock basement), and elevated evapotranspiration rates amplified drought-related impacts in NEB.

[1]The paper can be cited as: Pontes Filho, J. D., Souza Filho, F. D. A., Martins, E. S. P. R., & Studart, T. M. D. C. (2020). Copula-based multivariate frequency analysis of the 2012–2018 drought in Northeast Brazil. Water, 12(3), 834.

Societies adapt to the environment shaped by climate factors (CAMPOS, 2015) and, in the case of Ceará, this adaptation was centered on two pillars. The first was the construction of large dams, used as public policy to help cope with drought. These large reservoirs were designed to operate in Ceará's climate, taking into account its interannual rainfall variability, i.e., the drastic oscillations between wet and dry years (ANDREOLI; KAYANO, 2005; HASTENRATH, 2012).

The second was based on the transparent water allocation process and hydrosystems management supported by an early warning operation system (DELGADO *et al.*, 2018; FORMIGA-JOHNSSON; KEMPER, 2005; SANKARASUBRAMANIAN *et al.*, 2009; SOUZA FILHO; LALL, 2003), vital to Ceará's resilience to drought. These initiatives were successful in preventing migration and the devastating loss of life but were insufficient to address other serious economic losses resulting from the 2012 – 2018 drought.

Research has shown that the adaptive capacity built in Ceará State, e.g., hydraulic infrastructure and management actions, coupled with emergency measures taken to cope with the 2012-2018 drought reduced its vulnerability (CAMPOS, 2015; GUTIÉRREZ *et al.*, 2014). Despite the lessons learned, such measures are still bound by a "reactive" management paradigm. We evaluate that without proactive management and preventive drought measures, reduced efficiency was achieved by these past measures. Proactive drought management is the planning of preventive measures necessary to mitigate drought impacts.

One of the most striking social features of droughts is the loss or "washing away" of memory, which usually happens when the first rains arrive. It is this feature that makes most planning reactive. Our research team found that remnants of this memory can be used and has great potential for proactive drought planning. It would be possible, for example, to use frequency analysis of specific events as a memory holder, since it informs the estimated return period of an event, i.e., the expected recurrence interval of an event with magnitude equal to or greater than a specified one (HAAN, 2002). Frequency analysis is only possible through consistent monitoring. It enables the identification of current drought exceptionality and permits the use of this information as a preparation tool for mitigation of future droughts.

The univariate approach has traditionally dominated the drought frequency analysis. However, multiple aspects of drought characteristics present a dependence structure that can be entirely ignored by the univariate approach, resulting in an incomplete representation of the phenomenon (ALIDOOST; SU; STEIN, 2019; PONTES FILHO *et al.*, 2019; XU *et al.*, 2015a). For instance, drought with the same duration could present completely different impacts, depending on their respective severity. Shiau (2006) developed a way to calculate the return

period of a drought as a function of its duration and severity. Based on the understanding of drought from the Standardized Precipitation Index (SPI) of a rain gauge in Taiwan, he analyzed the bivariate nature of droughts by calculating the joint return period of drought duration and severity. His main contribution was the use of copula functions to model the complex dependence of drought characteristics. Copulas are functions capable of modeling the dependency structure flexibly by not restricting the use of the same distribution for its marginals (CHEN *et al.*, 2013; GENEST; FAVRE, 2007; LAZOGLOU; ANAGNOSTOPOULOU, 2018; NELSEN, 2006), and many applications were applied all over the world (KIM *et al.*, 2019; MONTASERI; AMIRATAEE; REZAIE, 2018; SONG; SINGH, 2010; TOSUNOGLU; KISI, 2016; TU *et al.*, 2016; ZHANG; XIAO; SINGH, 2015) primarily on a punctual approach.

The limitation of the punctual approach is its focus on a local region, but the occurrence of drought may cover large areas. Thus, regional analysis has proven to be more efficient for drought management than punctual approach (AYANTOBO *et al.*, 2018; AYANTOBO; LI; SONG, 2019). Regionalization techniques are essential to reduce random fluctuations of a point-based approach and homogenizing drought analysis (ESPINOSA *et al.*, 2019; RIBEIRO *et al.*, 2019b, 2019a). Clustering techniques that consider the point-wise correlation of temporal series is important and is increasing in use in hydrological applications (GIMENO *et al.*, 2010; SANTOS; PULIDO-CALVO; PORTELA, 2010; SOUZA FILHO; LALL, 2003; TOSUNOGLU; CAN, 2016; VICENTE-SERRANO *et al.*, 2004). Even though, those types of regionalization do not conserve any correlation with the political planning unit. Thus, the traditional use of hydrographic region's scale is proposed as it reinforces the correlation with socio-economic impacts felt in this planning scale. In this sense, this scale is more appropriate for droughts analysis for the water sector since it is the water planning unit defined by Brazilian water law and can be used as an essential planning scale for proactive drought management.

Many drought analyses have been performed but used either a univariate or point-scale approach. However, droughts have multivariate characteristics and may cover large areas. The purpose of this study was to use a statistical model capable of representing drought multivariate characteristics at a useful scale for decision-makers. The improved understanding of exceptional droughts by using proposed framework should help improving proactive drought management. We organized the article into six sections. Section 2 presents the study area, and the principal mechanisms causing rainfall in the area. Section 3 investigates the large-scale dynamics that caused the 2012-2018 drought event and the main consequences derived from this event. Section 4 presents the data and methods used to define and model drought and its

characteristics. Section 5 introduces the results of these analyses, including the duration and severity of the drought initiated in 2012 for each hydrographic region, and their univariate and bivariate return period. Section 6 places a summary with concluding remarks and discussions of the main results in comparison with the results from other authors.

4.2 Study Area

The State of Ceará is located in the Northern portion of the Northeast of Brazil (NNEB), Figure 10. The hydrographic regions' code number were defined as a function of latitude. The hydrographic regions located in the North were classified as HR01 to HR07, those located in the Central area are HR08 to HR10, and the Southern hydrographic regions are HR11 and HR12. Ceará has more than 90% of its territory inserted in the Brazilian semiarid region (characterized by low precipitation levels, less than 800 mm per year, high evaporation rates, and shallow soils). Such characteristics make the region remarkably vulnerable to droughts. This vulnerability is increasing due to permanent land degradation, which puts 94% of NEB into moderate to high risk of desertification (VIEIRA *et al.*, 2015).

Figure 10: Location of Ceará State, its hydrographic regions and main reservoirs (storage capacity greater than 100 hm³).

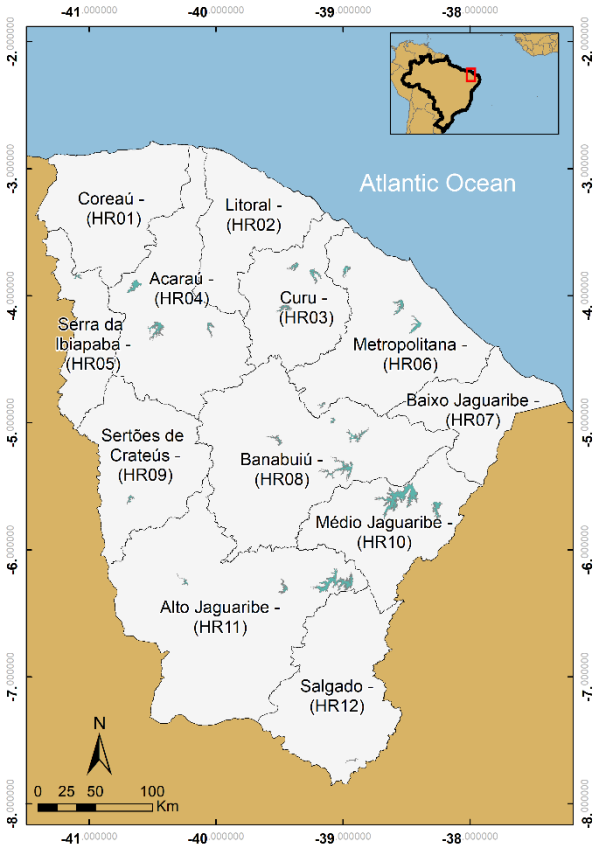

Source: Prepared by the author

The rainy season in Ceará State is characterized by a distinct seasonality, extending from December to July. The main rainy season occurs from February to May, depending on oceanic and atmospheric conditions, and the principal mechanism that influences rainfall in this period is the Intertropical Convergence Zone (ITCZ) (CAMPOS, 2015; HASTENRATH, 2012). When difference of the sea surface temperature (SST) of tropical north and south Atlantic, i.e. the Interhemispheric Tropical Atlantic Gradient (IHTAG), , is weaker, the ITCZ reaches its southernmost position, which usually occurs around March-April (HASTENRATH, 2012; HASTENRATH; HELLER, 1977; UVO *et al.*, 1998).

The interannual climatic variability on the NNEB is highly modulated by thermodynamic patterns that occur over the tropical Pacific and Atlantic Oceans. El Niño South Oscillation (ENSO) and, IHTAG, can perturb Walker and Hadley cells, causing drifts and consequently changing the intensity and period of the rainy season in the area (ANDREOLI; KAYANO, 2005; HASTENRATH, 2012; HASTENRATH; HELLER, 1977; KAYANO; ANDREOLI, 2004; MOURA; SHUKLA, 1981).

Depending on the intensity and period of the year in which it occurs, the ENSO warm phase is responsible for displacing the descending portion of the Walker cell. This phenomenon causes a zone of high pressure over NEB, which makes cloud formation in the region difficult and, consequently, influencing in years considered dry or very dry in the region (ANDREOLI; KAYANO, 2005; HASTENRATH; HELLER, 1977; UVO *et al.*, 1998). The IHTAG, on the other hand, is capable of causing drought in the region when abnormal warming of tropical North Atlantic SST occurs, which creates a low-pressure zone in this part of the Atlantic Ocean and attracts the ITCZ towards North, avoiding precipitation over South American continent (HASTENRATH; HELLER, 1977; HOUNSOU-GBO *et al.*, 2019; MOURA; SHUKLA, 1981; NOBRE; SHUKLA, 1996). Besides, the association of the positive phase of North Atlantic SST concomitant with an El Niño event provides accentuated regional impacts on the climatic condition (HOUNSOU-GBO *et al.*, 2016).

Despite the high-frequency interannual variability, there is also decadal climatic variability that can be influenced by low-frequency modes of SST anomalies. The pacific SST varies at a decadal time scale, a mode of SST variability known as Pacific Decadal Oscillation (PDO).

Kayano and Andreoli (2004) found a significant climate teleconnection between the precipitation in NNEB and PDO. The Atlantic Ocean also has its low-frequency variability mode referred to as Atlantic Multidecadal Oscillation (AMO) (ENFIELD; MESTAS-NUÑEZ; TRIMBLE, 2001; KERR, 2000). Linkages between AMO and seasonal climate variability over NNEB have also been found (JONES; CARVALHO, 2018; KAYANO *et al.*, 2018; KAYANO; CAPISTRANO, 2014; KNIGHT; FOLLAND; SCAIFE, 2006; LUCENA; SERVAIN; FILHO, 2011). Periods with simultaneously positive (or negative) PDO and AMO phases result in a more predictable behavior of rainfall in the region, with values below (or above) than normally expected (ROCHA; SOUZA FILHO; SILVA, 2019).

4.3 The 2012-2018 drought

The shock of the 2012-2018 drought raised awareness in Ceará's management community to the importance of proactive drought management, primarily due to the severity of its impacts. It was also an opportunity to better comprehend the complex interactions between ocean-atmosphere and its consequences in the rainfall over NNEB. The leading causes of this event were related to the serial combination of high and low-frequency anomalies in

SSTs that caused its persistence. Therefore, the 2012-2018 event can be understood as a series of consecutive one-year droughts.

Although El Niño is usually associated with dry periods and La Niña with wet periods on the NNEB, this drought started under the influence of a La Niña event. Rodrigues and McPhaden (2014), analyzing how the 2011-2012 La Niña event could have caused the drought in 2012, found two different types of La Niña events: (1) the cooling concentrated in the eastern Pacific, causing a cooling of the tropical North Atlantic and warming of the tropical South Atlantic; and (2) the cooling concentrated in the central Pacific, causing the opposite SST gradient in the IHTAG. The first type, the classical understanding of La Niña, can bring rain to the NNEB. The second is the one that caused the drought of 2012, which induced migration of ITCZ towards the north. This means that ENSO is a complex phenomenon and the full comprehension of its interactions with precipitation over the studied area is still in progress as new events occurs. Additionally, an upper-level convergence over NEB associated with an upper-level divergence in Amazonia during the main rainy season in 2012 contributed to this drought (MARENGO *et al.*, 2013).

The years of 2013 and 2014 did not present explicit forcing in the inter/intra annual scales, and AMO/PDO process may have influenced the drought in these years. In 2013, the ENSO phenomenon presented conditions of neutrality; although, ITCZ operated north of its climatological position in response to near neutral but still warming condition of surface waters in the tropical North Atlantic. The ITZC position, combined with westward anomalous displacement of humidity at high levels, contributed to rainfall below average in NNEB.

In 2014, neither El Niño nor IHTAG presented strong signals, and spatial variability of rainfall anomalies was found in NEB. However, a climatic condition that may have contributed to drought during the period was an anticyclonic anomaly detected in southeastern Brazil and considered one of the most critical factors of the 2014 – 2015 drought that affected southeast Brazil (NOBRE *et al.*, 2016). This system had an extension to NEB, affecting the area since 2012 (MARENGO *et al.*, 2017).

In 2015, the expansion of positive SST anomalies along the equatorial Pacific Ocean indicated the full establishment of the ENSO phenomenon. This El Niño persisted and gained force during 2015 and 2016, influencing the below-average rainfall in 2016 and 2017. In 2017, the El Niño condition retreated, and a La Niña configuration initiated. This state was favorable to indicate the end of the drought, but the warming of the North tropical Atlantic Ocean was also detected, negatively influencing the rain in NEB.

In 2018, IHTAG indicated a negative phase, especially around the end of the rainy season, and, in association with La Niña configuration over equatorial Pacific, contributed to rainfall around the climatological average over NNEB. This configuration provided enough rainfall to recover drought state in the majority of NNEB; however, few places still present persistence of this event. Figure 11 presents the time series of the cumulative rainfall anomaly and main climatic indexes that present teleconnections to precipitation in the region, NINO 3.4, IHTAG, PDO and AMO for the period of 2009 to 2018 (https://www.esrl.noaa.gov/psd/data/climateindices/list/). The accumulated rainfall deficit of the 2012 – 2018 drought is 1225 mm, 1.5 times the yearly climatological rainfall, 800.6 mm.

Figure 11: Anomalies of cumulative rainfall (mm), and oceanic index: Interhemispheric Tropical Atlantic Gradient (IHTAG), Nino 3.4, Atlantic Multidecadal Oscillation (AMO) and Pacific Decadal Oscillation (PDO).

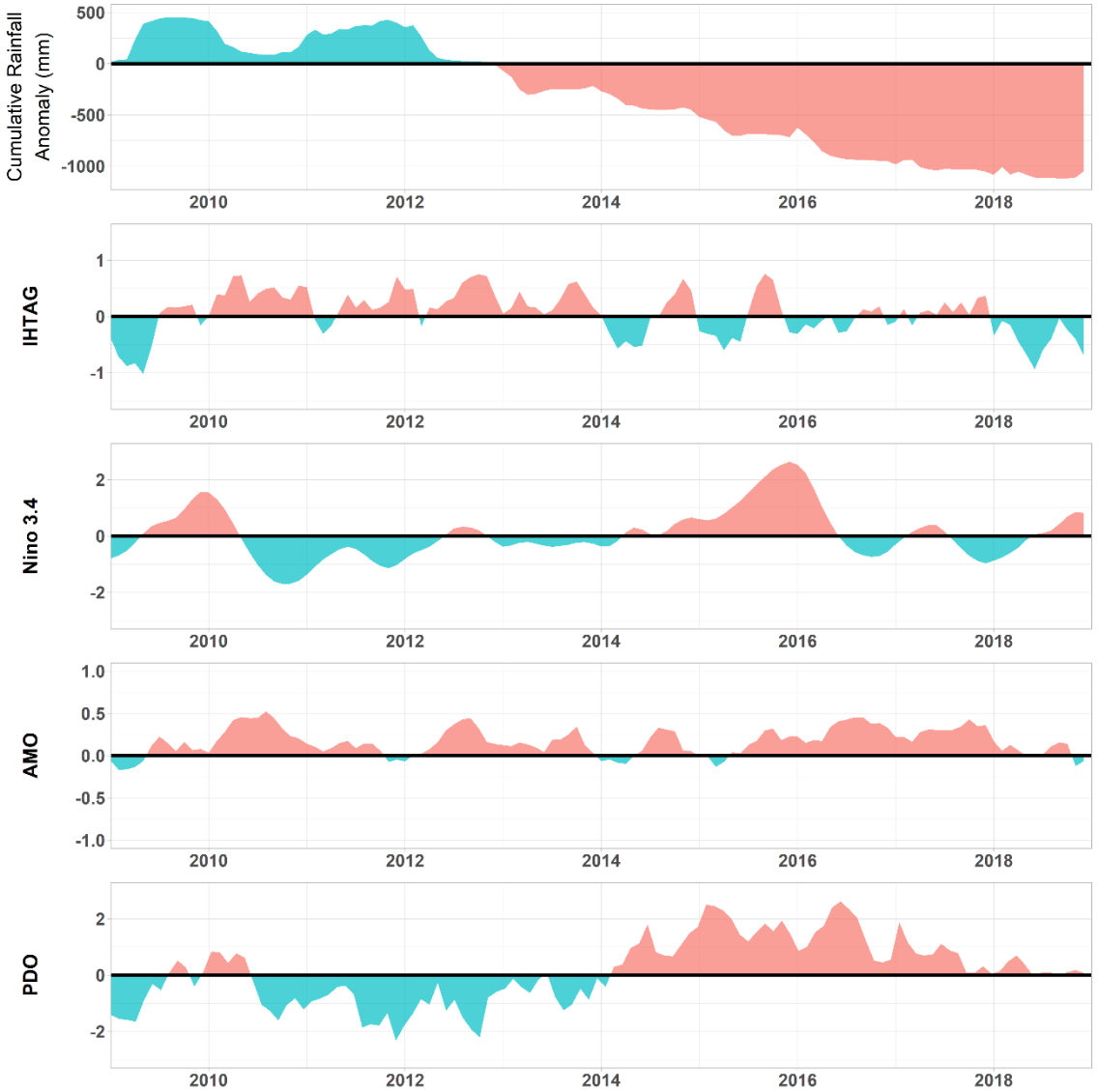

Source: Prepared by the author

The long duration and severity of the 2012 drought caused many impacts on the socio-economy and environment in NEB. Figure 12 presents the stored water volume per hydrographic region and the total accumulation in the state of Ceará. The total water storage capacity of Ceará State is 18.500 hm³ (26% in the North, 57% in Central and 17% in the South region). This storage water decreased 63% from 2011 to the end of 2016, with some hydrographic regions with total collapse. This issue was more accentuated and prolonged in Central and Southern regions, i.e. HR8 – HR12, which represents 74% of the state's total accumulation capacity. With the prolongation of the drought, the small and medium reservoirs (with storage capacity below 75 hm³ according to Ceará State's declaration nº 23.068/1994

(CEARÁ,)) started to collapse both in terms of quantity and quality, enhancing the costs of capturing and distributing water at longer distances.

Figure 12: Stored volumes for each hydrographic region in December of 2011 to December of 2018.

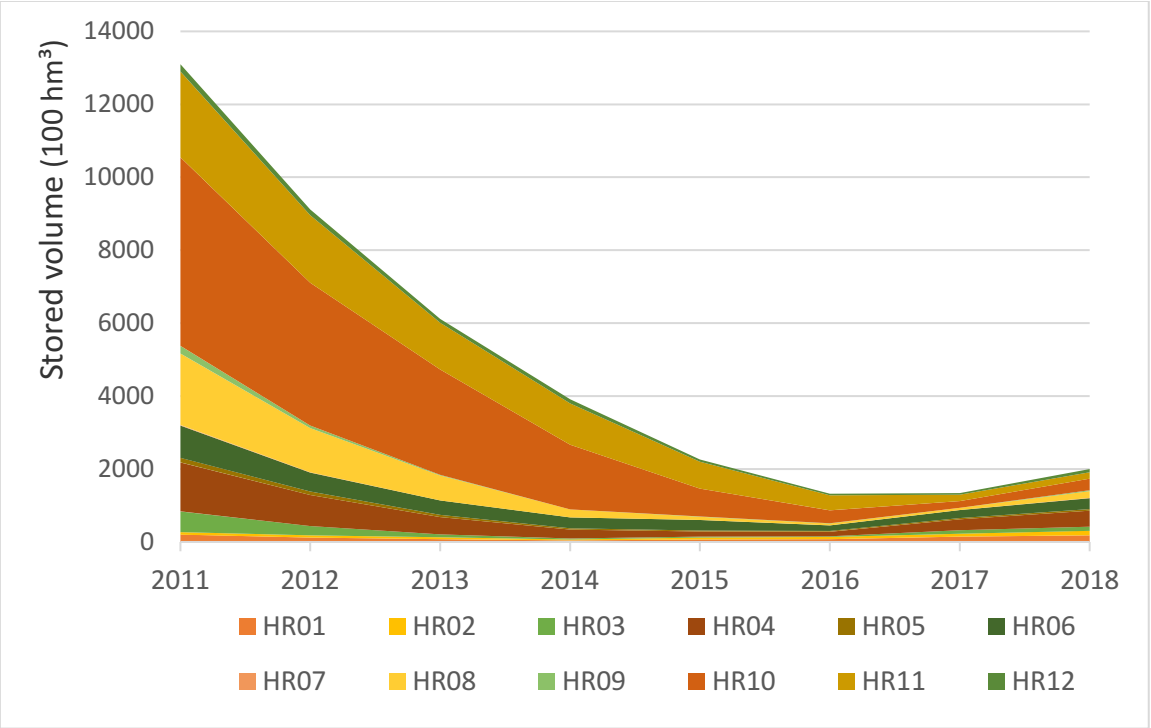

Source: Prepared by the author

The water shortage also affected the water quality of those reservoirs, especially regarding eutrophication and an increase in the concentration of salts due to the low inflow periods, higher evaporation, and anthropogenic actions. Santos et al. (2017), for instance, monitored the water quality of the biggest reservoir in the Ceará State (i.e. the Castanhão, located at HR10) from November 2011 to May 2014 and found it went from an initial oligotrophic condition, i.e. low nutrient values, in 2011 to a eutrophication condition, i.e. high nutrient values, with the decrease of its accumulated volume by 2014. Increased water treatment costs arose from this condition.

In response to this water shortage, Federal and State actions were taken to build a series of emergency pipelines, drill wells, construct water cisterns and distribute water through water tank trucks to meet the demands in rural and urban areas in Ceará. The reactive characteristic of the measures taken implied in increased associated costs as no previous planning for these actions existed.

The impacts on State's agriculture were felt at different timescales, depending on the type of agriculture used. In the first two years of the drought, 2012-2013, rainfed agriculture

was strongly impacted, and many farmers completely abandoned their cultures. The abandoned soil enabled natural vegetation, adapted to dry conditions, to recover even during prolonged drought periods. Irrigated agriculture, on the other hand, suffered practically no impact at the start of the drought, since the large multi-annual reservoirs guaranteed its supply. Those reservoirs initiated the drought with elevated accumulated levels regarding the previous rainy year of 2011. With the persistence of drought and the consequent decrease in accumulated levels, the reduction and posterior interruption of water use permits for irrigation were determined to save water for the prioritized human water supply, according to Brazilian water law.

In this sense, a series of crises management measures were promoted by Federal programs such as: *Programa Garantia Safra*, granted to farmers that lost at least 50 percent of their production; *Bolsa Estiagem*, that distributed US$40/month for smallholder farmers; subsidized prices for selling maize to feed animals; expansion of emergency credit lines for farmers, traders and industry sectors; and renegotiation of debt of farmers (GUTIÉRREZ *et al.*, 2014). Despite the devastating impacts on agricultural, livestock, and industrial activities, this extreme drought did not lead to human losses nor migration as happened in the past; this lower social disturbance is associated with government social programs (GUTIÉRREZ *et al.*, 2014)(CAMPOS, 2015).

4.4 Data and Methods

4.4.1 Data

The series of daily precipitation from 1911 to 2018 used to analyze drought in Ceará State was obtained from the Brazilian National Water Agency (http://www.snirh.gov.br/hidroweb/). The average areal rainfall for each of the twelve hydrographic regions of the Ceará State was obtained by interpolating the daily precipitation at each rain gauge according to the Inverse Distance Weighting (IDW) method with exponent two into grid points with 0.05º size. Further, the average of the interpolated values was extracted for those inside each analyzed area. The use of hydrographic region's scale tends to reduce random fluctuations of a point-based approach, homogenizing drought analysis, and reinforcing correlation with socio-economic impacts felt in this planning scale.

4.4.2 Drought Analysis

The drought analysis was based on the calculation of the Standard Precipitation Index (SPI) (MCKEE; DOESKEN; KLEIST, 1993) with 12 months aggregated timescale ($SPI12$). The time scale used for the calculation of the index is directly related to the time required for the effects of drought to be felt on the different activity sectors and the region's water resources (SILVA; SOUZA FILHO; ARAÚJO JÚNIOR, 2015). A new time-series was created with only December $SPI12$ values ($SPI12_{DEC}$) to represent the accumulated annual information. This discretization process was performed to remove the continuous information provided by SPI moving window. By doing so, the objective was to archive independent random variables that represent the total annual precipitation, smoothing the temporal series and avoiding spurious information of SPI influenced by above or below-average precipitation in months of the dry season (July to December).

The calculation of drought duration and severity characteristics for each hydrographic region was obtained through run theory, as proposed by Yevjevich (1967). Each drought event is defined as the proportion of time where all values of a variable X_t are below a selected truncation level. Specifically for SPI, the duration of a given drought event is determined by summing the periods that this event remained below a certain threshold, in this paper, $X_t = 0$. Shiau (2006) used this threshold as it avoids the division of spurious droughts that occurs inside one longer drought. This makes sense as social and environmental impacts are more significant in prolonged droughts than in consecutive shorter droughts. Figure 13 illustrates this process. Drought events 1, 2, and 3 are orange. The severity is given by the summation of SPI values during one event, according to equation 1:

$$S = -\sum_{i=1}^{D} SPI12_{DEC} \tag{1}$$

where S is the severity, and D is the duration, and $SPI12_{DEC}$ is the SPI value discretized for every December considering the aggregated time-period of 12 months.

Figure 13: Running theory to calculate drought duration D and severity S.

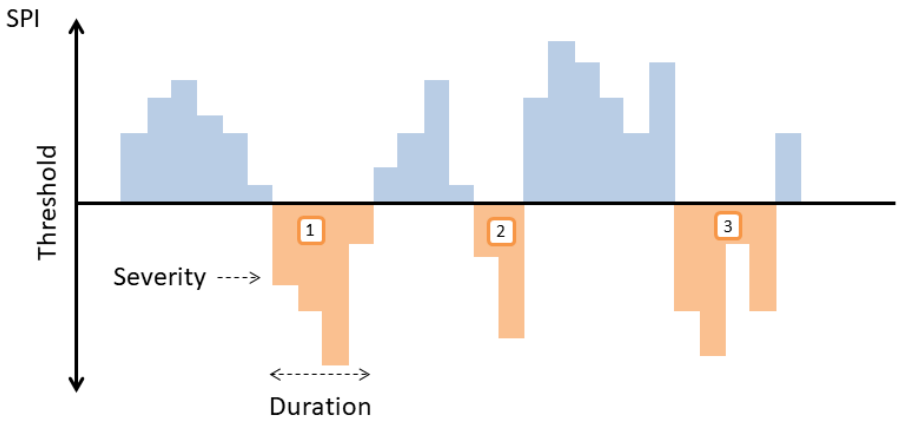

Source: Prepared by the author

4.4.3 Statistical Inference

Once the drought duration and severity characteristics were separated from the original time series by run theory application, data analysis could be performed to deduce properties of the variables samples and adjust to a population. The distribution function that better represents drought duration and severity has not yet established an agreement. Exponential and Gamma were proposed by Shiau (SHIAU, 2006) for univariate modeling the drought characteristics; however, many authors prefer to perform a goodness-of-fit test to find the families that best represent the analyzed sample for each region and drought (KIM *et al.*, 2019; KWON; LALL, 2016).

Thus, both duration and severity time series were adjusted for the univariate Log-normal, Exponential, Weibull, Gamma, and Logistic probability distribution families. The parameters were chosen based on the maximum likelihood estimation (MLE) method. The Akaike Information Criteria (AIC) indicated the candidate distributions that best fitted the data. AIC is a parsimonious estimator of the relative quality of statistical models that penalizes overfitting.

Regarding the bivariate model, this study focused on the use of copula functions to model the dependence structure among marginal distribution functions. The bivariate joint distribution function $H(d,s)$, where D and S are the random correlated variables, drought duration, and severity, with respective marginal distributions $F_D(d)$ and $F_S(s)$, is given by the copula function $C[F_D(d), F_S(s)]$, according to the equation 2:

$$H(d,s) = C[F_D(d), F_S(s)] = C(u,v) \quad (2)$$

Where $F_D(d)$ and $F_S(s)$ are equal to u and v, with $u, v \in (0,1)$.

The copula functions can be classified in Meta-elliptic and Archimedean copulas: the first is symmetric, presenting no tail dependence; the second is more flexible and can present upper or lower tail dependence. In this study, three Archimedean copulas, Clayton, Frank, and Gumbel, and two Meta-elliptic copulas, Gaussian and t-Student, were used as candidates to identify the family that was best suited to model the dependence structure between the duration and severity. Equations 3, 4, 5, 6, and 7 present the formulations of the candidate copula families, where θ, ρ, and v are the copula function parameters.

Clayton $$(\mathrm{u_1}^{-\theta} + \mathrm{u_2}^{-\theta} - 1)^{\frac{-1}{\theta}}) \quad (3)$$

Frank $$-\frac{1}{\theta}\log\left(1 + \frac{(\mathrm{e}^{-\theta\,\mathrm{u_1}} - 1)(\mathrm{e}^{-\theta\,\mathrm{u_2}} - 1)}{(\mathrm{e}^{-\theta} - 1)}\right) \quad (4)$$

Gumbel $$\exp\{-[(-\ln \mathrm{u_1})^{\theta} + (-\ln \mathrm{u_2})^{\theta}]^{\frac{1}{\theta}} \quad (5)$$

Gaussian $$\phi_\rho(\phi^{-1}(\mathrm{u_1}), \phi^{-1}(\mathrm{u_2})) \quad (6)$$

t-Student $$\mathrm{T}_{\rho,\mathrm{v}}(\mathrm{T}_{\mathrm{v}}^{-1}(\mathrm{u_1}), \mathrm{T}_{\mathrm{v}}^{-1}(\mathrm{u_2})) \quad (7)$$

The Inference Function from Margins (IFM) method (JOE, 1997) was used to estimate copula parameters. IFM is a parametric method that consists of the previous definition of marginal distributions used to transform samples in the (0,1) interval. Thus, transformed samples are jointly modeled by estimating the parameters for the families of the candidate copula using the maximum likelihood method. The minimum value of AIC was used to find the best fit model around the candidate copulas. Brechmann and Schepsmeier (BRECHMANN; SCHEPSMEIER, 2013) defined the AIC relationship with a bivariate copula model and its respective parameter (θ), according to equation 8.

$$AIC = -2\sum_{i=1}^{N} ln[C\ (u_1, v_1|\theta)] + 2k \quad (8)$$

Where, $i = 1, \ldots, \mathrm{N}$ are the observations of the variables modeled and k the number of estimated parameters in the model.

4.4.4 Frequency Analysis

To better prepare for the occurrence of future droughts, one analysis that can be integrated into the risk management is the estimation of return periods of past drought events through a process known as frequency analysis. Independent and stationary time series are needed to perform the frequency analysis (HAAN, 2002).

4.4.4.1 Univariate return period

The calculation of the return period represents the expected period between the occurrence of two events with the same or superior magnitude. The return period of drought duration (T_D) and severity (T_S) are described as a function of the expected interarrival time $E(L)$ and the cumulative distribution functions (CDF) of the drought characteristic $F_D(d)$ and $F_S(s)$, as expressed in equations 9 and 10 (KWON; LALL, 2016; SHIAU; SHEN, 2001; SHIAU, 2003, 2006). For the return period of a time series with annual recurrence, such as annual maxima precipitation, the $E(L)$ is equal to one. However, droughts are not supposed to occur every year, and $E(L)$ is found by estimating the mean value between the occurrences of droughts.

$$T_D = \frac{E(L)}{P(D \geq d)} = \frac{E(L)}{1 - P(D \leq d)} = \frac{E(L)}{1 - F_D(d)} \tag{9}$$

$$T_S = \frac{E(L)}{P(S \geq s)} = \frac{E(L)}{1 - P(S \leq s)} = \frac{E(L)}{1 - F_S(s)} \tag{10}$$

4.4.4.2 Bivariate return period

According to Shiau (2006), the joint return period of duration and severity can be defined in two cases: the return period for $D \geq d \; or \; S \geq s$ and return period for $D \geq d$ and $S \geq s$. Both definitions of joint return period for copula-based drought events are described by equations 11 and 12, respectively:

$$T_{DorS} = \frac{E(L)}{P(D \geq d \; or \; S \geq s)} = \frac{E(L)}{1 - F_{DS}(d, s)} = \frac{E(L)}{1 - C\big(F_D(d),\, F_S(s)\big)} \tag{11}$$

$$T_{D\&S} = \frac{E(L)}{P(D \geq d, S \geq s)} = \frac{E(L)}{1 - F_D(d) - F_S(s) + F_{DS}(d,s)} = \frac{E(L)}{1 - F_D(d) - F_S(s) + C\left(F_D(d), F_S(s)\right)} \quad (12)$$

where T_{DorS} is the return period for $D \geq d$ *or* $S \geq s$; $T_{D\&S}$ is the return period for $D \geq d$ and $S \geq s$.

4.5 Results

4.5.1 Drought Analysis

Droughts are, by definition, extreme events and any proactive measure must be previously defined based on magnitude and frequency of occurrence. In drought-prone areas such as the Brazilian Semi-arid region, the high interannual variability of hydrologic conditions must be considered on the standard operational routine, and only exceptional events should justify special treatment and institutional intervention (AWANGE; MPELASOKA; GONCALVES, 2016). Therefore, a scientific criterion is required to quantify the frequency of each event.

Figure 14 indicates the SPI calculated for the mean precipitation over the Ceará State for the aggregated time-period of 1 to 35 months. The darker colors in 2012-2013 indicate that this was the most critical period of the analyzed drought, and the following individual years were smoothed. Therefore, the gravity was the combination of its strong beginning with the abnormal sequence of dry years.

Figure 14: SPI for the aggregated period of 1 to 36 months, from 1973 to 2019. Warm colors represent periods of drought in Ceará State.

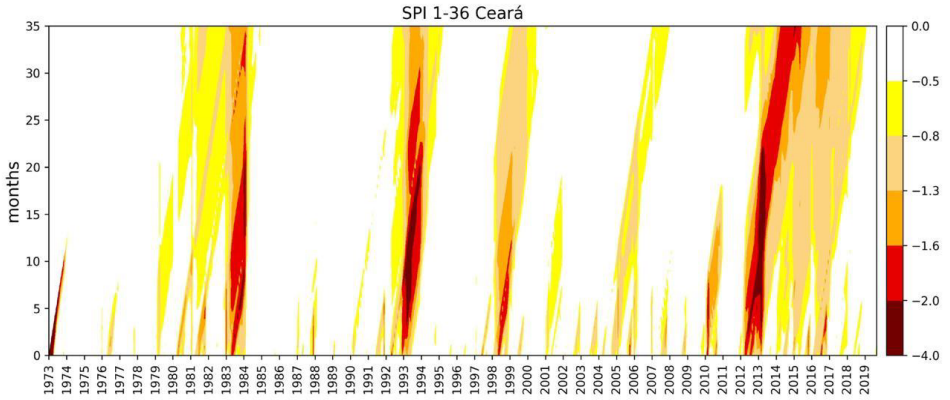

Source: FUNCEME (2019).

Drought events for the twelve hydrographic regions of Ceará State were identified using $SPI12_{DEC}$. For the sake of simplicity, $SPI12_{DEC}$ will be treated by SPI for now on. The SPI values for the 2011 – 2018 drought have exceeded the extreme condition (threshold equals -2.0, according to Mckee, 1993) for the majority of hydrographic regions during the drought onset in 2012. However, it was not the first time a drought with such magnitude had occurred in the region, as the events around 1920, and during the 1950s decade, as shown in Figure 6. The columns in Figure 6 also shows the spatial coverage of extreme events, such as the warm colors at the dry years of 1915, 1919, 1932, 1958, 1983, 1993 and 2012, and the cold colors at the wet years of 1917, 1924, 1964, 1974 and 1985. This fact is associated with large scale systems such as ENSO teleconnections and Atlantic circulation. This regional behavior is detrimental to drought management as all basins are uniformly affected, making it challenging to transfer water between hydrographic regions.

From Figure 15, it is also possible to see that the drought that started in 2012 has different ending times. For the hydrographic regions closer to the ocean, it ended between 2016 and 2017, indicated by light green colors. For those regions located more central and in the southern regions, the drought persisted until 2018, with no clear definition of ending for some of them yet. Also, sequential drought years such as the analyzed one and covering almost all hydrographic regions can present enormous negative impacts and were detected in 1930 – 1933, 1941 – 1943, 1951 – 1956, 1979 – 1983 and 1990 – 1993, showing the high climatic variability existent in the region.

Figure 15: SPI values for the 12 hydrographic regions of Ceará State organized from northern to southernmost position, HR01 - HR12. Warm colors represent dry years and cold colors represent wet years. Spatial coverage of extreme events can be visually detected.

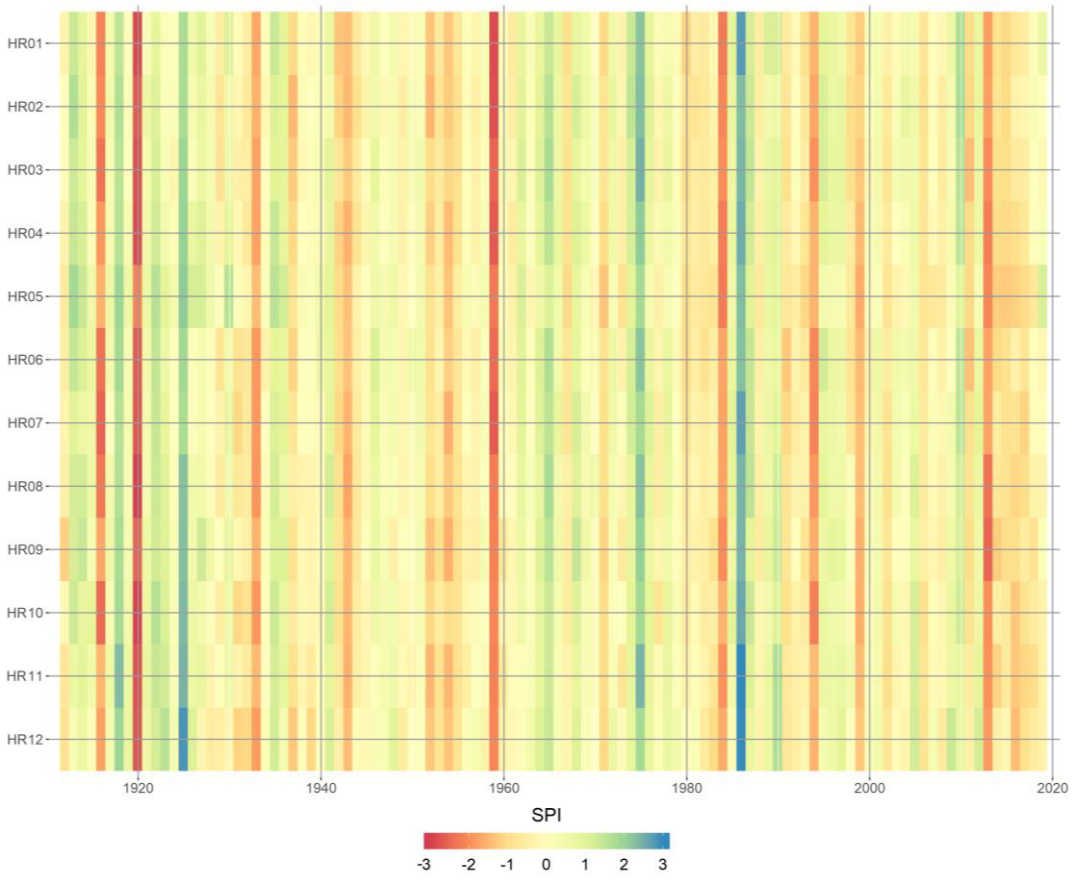

Source: Prepared by the author

The analysis of the descriptive statistics of drought events (Table 4) showed that the hydrographic regions presented between 22 and 26 drought events over the period 1911 - 2018. In this period, a drought occurs every 4 to 5 years in each hydrographic region in Ceará State, as shown by the average inter-arrival time. In general, in the North, there were more droughts, however, shorter in duration and less severe than in the central and southern regions, where generally fewer droughts happened, but longer lasting and more severe. The longest drought occurred in region 08, aged 10 years, and the most severe in region 11, both located in the central and southern regions. HR08 presents the highest coefficient of variation (CV) for both duration and severity, indicating that this hydrographic region has the highest exposure to extreme droughts. Table 4 also shows that for most hydrographic regions, the current drought is the most severe and prolonged ever recorded.

Table 4: Descriptive statistics of drought events and the variables duration and severity by river basin in the period 1911-2018. In bold, when the current drought event initiated in 2012 is equal to the maximum event in time series.

Region	Nº Drought Events	Inter-Arrival Time	Duration (years)				Severity			
			Max	2012 -2018 drought	Mean	CV	Max	2012 -2018 drought	Mean	CV
HR01	25	4.32	6	5	2.08	0.71	**5.10**	**5.10**	1.69	0.91
HR02	26	4.15	6	5	2.00	0.85	5.06	4.27	1.65	0.93
HR03	26	4.15	6	5	2.00	0.82	**5.11**	**5.11**	1.64	0.91
HR04	25	4.32	**6**	**6**	2.04	0.74	**6.01**	**6.01**	1.73	0.95
HR05	24	4.5	**6**	**6**	2.04	0.73	**7.47**	**7.47**	1.85	0.95
HR06	26	4.15	6	5	2.00	0.85	**4.85**	**4.85**	1.69	0.93
HR07	26	4.15	**7**	**7**	1.96	0.82	**5.38**	**5.38**	1.62	0.98
HR08	22	4.91	10	7	2.64	0.90	**6.76**	**6.76**	1.92	1.01
HR09	22	4.91	**6**	**6**	2.36	0.77	**7.07**	**7.07**	1.99	0.91
HR010	23	4.7	**7**	**7**	2.39	0.76	**6.24**	**6.24**	1.85	0.89
HR011	23	4.7	**7**	**7**	2.43	0.71	**7.54**	**7.54**	1.85	0.97
HR012	23	4.7	**7**	**7**	2.43	0.79	**5.88**	**5.88**	1.83	0.94

Source: Prepared by the author

Although this analysis indicated that the 12 hydrographic regions of Ceará State have similar univariate descriptive statistics, the dependence structure between modeled variables dictates the joint behavior that is the object of analysis in this paper. To be able to model the joint distribution, the construction of the marginal distribution approach was used. Using the AIC as decision criteria to choose best-fit distributions, the duration series were best modeled by Log-normal distribution, while an Exponential distribution better represented the severity series.

Figure 16 shows the scatterplot of drought severity and duration. The 2012-2018 drought is one of the most adverse events ever recorded for most hydrographic regions, being compared to the droughts of 1951-1956 and 1978-1983. The dependence structure of drought duration and severity presented a tendency to become narrowly correlated with the increase of the values showing an upper tail correlation, Figure 7. Thus, a simple linear regression model hardly models this kind of asymmetric correlation. Copula functions, however, can meet this type of dependence structure. The drought initiated in 2012 is plotted in red. This analysis agrees with the one presented in Table 4, putting this event as one of the most outrageous ever recorded for all the hydrographic regions, which associated with population growth, increased water consumption and the reactive measures taken may explain the massive impacts caused by this drought.

Figure 16: Scatterplot of duration D and severity S of the recorded droughts by hydrographic region. In solid red, the drought with onset in 2012 and highlighted are the periods of the most extreme events.

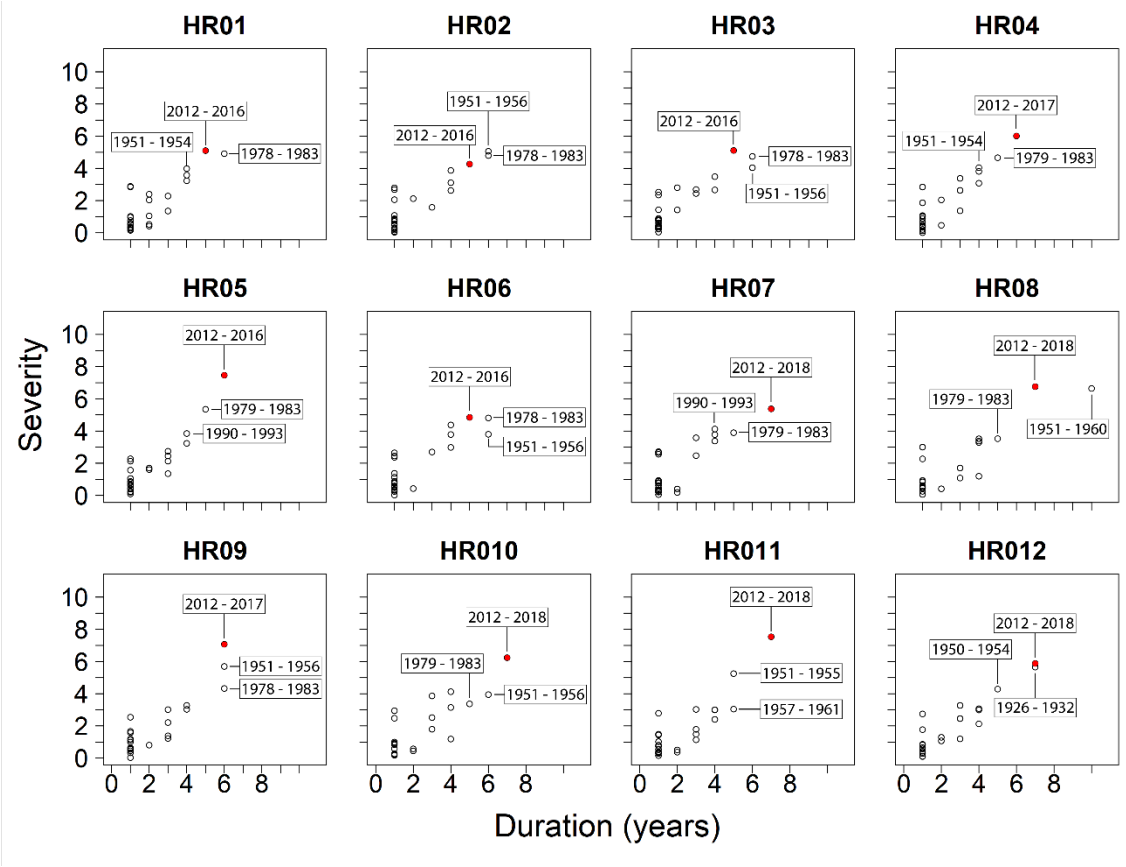

Source: Prepared by the author

By knowing the marginal distributions, the copula functions could be fitted to the data. The Survival Clayton (180º rotated Clayton) and Gumbel, both asymmetric Archimedean copulas, were chosen. Table 5 shows the marginal distribution function, the copula functions, their respective parameter, and the Kendall's Tau correlation coefficient (τ) for each hydrographic region. The moderate τ values show that the founded duration and severity are not highly correlated. One possible reason for this is that the drought threshold equals zero, which selected a high number of droughts that lasted only one year. The asymmetric behavior of drought characteristics provided by this threshold is still able to be modeled by taking advantage of copula capabilities to model tail dependence. Also, this threshold is still adequate as it incorporates the impacts of drought enhancement and recovery. This moderate correlation additionally shows the importance of doing a multivariate analysis as drought duration does not necessarily indicate extreme severity.

Table 5: Marginal distribution functions and Copula functions (associated parameters).

Hydrographic Region	Duration	Severity	Copula
HR01	Log-normal ($\mu = 0.53, \sigma = 0.61$)	Exponential ($\lambda = 0.59$)	Gumbel ($\theta = 2.26, \tau = 0.56$)
HR02	Log-normal ($\mu = 0.43, \sigma = 0.67$)	Exponential ($\lambda = 0.61$)	Survival Clayton ($\theta = 1.78, \tau = 0.47$)
HR03	Log-normal ($\mu = 0.44, \sigma = 0.65$)	Exponential ($\lambda = 0.61$)	Gumbel ($\theta = 2.38, \tau = 0.58$)
HR04	Log-normal ($\mu = 0.49, \sigma = 0.64$)	Exponential ($\lambda = 0.58$)	Survival Clayton ($\theta = 2.56, \tau = 0.56$)
HR05	Log-normal ($\mu = 0.50, \sigma = 0.63$)	Exponential ($\lambda = 0.54$)	Survival Clayton ($\theta = 2.28, \tau = 0.56$)
HR06	Log-normal ($\mu = 0.43, \sigma = 0.67$)	Exponential ($\lambda = 0.59$)	Survival Clayton ($\theta = 1.70, \tau = 0.46$)
HR07	Log-normal ($\mu = 0.43, \sigma = 0.64$)	Exponential ($\lambda = 0.62$)	Survival Clayton ($\theta = 1.56, \tau = 0.44$)
HR08	Log-normal ($\mu = 0.65, \sigma = 0.77$)	Exponential ($\lambda = 0.52$)	Survival Clayton ($\theta = 2.32, \tau = 0.54$)
HR09	Log-normal ($\mu = 0.60, \sigma = 0.7$)	Exponential ($\lambda = 0.50$)	Survival Clayton ($\theta = 2.33, \tau = 0.54$)
HR010	Log-normal ($\mu = 0.62, \sigma = 0.70$)	Exponential ($\lambda = 0.54$)	Survival Clayton ($\theta = 1.90, \tau = 0.49$)
HR011	Log-normal ($\mu = 0.66, \sigma = 0.68$)	Exponential ($\lambda = 0.54$)	Survival Clayton ($\theta = 2.23, \tau = 0.53$)
HR012	Log-normal ($\mu = 0.62, \sigma = 0.71$)	Exponential ($\lambda = 0.55$)	Survival Clayton ($\theta = 3.20, \tau = 0.62$)

Source: Prepared by the author

4.5.2 Frequency Analysis

As stated by Haan (2002) (HAAN, 2002)in order to perform frequency analysis, primarily is necessary to check for independency and stationarity of the SPI time series. The independency was achieved by the discretization of the $SPI12$ into $SPI12_{DEC}$ as discussed in section 4.2. Figure 17 shows the autocorrelation to the time series of $SPI12$ and $SPI12_{DEC}$ for the HR04 as an example. The $SPI12$ time series presented strong serial dependence; i.e. values at some time t are statistically dependent to other lagged value, due to the moving window used to compute $SPI12$ values. The discretization performed by using $SPI12_{DEC}$ time series provided the required independency to perform frequency analysis.

The Mann-Kendall (MK) test (MANN, 1945; KENDALL, 1975) was used to detect the trends in $SPI12_{DEC}$ time series for the hydrographic regions, which is commonly used in hydrology and meteorology (PAN; CHEN; LIU, 2018). The null hypothesis of no trend was tested against the alternative hypothesis of monotonic trend (not shown). From the 12

hydrographic regions tested, only 2, HR05 and HR09, presented statistically significant downward trend at a significance level of 0.05 in the $SPI12_{DEC}$ time series. Therefore, for those regions the return period can be expected to be overestimated, which means that more frequent events can happen. However, those regions have smaller population density and do not contribute to the water transfer systems that provide water to coastal areas with higher population densities.

Figure 17: The differences between autocorrelation of time series of SPI12 and the discretized $SPI12_{dec}$ for HR04. The SPI12 time series presented strong autocorrelation due to the moving window used to compute its values.

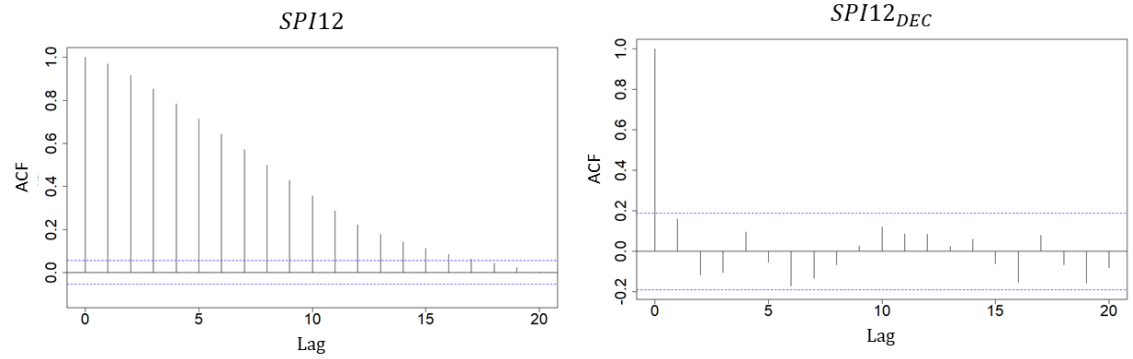

Source: Prepared by the author

Once the considerations to perform frequency analysis are analyzed, the joint distribution function modeled based on the marginals and using copula functions can calculate the return period as indicated by equations 7 and 8. Figure 18 presents return periods for the hydrographic regions for both the "and" and "or" cases. The return periods are presented in the form of contour lines. Different combinations of drought duration and severities can provide the same value for the return period. In the "or" case, those contour lines do not cross the axes, while the "and" cases are bounded by horizontal and vertical axes. It can be seen that "and" cases have higher return periods than the "or" ones, as the first analysis is more restrictive than the second. The information provided by Figure 9 can also specify the return period of a given event by providing its duration and severity. This functionality enables its use in proactive drought plans as the return period of any given drought can easily be found by providing the associated duration and severity. The 2012 event is highlighted in red. Most of the drought events that occurred in all hydrographic regions has a return period below the 64-year isoline. More extreme events, such as 1930 – 1933, 1941 – 1943, 1951 – 1956, 1979 – 1983 and 1990 – 1993, in addition to the 2012 – 2018 event have a longer return period.

Table 6 summarizes the information from return period for univariate, duration and severity, and multivariate, "or" and "and" cases for these droughts and rank those return periods with the set of events recorded. The comparison between univariate return periods (T_D and T_S) of the 2012-2018 drought for all analyzed regions presented no clear pattern of which one presents the highest values. For HR05, HR08, HR09, and HR11, hydrographic regions located in South, Central and Southern regions, $T_S > T_D$, for the others $T_D > T_S$.

It is important to observe that compound events must satisfy following inequalities: $T_{D\text{or}S} < \min(T_D, T_S)$, i.e. the compound return period for the "or" case must be inferior to the minimum of univariate return period of those drought characteristics. As it is a more permissive event, only one of the two conditions must be satisfied. Also, $T_{D\&S} > \max(T_D, T_S)$ implies that the compound return period for the "and" case must be superior to the maximum of the univariate return periods. As it is a more restrictive event, both conditions must be satisfied. Therefore, the joint return periods for the "and" cases are consistently higher than the univariate approach. These results indicate the necessity to consider the joint relationship between drought characteristics to real represents its recurrence as the correlation between drought characteristics are proportional to its damage potential. The rank also shown in Chart 1 put the 2012-2018 drought as one of the three highest most exceptional droughts that occurred between 1911 – 2018 for all hydrographic regions. Also, although more extended droughts had occurred in some hydrographic regions, the severity of this drought is highlighted, indicating the importance of multivariate analysis of drought events.

Figure 18: The drought return period of the "or" and "and" cases, i.e. T_DorS and T_(D&S), for each hydrograph region. Contour lines correspond to the return period (years).

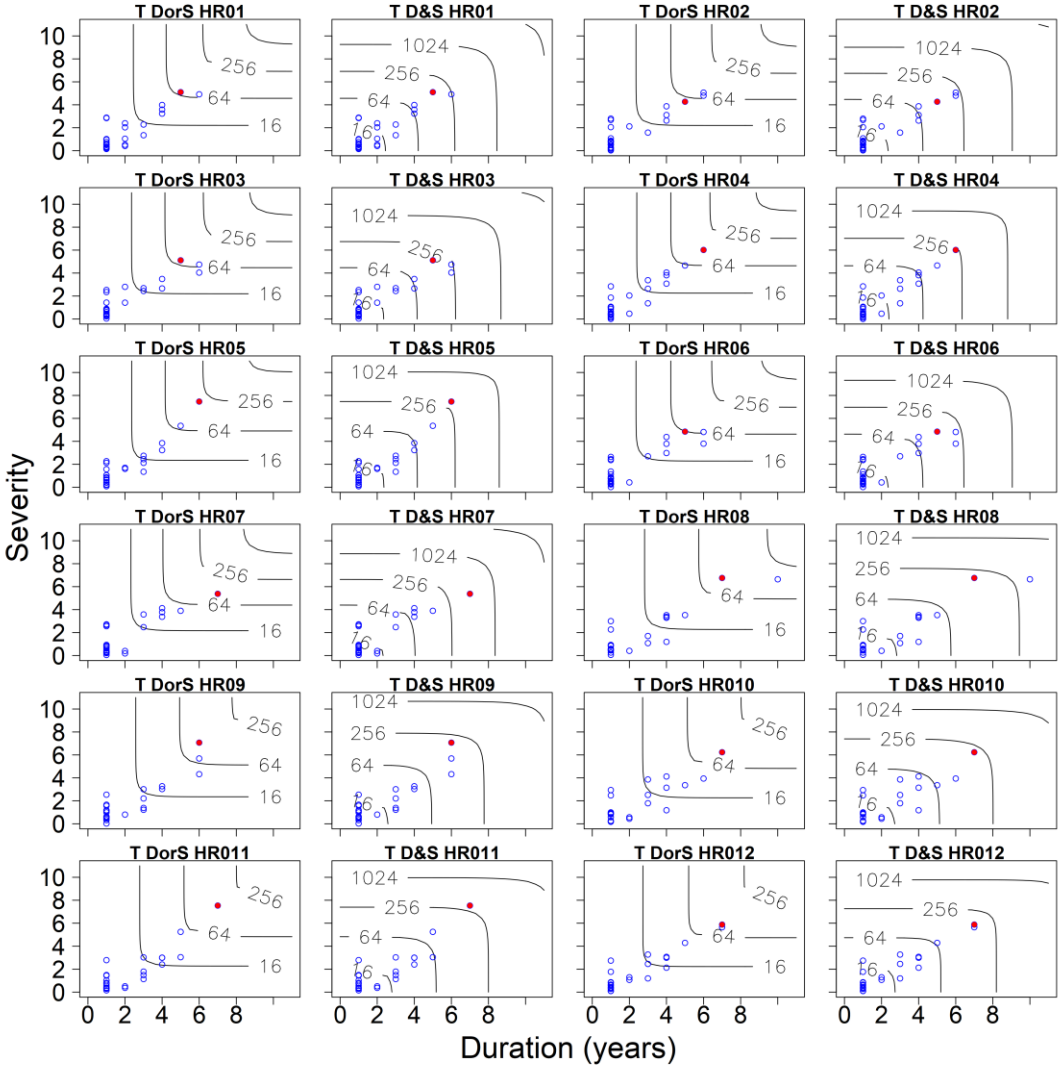

Source: Prepared by the author

Table 6: Description of the 2012 onset drought event for each hydrographic region. The univariate return period (years) of drought duration (T_D) and severity (T_S), and the bivariate T_DorS and T_(D&S) return periods (years).

Hydrographic region	Drought period	T_D	T_S	T_{DorS}	$T_{D\&S}$	Rank in the set of events		
						Duration	Severity	Joint
HR01	2012 - 2016	113	88	72	155	2	1	2
HR02	2012 - 2016	106	56	52	124	3	3	3
HR03	2012 - 2016	115	94	77	157	3	1	3
HR04	2012 - 2017	206	141	131	234	1	1	1
HR05	2012 - 2017	223	254	191	313	1	1	1
HR06	2012 - 2016	106	73	63	136	3	1	3
HR07	2012 - 2018	465	117	115	499	1	1	1
HR08	2012 - 2018	106	165	98	188	2	1	2
HR09	2012 - 2017	111	168	102	193	1	1	1
HR010	2012 - 2018	161	136	112	215	1	1	1
HR011	2012 - 2018	160	275	150	309	1	1	1
HR012	2012 - 2018	152	119	110	171	1	1	1

Source: Prepared by the author

Drought risk for any region is a product of the region's exposure to a predefined event and the vulnerability of society to this event (WILHITE, 2005). The return period can express the drought exposure as it incorporates the probability of occurrence of an event. Therefore, it is interesting to analyze the exposure to drought hazard at the different hydrographic regions of an event with similar characteristics of the 2012-2018 drought. Thus, the return period of an event with average characteristics of the analyzed drought in the 12 regions (duration equals 6 years and severity equals 6) was calculated, Figure 19. It shows a clear distinction between North regions with Central and South areas. The south is the region with more susceptible to severe and persistent drought as the 2012-2018 event and it is where the main reservoirs are located. The North is less affected by long drought as it is affected by intra-annual variability caused by oceanity conditions. Also, it is less dependent to ITCZ position as even a slight modification of its climatological position can still provide precipitation to the area. On the contrary, precipitation in the Central and Southern regions are more dependent on ITCZ, and consequently, to IHTAG modulation.

Figure 19: Exposure to drought hazard of an event with average characteristics of the 2012-2018 event. The lower the return period the higher the exposure to drought hazard.

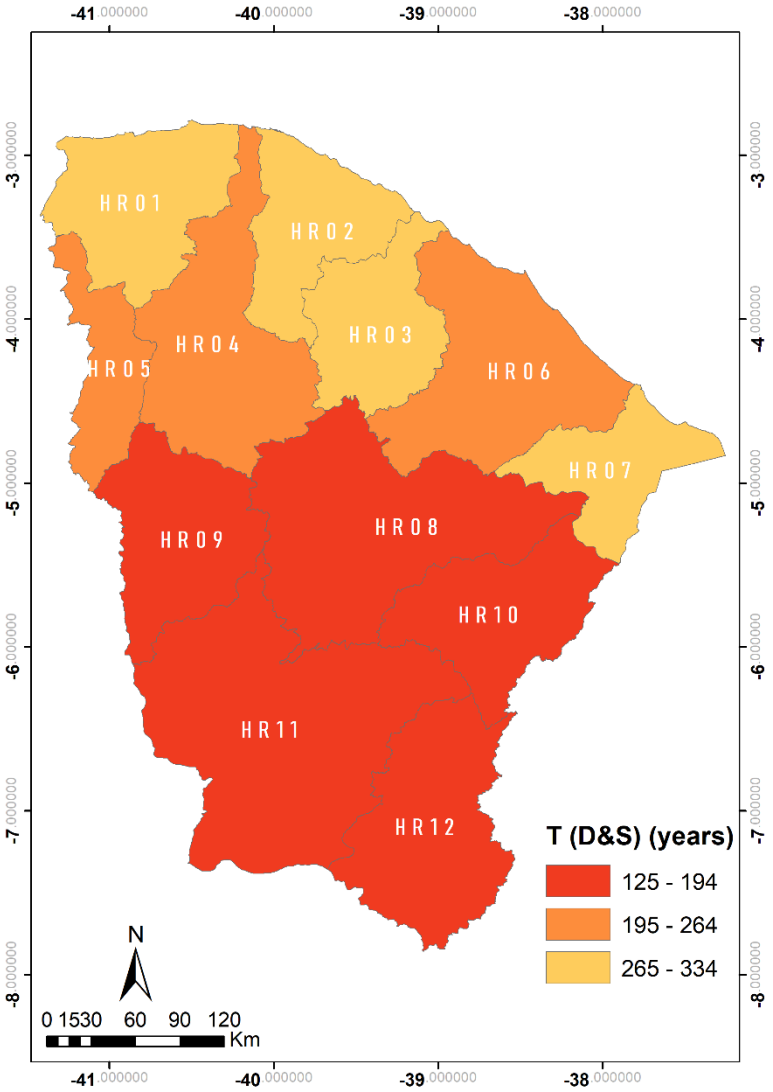

Source: Prepared by the author

The presented drought frequency analysis indicates the recurrence of an event with magnitude equal to or greater than the one of the 2012-2018 drought for each hydrographic region in Ceará. It indicates that the joint return period is always greater than the univariate approach. This result indicates the necessity to consider the joint characteristics to understand the real exceptionality of extreme events. Another impressive result was that the Northern areas are less susceptible to exceptional droughts, such as the analyzed one. As the main reservoir storage capacity is localized in Central and South regions, it indicates that the Ceará's water reserves are concentrated in the more vulnerable areas to jointly occurrence of prolonged and severe droughts.

4.6 Discussions and Conclusions

The Northeast of Brazil (NEB) has experienced one of its worst droughts ever recorded, from 2012 to 2018. The leading causes were associated with anomalies in SST at equatorial Pacific and Atlantic oceans caused by low frequency, decadal, and high frequency, within year to years variability modes. The serial combination and association of the climatic phenomenon (i.e. La Niña with the cooling occurring at central Pacific, the prevalence of tropical North Atlantic warming, AMO/PDO low-frequency modulations and El Niño), influenced the ITCZ and the Walker Circulation Cell to inhibit the occurrence of precipitation over NNEB. In Ceará State the accumulated rainfall deficit of the 2012 – 2018 drought was 1225 mm, 1.5 times the yearly climatological rainfall.

NEB is known as a drought-prone region with considerable adaptive capacity, both in terms of increased water infrastructure and management. This resilience is based on learnt experiences, acquired from its drought antecedents. This capacity has recently been questioned due to the magnitude of the current drought and the emergency measures that were needed to cope with it. Those measures helped to mitigate social damage that historically occurred in the most extreme droughts, such as human losses and massive migration (CAMPOS, 2015); however, they were taken under a “reactive” management paradigm, which could not handle some of the higher economic losses suffered by the Ceará State.

We believe that proactive drought management can deal with some of the issues not addressed by its “reactive” predecessor. As stated by Gutiérrez et al (GUTIÉRREZ *et al.*, 2014), this drought was the trigger needed to start a discussion towards proactive drought management in NEB. Institutional relations between different public bodies and forums discussing the topic of drought have improved their performance by establishing monitoring processes and by incorporating active memory to elaborate proactive drought plans. To preserve this memory, frequency analysis of past events can be used in proactive drought plans as it enables a scientific identification of drought recurrence, which can be used as a preparation tool for mitigation of future droughts.

The univariate approach to calculate drought return period has traditionally dominated the drought frequency analysis and it is a common practice in Brazil (AWANGE; MPELASOKA; GONCALVES, 2016; BRITO *et al.*, 2018; CUNHA *et al.*, 2018; MARENGO *et al.*, 2017; MARTINS *et al.*, 2018; PORTELA *et al.*, 2015a). Martins et al. (2018) estimated the return period of the 2012-2016 drought that occurred on the most significant water system in NEB, São Francisco River Basin, as 135 years using the univariate approach. However, the

impact caused by a drought event may vary according to its duration and severity. Although these characteristics are correlated, their associated behavior can provide synergetic impacts that could be missed by a univariate approach.

The framework of bivariate frequency analyses can represent the exceptionality of drought events as the correlation between droughts characteristics are proportional to its damage potential, i.e. the negative impacts associated with a short drought but extremely severe may be stronger than another longer but less severe drought. Copula functions were useful to accurately model the dependence structure of drought characteristics as they presented different marginal distributions and due to observed upper tail dependence in the joint behavior. Thus, Gumbel and Survival Clayton asymmetric Archimedean copulas were chosen.

The hydrographic region was chosen as the planning scale in line with Brazilian water law that states it as the territorial management unit. There are significant benefits to use this scale, including better representation of socio-economic and environmental relationship existent between water supply and demand (e.g. precipitation, runoff, water reserves accumulated in reservoirs, associated demands for agricultural and urban uses, etc.). Also, it benefits from the capability to consolidate information that could otherwise randomly fluctuate in a point-based analysis.

The 2012-2018 drought in Ceará State had the highest mean bivariate return period ever recorded, presenting long persistence, substantial severity and spatial coverage. The mean joint return period, considering the "and" case, was 240 years (maximum of 499 years in HR05). The mean univariate return period of the 2012-2018 droughts for the 12 hydrographic regions located in Ceará State was 169 years for the duration (maximum of 465 years in HR07), and 141 years for drought severity (maximum of 275 years in HR11). The bivariate analysis consistently presented higher values than the univariate, indicating the necessity to consider the joint behaviors to avoid underestimation of drought impacts. Similar characteristics to this drought were presented earlier in the 1951-1956 and 1978-1983 events for some regions, with a mean joint return period of 145 and 135 years, respectively.

The severity of this drought was influenced by the first two years, 2012 and 2013, added to the long final sequence; Although the devastating impacts suffered from the current drought, having started with the most severe part of the drought served as a critical warning. This opportunity increased the capability to mitigate drought effects in the area, but early warning and monitoring systems must be prepared to anticipate actions in future droughts that may not start with the same severity. Most of the other events presented a bivariate return period of inferior to 64 years for all hydrographic regions. Ceará State is more likely to present another

drought with the same characteristics as the one here analyzed than California to a drought that occurred over the same period, 2012-2015, which has a return period estimated in 1400 years by Kwon and Lall (2016). This fact reflects the extreme variability and frequent drought recurrence existent in the region, showing the necessity to proper cope drought events with state-of-art techniques.

Knowing the exposure to drought is fundamental when planning measures to mitigate drought. The analysis presented here can inform decision-makers as to which areas are more susceptible to the occurrence of future droughts. This analysis indicated that the northern region of Ceará State is less susceptible to severe and persistent drought, such as the 2012-2018 event. Possible explanations are the intra-annual variability caused by proximity to the ocean. Another fact is that the higher latitudes are less impacted by ITCZ positioned north of its climatological position. Therefore, in the Central and Southern regions, which concentrate 74% of State's potential storage capacity, an extreme event can be more recurrent and water security can be compromised. Such analysis can be incorporated in drought plans to detect more exposed areas to drought. A limitation of the present approach is that it reflects meteorological drought exposure and does not consider water transfer between hydrographic regions, which may cause different drought risk depending on where the supply is provided.

Classical approaches such as univariate analysis underestimates events frequency, others cannot be associated with impacts if analyzed at inappropriate scales. This paper has argued that considering simultaneously drought duration and severity at a useful scale improves risk assessment. The presented framework has shown that hydrographic region scale is adequate to couple drought impacts with the awareness given by bivariate analysis. Copula functions were vital to jointly modeling drought characteristics as other models cannot cope with their asymmetric behavior. This framework can be replicated in drought plans for other regions, serving as a tool to previously prepare measures adapted to the risk exposure in each region. Further investigation should analyze the scale that best represents specific impacts such as reservoir operation, water transfer between regions, and urban and agricultural supplies. Also, efforts should be made to understand the influence of events with different expected intervals with potential impacts on reservoirs levels, streamflow volumes and ecosystem thresholds. There are several changes that need to be made in order to mitigate drought impacts and transforming statistical information into useful information for decision-makers is one of them.

5 THE DYNAMICS OF SPATIO-TEMPORAL DROUGHTS IN NORTHEAST BRAZIL

5.1 Introduction

Drought is a natural phenomenon associated with climate variability, characterized as a period when water availability is lower than the average values for the region. Due to this difficulty in monitoring the drought onset, a better understanding of the spatio-temporal distribution of drought and its evolution characteristics is important for proactive drought management (LIU *et al.*, 2018).

Drought monitoring has advanced and many different methods to monitor drought have been proposed. For example, different drought index, such as the Palmer Drought Severity Index (PDSI) (PALMER, 1965), Standardized Precipitation Index (SPI) (MCKEE; DOESKEN; KLEIST, 1993), and Standardized Precipitation Evapotranspiration Index (SPEI) (VICENTE-SERRANO; BEGUERÍA; LÓPEZ-MORENO, 2010). Despite the drought index used, drought characteristics can be identified from historical time series data based on the run theory (YEVJEVICH V, 1967). By using run theory, each drought event can be analyzed separately from the original time series. This technique gained popularity in drought analysis as it allows univariate and multivariate frequency analysis, and comparisons between different drought characteristics (ESPINOSA *et al.*, 2019; LIU *et al.*, 2019a; SHIAU, 2006).

The disadvantages of these analysis based on run theory is that it considers only the time component of the drought. As droughts are a widespread phenomenon, its analysis should consider the spatial component to better cope with real impacts. The first studies that considered the influence of area on drought analysis considered drought as a phenomenon with a fixed spatial extent and regionalized the precipitation data using Thiessen polygons or homogenous regions using statistical clusterization such as Principal Component Analysis (PCA) or K-means (PORTELA *et al.*, 2015a; VICENTE-SERRANO, 2006; ZHOU; LIU; LIU, 2019). However, these approaches are limited as meteorological droughts do not respect physical, political or homogenous borders.

Currently, the characteristics of droughts in space dimensions have attracted more attention. Starting from the concept of depth-area-duration analysis, (2005) constructed a series of severity-area-duration (SAD) curves to relate the areal extent of each historical drought to its severity. To better understand drought the evolution process of droughts in space and time, simultaneously, Lloyd-Hughes (2012) developed a 3-dimensional (longitude, latitude, and time) method based on the spatial clustering algorithm proposed by Andreadis et al. (2005). Herrera-

Estrada et al. (2017) presented an analysis of how drought moves in time and space and Diaz et al (2019) tracked drought centroid to understand drought dynamics. Following these studies, 3D drought analysis that tracks spatio-temporal development of droughts is demonstrating a promising area for improvement for better drought monitoring and early warning (LUO *et al.*, 2022; XU *et al.*, 2015b; ZHOU *et al.*, 2021).

These studies have advanced the spatio-temporal understanding of droughts. However, the studies fall into the following dilemma of complexity. To reduce the dimensionality, ignoring other faces of the problem; or to over-complexify, making it difficult for managers and decision-makers to analyze. For example, Wen et al. (2020) used a 3D clustering algorithm to analyze a large number of drought characteristics (drought duration, drought area, drought mass, drought volume, drought density, drought aggregation index, and longitude and latitude coordinates of centroid). Also, Herrera-Estrada and Diffenbaugh (2020) used seven different drought characteristics to characterize landfalling droughts from a 3D analysis, such as cluster area, growth rates, intensities, intensification, duration, distance, and maximum extent. Many drought characteristics analyzed makes it difficult for the decision-maker to take early action due to the high amount of information. Furthermore, the understanding of how characteristics accelerate and decelerate in time and space has not yet been analyzed. Previous analyses used to identify droughts in the 3 dimensions and analyze the direction and trajectory of migration (DIAZ *et al.*, 2019, 2020; HERRERA-ESTRADA; DIFFENBAUGH, 2020; ZHOU; LIU; LIU, 2019). Understanding how each event evolutes in terms of its spatio-temporal characteristics is important to improve understanding of the evolution of droughts.

In recent years, Brazil has been advancing its official drought monitor, which uses participatory information to diagnose where the drought areas are located (MARTINS *et al.*, 2015). However, little spatiotemporal analysis has been made and there is a need for more research on how to use spatiotemporal analysis to improve drought characterization and management in Northeast Brazil (Brito et al., 2021).

The present work aims to fill this gap by analyzing the spatiotemporal patterns and dynamics of drought events in Northeast Brazil. The study area is divided in two main analysis. The first analysis how each drought event evolutes according to the growth curve, growth rate and acceleration. The second aims to understand mean characteristics of drought events according to the place its centroid was originated. The results of this study will provide valuable information for drought monitoring, forecasting, and management in Northeast Brazil, and will contribute to the advancement of the field of spatiotemporal analysis of drought.

5.2 Materials and methods

This paper is divided into in two phases, drought spatio-temporal definition and drought spatio-temporal analysis. The definition has four steps: data processing, drought definition in one dimension (1D), in two dimensions (2D) and in three dimensions (3D). The analysis is divided into two parts. The first focuses on observing the dynamics of drought evolution inside the drought event, and the second focuses on searching for patterns and relationship between mean drought characteristics.

The first step for drought spatio-temporal definition is data processing is the first step. It requires gridded data to support the spatial analysis. Meteorological drought is often classified as below-average precipitation for a given area. As precipitation is the most worldwide climatic information, we chose this variable to make further analysis.

This study was performed in Northeast Brazil, which is known as a drought-prone area that faces recurrent multi-year droughts. We use monthly total precipitation data from the University of East Anglia/Climate Research Unit (CRU), CRU TS v 4.05 at 0.5° x 0.5° resolution from 1950 – 2018 (HARRIS *et al.*, 2020). The CRU TS v 4.05 time series has been available since 1901, but we chose only to use data from the mid-20th century onwards as the region did not have many rain gauges at the begging of the century.

The second step is to define drought. The well-known Standardized Precipitation Index (SPI) (MCKEE; DOESKEN; KLEIST, 1993) was used as it is the drought index recommended by the World Meteorological Organization. SPI has the advantages of simplicity as it uses only precipitation, presents standardized information, making it easy to compare its values across different regions, and ability to provide information in different timescales, being able to be used as proxies for agricultural, hydrological, and socioeconomic droughts using different time scales (HAYES; ALVORD; LOWREY, 2007; PONTES FILHO *et al.*, 2019).

The perception of drought varies according to users' specific interests, making it impractical to have a single completely adequate definition (PALMER, 1965). Users perceive droughts differently as the water shortage can affect them at different times. Shorter time scales, such as 1 to 3 months, can be more critical to agricultural users that do not irrigate their cultures. More extended periods, such as 6 to 12 months, can relate to hydrological impacts on urban and irrigation water supplies. Thus, the aggregation period and the threshold chosen can strongly impact drought analysis.

The identification of spatial-temporal drought is the third step. It involves dividing interconnected grids into clusters and extracting continuous grids at both spatial and temporal

scales to construct a three-dimensional (longitude, latitude, and time) drought structure. The algorithm uses the following sequence.

The gridded precipitation data is converted to SPI values using the chosen time-scale. We analyzed SPI for the 3, 6, 12 and 24 time-scale. Run theory is applied for each grid cell as the traditional 1D analysis. It identifies the periods when the drought index is below the drought threshold. The values are converted into a binary format (0/1), assigning whether it is (1) or not (0) under drought conditions.

For the 2D analysis, the algorithm scans all grid cells below the drought threshold for each time or snapshot. When the first cell value equals "1", indicating that the grid is under drought, the algorithm creates a drought event and searches for the 9x9-1 neighbors, excluding the center grid. If a neighbor cell also has the "1" value, it is included in the same drought event, forming a cluster. A new cluster event is created if another cell in the same snapshot has the "1" value, but it is not contiguous to any previous cluster. A minimum initial area of 1.6% of the total is required to analyze more regional events (XU *et al.*, 2015b).

The 3D analysis connects spatial clusters through time. We link clusters with overlapping grid cells between time t and time $t+1$. An ID is assigned to each spatial cluster. If two or more different clusters are merged sometime after their formation, the ID of the oldest is conserved for all clusters (Figure 20). To connect a cluster in time t with $t+1$, a minimum overlap area is required to eliminate ambiguous drought events. A threshold of overlap area of 1.6% was chosen in this study following Li et al. (2020).

A sensitive analysis of the temporal and spatial parameters used here, the time-scales used in the SPI and the minimum initial area and minimum overlap area, is provided to understand how these parameters can affect drought characterization.

An important consideration in the proposed algorithm is that if a cluster splits into two or more clusters, they all keep the same initial ID. This is a modification of the algorithm used by Diaz et al. (2019) and Herrera-Estrada et al. (2017), whose analysis conserved only the areas of the largest clusters. We chose this path as droughts can be onset in different regions at the same time due to different precipitation mechanisms that affect each region. Therefore, conserving only the largest area can cause an artificial interruption of an event that still occurs or even the complete ignoration of an event that happened simultaneously but in different regions.

Figure 20: Definition of spatial-temporal drought events by the three-dimensional clustering algorithm. Panel (a) shows three cluster events at time t=1. Panel (b) shows two clusters at t=2.

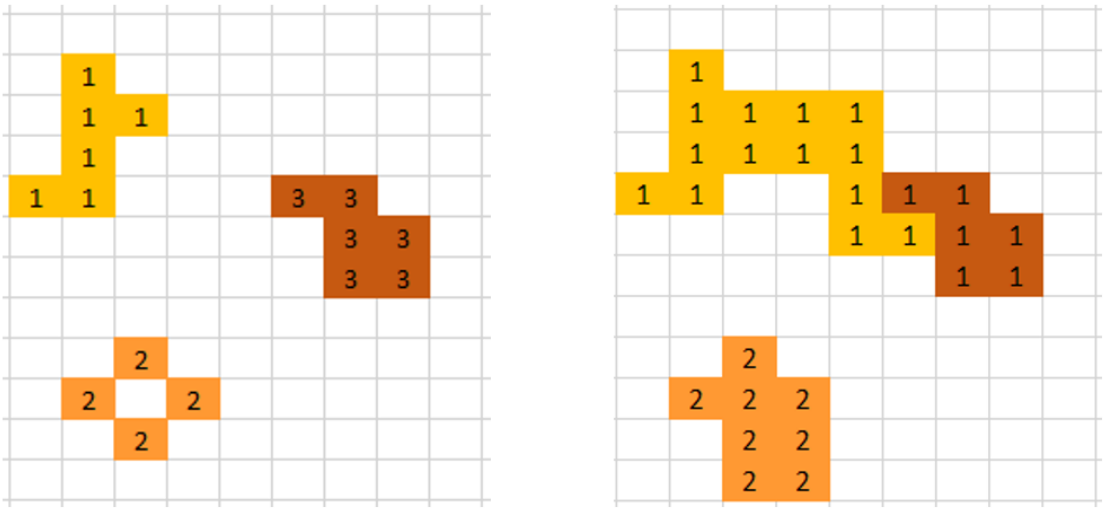

Source: Prepared by the author

After the clusters are defined, we divide the analysis of drought characteristics in two parts. The first analysis is to understand drought dynamics during each event. The second is to understand drought patterns of average characteristics.

For the first part, three drought characteristics were studied: centroid, severity, and area. Centroid is the geographic coordinates of the mass center of the affected area. The severity shows the sum of severity at all gridded cells affected. The spatial extent informs how widespread the event was. Drought duration was not chosen to be analyzed since it is present in all the other three drought characteristics.

To understand how the drought event evolves we propose to analyze droughts using three evolution measures: Growth curve, growth rate and acceleration analysis. The growth curve is the cumulative sum of the characteristic value. The growth rate is the first derivative and shows the instantaneous value at a given moment. Acceleration is the second derivative and informs whether the characteristic is intensifying or not (Table 7). The first application of growth curve, growth rate and acceleration analysis was proposed by Utsunomiya et al (2020) as an effort to monitor COVID-19 spread and is here adapted for understanding drought behavior.

Table 7: Description of measures used in this study to characterize drought.

Characteristic	Evolution Measure	Equation	Description
Centroid	Growth Curve	$d_t = \sum_{i=1}^{t} v_i$	Cumulative distance of the centroid path (km). Where d_t is the centroid growth curve at instant t, and v is the instantaneous centroid velocity.
	Growth Rate	$v_t = dist(C_t, C_{t-1})$	Instantaneous centroid velocity (km/month). Where v_t is the velocity at moment t, C_t is the centroid position in the instant t, and $dist$ is a function that represents distance, in this case we used the Euclidian distance.
	Acceleration	$a_{c,t} = \frac{(v_t - v_{t-1})}{dt}$	The rate of change of the centroid velocity with time (km/month²). Where $a_{c,t}$ is the instantaneous centroid acceleration at instant t, and v is the instantaneous centroid velocity.
Severity	Growth Curve	$M_t = \sum_{i=1}^{t} s_i$	The cumulative sum of the drought index value at the drought cluster ([SPI]). It gives the idea of total magnitude of drought severity s.
	Growth Rate	$s_t = \frac{\sum_{i=1}^{u} SPI_{i,t}}{u}$	Mean of cluster's drought index value at instant t ([SPI]/month). The $SPI_{i,t}$ is the index value at grid cell i and instant t; u is the number of grid cells belonging to the cluster.
	Acceleration	$a_{s,t} = s_t - s_{t-1}$	The rate of change of the severity with time ([SPI]/month2). Where $a_{s,t}$ is the instantaneous severity acceleration at instant t, and s is the instantaneous severity.

Characteristic	Evolution Measure	Equation	Description
Area	Growth Curve	$CumA = \sum_{i=1}^{t} A_i$	The cumulative sum of the drought area A over the time the event persists (km²).
	Growth Rate	$A = \sum_{i=1}^{u} Area_{i,t}$	The drought area at a given moment (km²/month). The $Area_{i,t}$ is the area of each grid cell i and instant t.
	Acceleration	$a_{a,t} = A_t - A_{t-1}$	The rate of change of the drought spatial extent with time (km²/month²). Where $a_{a,t}$ is the instantaneous area acceleration at instant t, and A is the instantaneous area.

Source: Prepared by the author

The second part aims to understand drought patterns and relationship between characteristics. To have this understanding, drought centroid, severity, area ,and duration were analyzed. The centroid of the onset and offset of drought events were taken to investigate the possibility of having an area with higher probability of starting more dangerous drought events. With dangerous we mean events with longer duration, more severe and affecting bigger areas. The study area was divided into seven zones to try to understand if there are regions more prone to more dangerous events (Figure 21). The seven zones were divided to better comprehend drought characteristics at regions influenced by different climatic conditions. The northern part of the study area is predominantly influenced by the Intertropical Convergence Zone (ITCZ), the eastern part is more influenced by southeast trade winds, and the southern part is primarily governed by cold fronts. (COSTA *et al.*, 2018; HASTENRATH, 2012; NOBRE; SHUKLA, 1996; UVO *et al.*, 1998). Due to this divergence, it is important to understand the dynamics of droughts that had their onset influenced by these precipitation mechanisms.

Figure 21: The seven zones selected to analyze drought characteristics.

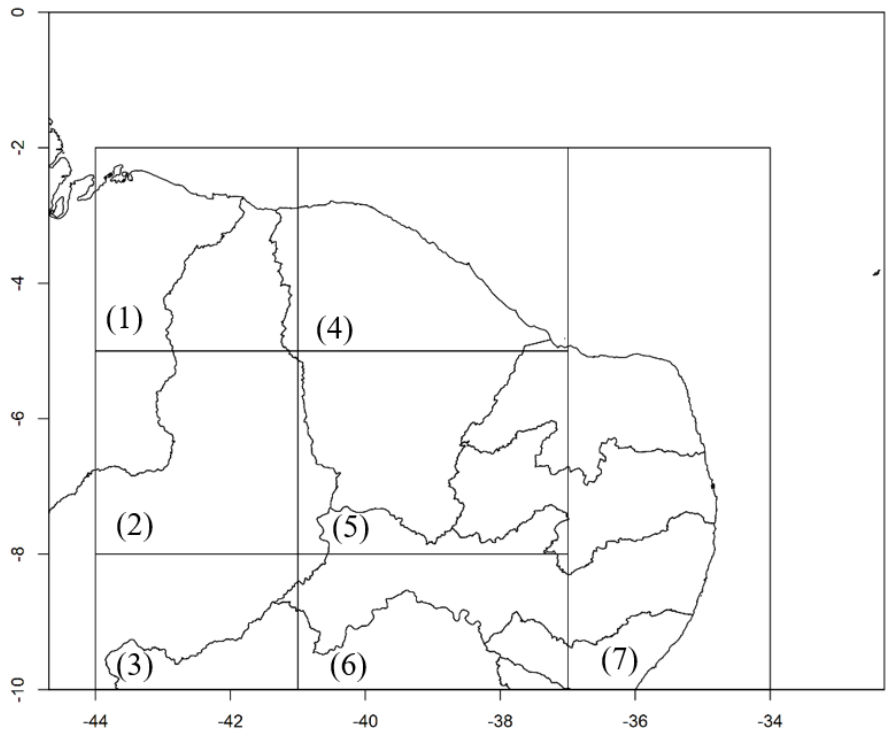

Source: Prepared by the author

5.3 Results

5.3.1 Intra-event analysis of drought dynamics

The drought spatio-temporal analysis of droughts permit understanding where its onset was, how it evolved, the regions where it affected, where it remained the longest. This information is important to decision-makers to create coping measures to deal with future droughts. The 2012-2014 drought event in Northeast Brazil, for instance, is presented in Figure 22 using SPI 12 and threshold -1. To describe Figure 22, we can see that In (a), The gray cells are the ones that do not face drought, while the red cells are the ones under drought. When all the region does not face drought, the region is marked in green. In (b), the red mark is where the drought centroid started and the blue mark is where it finished. The black line tracks the centroid's path. In (c), (d) and (e), the red lines informs the magnitude of the growth curve, growth rate and acceleration evolution measures.

Figure 22: Spatio-temporal analysis of the 2012-2014 drought event in Northeast Brazil using SPI 12, threshold -1.

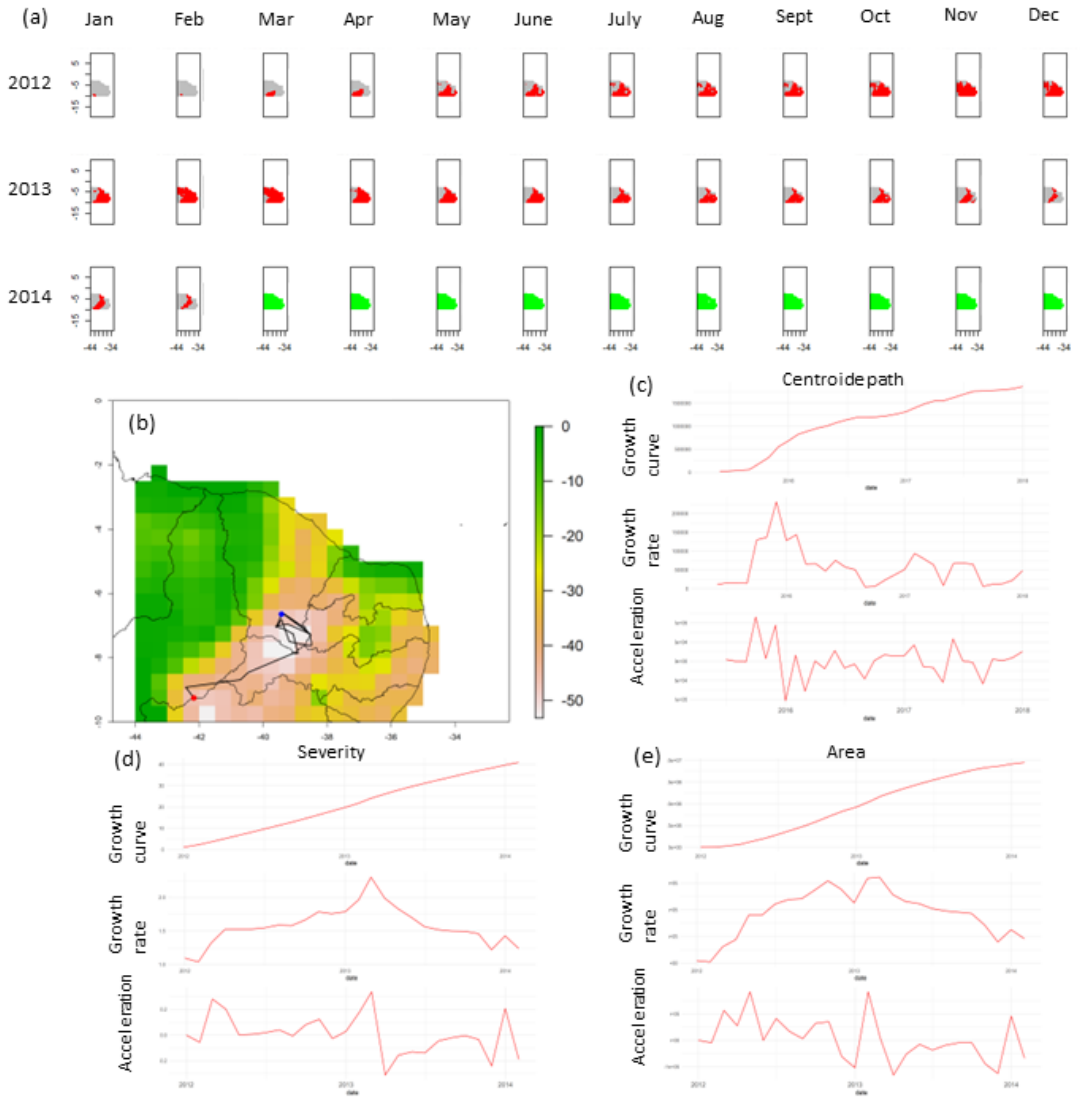

Source: Prepared by the author

The event started in 2012 in the south-west part of the studied region, between the borders of Piaui and Bahia states. During this year, drought expanded in area, affecting almost all the grid cells. By the middle of 2013, the drought reduced its impacted area and the severity. From the centroid path point of view, the drought started by travelling a great distance, but when it reached its maximum extent, its centroid remained stationary in the center of the study area. When the drought lost strength, the centroid remained in this area, as the drought was extinguished from the sides, remaining in the northern, central, and southern portions. The most affected area was the Central and South-West regions, with lower severity in the West. Figure 22 gives an overview of the drought event. It is possible to see the main affected areas and understand how drought evolved in time and space.

Although the information brought by figure 22 is innovative and can give an overview of the drought, the discovery of patterns that can help plan and anticipate new events is only possible when comparing historical events. To do this, the strategy of analyzing average characteristics of events separated by the region of drought initiation was used and will be presented in the next section.

Other important drought events for understanding the spatio-temporal evolution of droughts in the study region are presented as Appendices. The five main events selected were the 1950-1956, 1957-1961, 1980-1984, 2012-2014, and 2015-2018 droughts. These events were selected for their temporal scope, all with more than two years duration, and spatial, and the severity of the events.

The 1950s proved to be a very dry period, with virtually the entire decade featuring drought in some region. In general, all five events analyzed presented a predominance of the centroid by the central region of the study area. Some droughts presented patches of more intense severity in an isolated way, such as the 1950-1956 and 1957-1961 droughts. The others, on the other hand, usually presented warmer regions, such as the 1980-1984 drought that affected the eastern region more, and the 2015-2018 drought, which affected the northeastern region less.

5.3.2 Searching for patterns and relationship between mean drought characteristics

The analysis of drought mean characteristics was started by establishing the drought's onset region. The study area was divided in seven different regions and the mean characteristic of each event was analyzed.

Figure 23 gives an overview of the mean characteristic of each drought event separated by regions. It is possible to see that droughts that its centroid was in region 5 during its onset presents the highest mean duration, severity, and area. The characteristics of droughts from other areas do not present a clear pattern such as the ones from region 5.

Figure 23 also presents a 4D analysis, by showing how droughts characteristics are related to each other in the four dimensions (duration, severity, area, and region of centroid's onset). The severity and duration are in the y and x axes, the size of the bubble is related to the affected area and the color is related to where the region of centroid during its onset. It is clear from this picture that droughts from region 5 present the most important events in terms of duration, severity, and area. These results suggest the drought monitoring at region 5 is

fundamental and higher-level observation should take place for droughts that are onset at this region as they have potential to have more impacts in the region.

Despite the higher average values presented for droughts that was onset at region 5, drought characteristics for this region presented also higher variability. This result may be related to the fact that this area presents strong orographic influence, especially in the South part of this region, which tends to present a different behavior and increase noise in the classification of drought characteristics.

Figure 23: Boxplots of drought duration, area (km²), and severity for droughts in each region of Northeast Brazil using SPI 3. Figure also shows a 4D analysis of duration, severity, area, and region of centroid's onset.

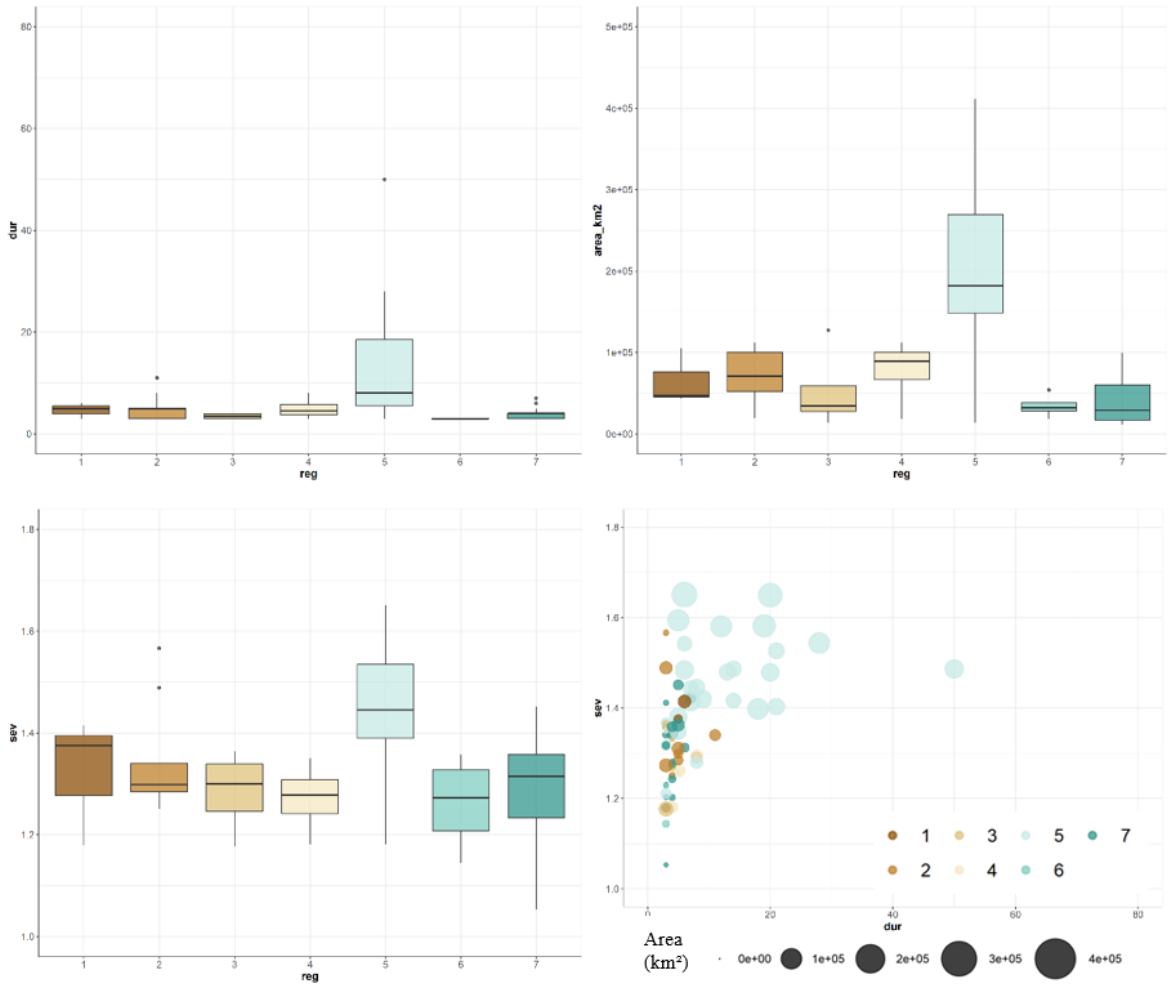

Source: Prepared by the author

The correlations between variables are presented in figure 24. Severity and area present stronger correlation then each characteristic with duration, especially for the lower values. Region 5 shows most drought events, and the events with higher magnitude in every

characteristic, showing that this region is more prone to develop droughts and to develop droughts with higher capacity to impact socio-economic aspects in Northeast Brazil. Therefore, this region should be always well monitored by drought monitor.

Figure 24:Scatter-plot of duration, severity area and region of centroid's onset.

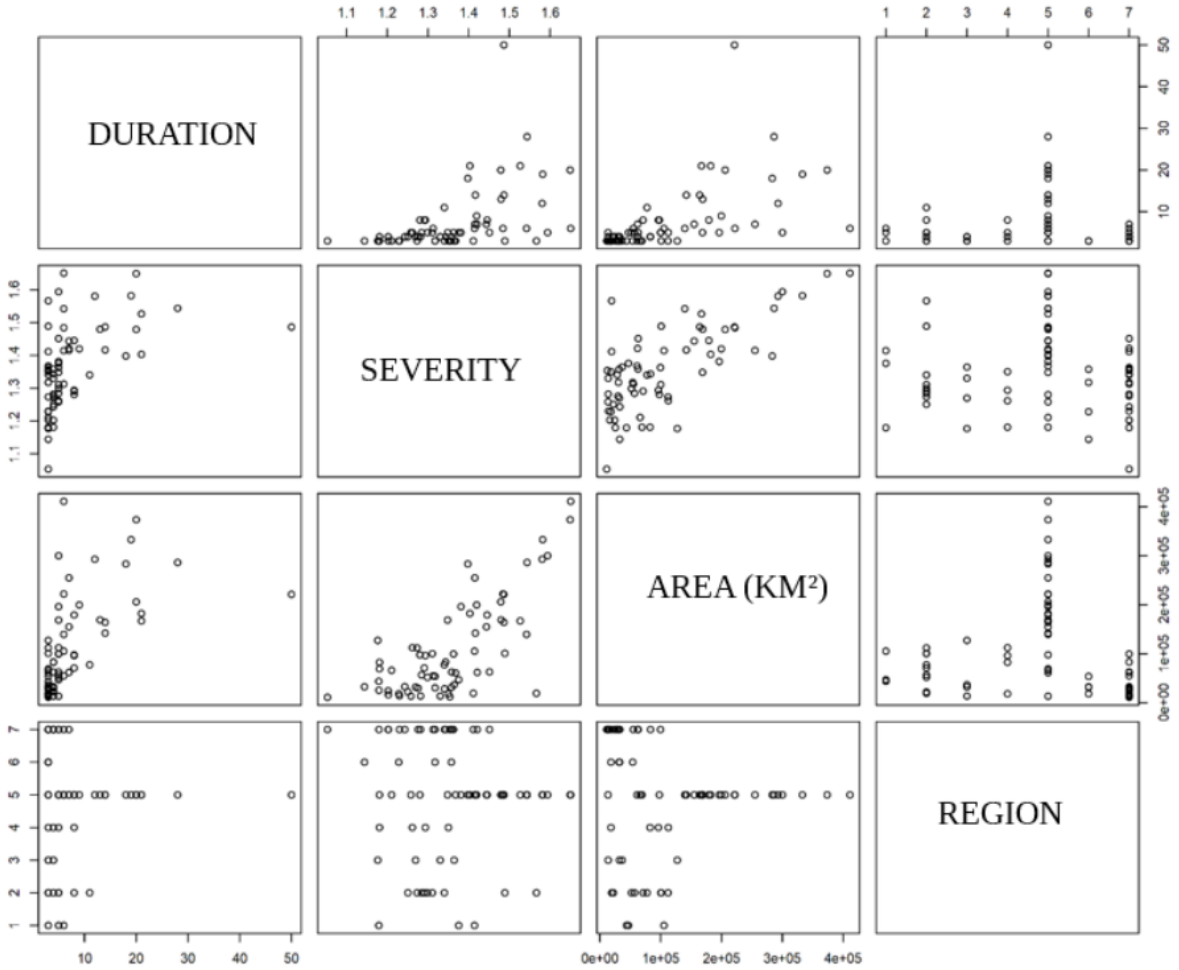

Source: Prepared by the author

5.4 Sensitive analysis

A sensitivity analysis was carried out to investigate the temporal and spatial characteristics of drought. The temporal component was evaluated using different time scales of the Standardized Precipitation Index (SPI) at 3, 6, 12, and 24 months. For the spatial analysis, two parameters were tested, namely, the minimum initial area and the minimum overlap area.

The results for the temporal sensitivity analysis, presented in Figure 25, show that the drought characteristics vary with different SPI time scales. Specifically, drought duration and centroid velocity increase with the time scale. Longer aggregated periods, such as SPI 12 and SPI 24, are associated with prolonged drought events and smaller centroid velocity. Longer

time scales result in less abrupt changes in the time series, making it more difficult for small precipitation events to end a prolonged drought event. Moreover, longer aggregated periods conserve more information, resulting in smaller changes in area between consecutive months. However, the signal for mean area and mean severity was not as clear. SPI 6 exhibited different behavior than the other time scales, presenting a stronger variance. These findings can be attributed to the strong interannual variation in the study area, that can present noise in the 6 months aggregated time scale.

Figure 25: Boxplot of the temporal sensitivity analysis of drought characteristics by considering different temporal time-scales (3, 6, 12 and 24 months).

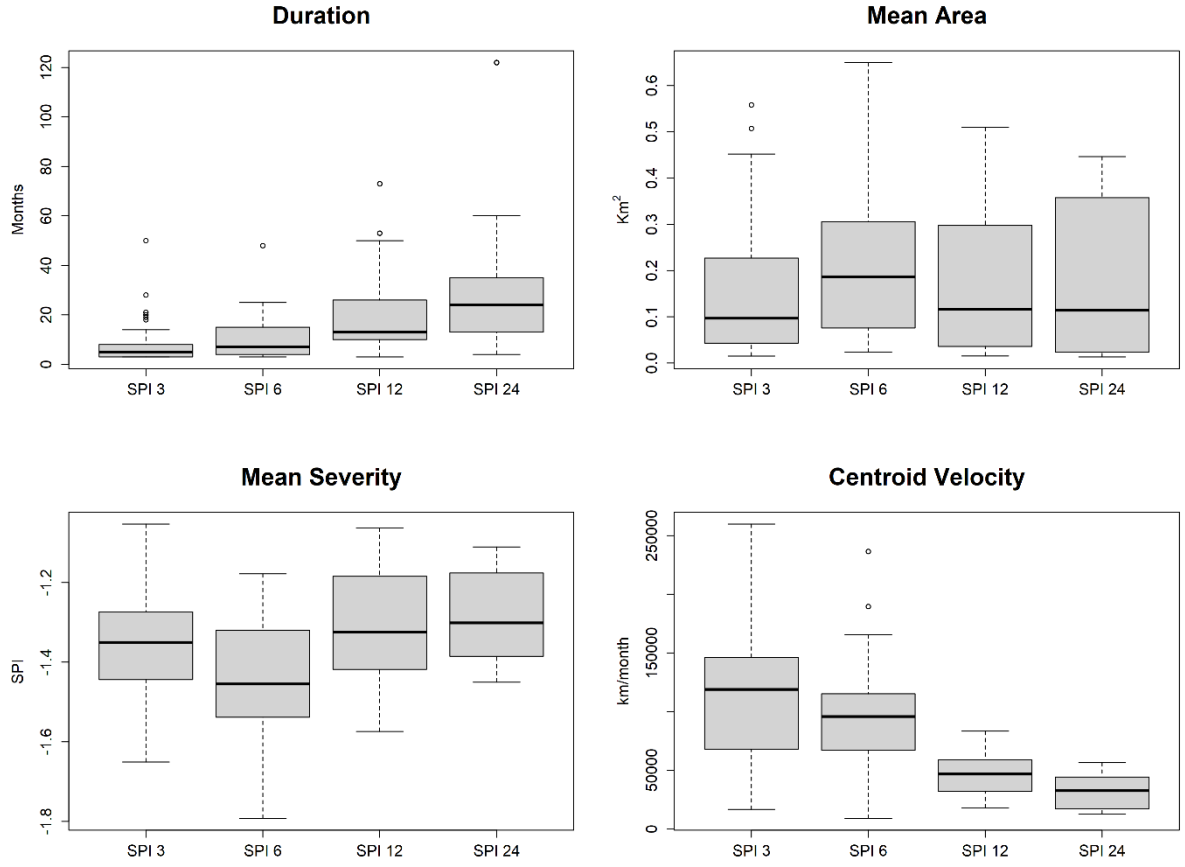

Source: Prepared by the author

In the spatial sensitivity analysis, a threshold of 1.6% was initially used for both the minimum initial area and the minimum overlap area. The 1.6% threshold was conserved for one parameter while the other was changed for the sensitivity analysis, later the inversion procedure was performed to analyze the other parameter. The sensitivity analysis of different spatial thresholds (0.8%, 1.6%, 3.2%, 4.8%) was performed for SPI 12 for the two spatial

parameters. For the studied area, these percentages correspond to 1, 7, 14, and 21 contiguous pixels needed to start a drought event (minimum initial area) and to connect the event with the following month (minimum overlap area). To understand whether these thresholds are too restrictive or too permissive, the sensitivity analysis was performed (Table 8).

Table 8: Spatial sensitive analysis of drought events captured at different spatial thresholds (0.8%, 1.6%, 3,2% and 4,8%) for the two spatial parameters, minimal area and overlap area.

Thresholds	Minimal Area			Overlap Area		
	Nº events	Duration (month)	Area (km²)	Nº events	Duration (month)	Area (km²)
0.8%	55	8	77.55	22	13	1149.72
1.6%	22	13	1149.72	22	13	1149.72
3.2%	17	20	2185.02	22	13	1149.72
4.8%	15	25	3487.91	22	13	1149.72

Source: Prepared by the author

The minimum area parameter was found to have strong influence on the number of drought events registered in the period. Lower values permitted the characterization of less spread events and presented shorter duration and less widespread area. For instance, the less restrictive threshold, 0.8%, registered 55 drought events, while the more restrictive, 4.8%, registered only 15 events. The inverse effect was found in the duration and area variables. The lower the thresholds, the shorter and less spread was the median event. On the other hand, the overlap area parameter did not present any variation on the number of drought events registered, accounting for 22 events for all thresholds.

Therefore, the spatial sensitivity analysis showed that the thresholds of the two parameters affect the characterization of drought events unevenly. The minimum area criterion has an important effect, defining many events that are more isolated and end up off-setting quickly, causing less damage to the environment. The area overlap criterion did not show any change in the definition of drought events.

Therefore, the temporal and spatial sensitivity analysis clearly demonstrated the importance of carefully consider the threshold values of temporal and spatial parameters when using the SPI to characterize drought in similar areas.

5.5 Discussion and conclusions

The intra-event analysis of drought dynamics was divided into three stages: growth curve, growth rate and acceleration. Although drought tracking spatio-temporal migration has been evaluated in previous studies (DIAZ *et al.*, 2020; ZHOU; LIU; LIU, 2019), the researchers did not focus on how drought characteristics evolve during the event. In this study, I proposed the use of growth curve, growth rate and acceleration to figure out how severity, area and centroid path can change during each event. The proposed curves give insights on how droughts evolve in time and space by showing when the event is accelerating and decelerating in each drought characteristic. This is important to understand drought evolution by its different faces. These curves were proposed by Utsunomiya et al (2020) to monitor COVID-19 spread. The theorical model for COVID-19 spread was clear and provided a formulation that could be used to forecast, but the same results were not found when analyzing drought characteristics. The complex climatic variability and small amount of drought events make the intra-event analysis difficult to find patterns. Therefore, we needed to migrate the analysis by looking at the mean behavior of different drought characteristics.

The northeastern region of Brazil is known for its long and severe and widespread drought periods, which are a result of strong spatio-temporal climatic variability due to a complex meteorological system that influence rainfall patterns in the region. Oceanic and atmospheric factors, such as the Sea Surface Temperature (SST), the Atlantic dipole, and the El Niño Southern Oscillation (ENSO), play important roles in the occurrence of droughts in the region. The presence of the Atlantic dipole, which is characterized by a difference in SST between the north and south tropical Atlantic ocean temperature, has been linked to drought in the northeastern region of Brazil, especially in the northern part as it plays an important role in the seasonal displacement of the ITCZ reaching its southernmost position from March to May (HASTENRATH, 2012; UVO *et al.*, 1998). Less precipitation in the region is associated with warmer SST in the Tropical North Atlantic (TNA) and strong Southeast trade winds (Nobre & Shukla, 1996). When analyzing the last two milenia precipitation in Northeast Brazil, Utida et al. (2019) found consistent dry periods when the ITCZ was in a mean position northern than its climatology. In contrast to the northern region, precipitation in the eastern coast is modulated by breeze circulation and easterly waves disturbance (GOMES *et al.*, 2015). In addition to these Atlantic Ocean factors, the ENSO also plays an important role in influencing the precipitation patterns in the northeast (HASTENRATH, 2012). During an El Niño event, the SST in the central and eastern Pacific Ocean rises, causing a shift in the atmospheric circulation that results

in reduced rainfall in the northeastern region of Brazil. The region is also affected by multidecadal variability (KAYANO; ANDREOLI, 2004), highlighting the complexity in understanding and forecasting drought behavior in the region.

As the precipitation mechanisms that govern the northern and eastern regions of northeast Brazil are different, it is plausible that drought events that started in each region face different characteristics. However, this paper advanced the characterization of drought dynamics as it reveals that droughts that start in the east do not develop to impact the whole region. On the other hand, droughts that started in the central part of Northeast have more probability to develop and impact the whole study area. This is because the ITCZ have more difficulty to displace at most central regions, and this results in longer, more severe and more widespread droughts that have their onset in this region.

Due to no previous spatio-temporal study on using the 3D clustering algorithm in Northeast Brazil was made, it is difficult to compare the results found in this study. However, using different methodology, Brito et al. (2021) analyzed the spatio-temporal behavior of drought events in Northeast Brazil using the official Drought Monitor as a data-source. The authors found that from 2014 to 2019, over 75% of the Northeast region of Brazil (NEB) area registered exceptional drought. The methodology used, however, dealt with duration and area of events as singular characteristics, do not using an integration technique to understand their relationships, such as the 3D cluster algorithm. Silva et al. (2019) found that more centralized regions of Northeast Brazil were drought hotspots, which is in accordance with my results.

Sensitivity analysis using SPI 3, 6, 12 and 24 found that different time scales influence drought characteristics, particularly in terms of duration and centroid velocity. Longer time scales were associated with prolonged drought events, with smaller centroid velocity and less abrupt changes in the time series, making it difficult for small precipitation events to end prolonged drought events. Moreover, longer aggregated periods conserved more information, resulting in smaller changes in area between consecutive months. It also found similar results to central area being more prone to prolonged, severe and widespread drought events and that droughts that started at the eastern coast usually do not migrate to other more central or northern areas of Northeast Brazil. The spatial sensitivity analysis showed that the minimum area criterion significantly affects the number of drought events recorded, while the overlap area criterion did not vary the number of drought events recorded. The threshold chosen in this study, 1.6% of the studied area for minimum initial area and for minimum overlap area was considered adequate to characterize drought events that have more potential to cause impacts on environment and society.

The results of this study will contribute to a better understanding of drought dynamics, which can aid in improving drought monitoring and prediction. The intra-event analysis can be used for ongoing monitoring of drought events and to give insights to cope with adverse effects of droughts. Additionally, the findings of this study can provide valuable information for decision-makers, such as water resource managers and policy-makers, in their efforts to mitigate the impacts of drought in Northeast Brazil by knowing the region more prone to develop drought with higher potential to provide socio-economic impacts.

6 CONCLUSIONS AND RECOMENDATIONS

This thesis has significantly contributed to our understanding of drought events by developing multivariate analysis frameworks that are useful for drought planning and management. The main hypothesis was that multivariate drought analysis provides sufficient gain of information to justify its use in drought planning and management. This study has shown that incorporating multivariate analysis in the study of droughts allows for the visualization and integration of interdependent variables in the analysis, resulting in a sufficient gain of information that justifies its use. However, incorporating this information in planning and decision-making can be challenging due to the increased complexity involved. It is essential to ensure that decision-makers can comprehend the new information effectively. Through the tools created through this research, it is expected that these difficulties will be diminished and that the incorporation of these multivariate analyses will be encouraged in the planning and management of future droughts.

This thesis aimed to achieve three specific objectives: (i) to develop a monitoring and early warning system based on the persistence of droughts using conditional probability theory; (ii) to provide a framework to include multivariate frequency analysis in drought planning and management; and (iii) to develop a spatial-temporal drought analysis that identifies patterns to aid in early warning and decision-making. Each of these objectives is presented in this thesis as an independent paper in the form of chapters.

The first paper proposes an innovative framework for monitoring and early warning of droughts using copula functions, which can model the complex dependence structures between total and given precipitation. The resulting Continuous Drought Probability Monitoring System (CDPMS) model calculates the likelihood of drought onset by the end of the rainy season, based on the compounding effect of monthly rainfall. The concept of drought thresholds is used to translate information from the drought index to absolute precipitation values, which is easier for decision-makers to understand. The framework was assessed in mainland Portugal and demonstrated its capacity to anticipate droughts and improve performance as it gains more information over time. This approach has already been applied in Pakistan, and the results show that CDPMS is a valuable tool for monitoring and early warning of droughts, improving drought understanding and ability to cope with future droughts.

The second paper focuses on the importance of multivariate frequency analysis in drought memory and proactive drought planning. This paper presents a framework for multivariate frequency analysis at a territory scale that considers drought duration and severity

simultaneously. The proposed framework was used to investigate the bivariate return period of the 2012-2018 drought in northeast Brazil and found that analyzing drought duration and severity together can improve risk assessment. The results showed that the 2012-2018 event had the highest bivariate return period ever recorded, 240 years, and identified events with similar duration but less severity. The proposed framework is already being used as a tool in proactive drought plans for the region, demonstrating its institutional relevance.

The third paper explores the dynamics of spatio-temporal relationship between drought events. While the second paper proposed a framework for regionalized analysis of droughts, the third paper argues that droughts do not respect political or geographic borders and another way to monitor and assess drought risk is to understand how it moves, connects, and splits over time and space. Thus, the chapter provides a simple framework to visualize drought evolution over time and space, which includes a 3D analysis of lat, long, and time. The chapter proposes two different analyses: intra-event analysis of drought dynamics and searching for patterns and relationships between mean drought characteristics. The results show that the central part of the Northeast region developed longer, more severe, and more widespread droughts than any other area, indicating the need for proactive drought plans in this region.

In summary, the innovations presented in this thesis are: (i) the first paper introduced a novel solution that utilized copula functions to predict drought occurrence; (ii) the second paper provided a framework for incorporating multivariate information into drought planning, making a technological contribution; and (iii) the third paper presented an innovative approach to monitoring the spatiotemporal dynamics of droughts and identifying patterns that can facilitate early warning and monitoring in Northeast Brazil.

Therefore, this thesis presents three different papers that use multivariate analyses, and each present a framework to improve understanding of droughts. Each framework was developed independently with its own specific purposes, but considering multiple variables, and simplifying results for decision makers. These frameworks are independent and replicable to other regions, but they were not created requiring the application of more than one at the same time.

The results of this thesis demonstrate that multivariate analysis enhances understanding of drought events and can effectively inform drought planning and management. The developed monitoring and early warning system illustrated that it is possible to anticipate and mitigate drought impacts by modeling complex dependence structures between total and given precipitation. Moreover, the proposed multivariate frequency analysis framework improved risk assessment by simultaneously considering drought duration and severity at the

hydrographic region level, and is now used as a planning tool in new proactive drought plans for the studied region. Finally, the proposed spatial-temporal drought analysis framework revealed the central part of Northeast region to be more susceptible to prolonged, severe, and widespread droughts compared to other areas, which is vital for preparing for future events that originate in this region.

For future work, each study has its own set of recommendations. In the first study, the prediction of drought occurrence can be improved by explicitly incorporating climatic indices, such as ENSO, and applying the model to different climatic zones. Additionally, the copula-based model can compare its flexible advantages with other models to see whether this capacity enhances performance. In the second study, further research can be conducted to explore the impact threshold and analyze the dependence structure that correlates water reservoirs with meteorological drought. For the third study, advancing the research can be achieved by using clusterization for modes of climate variation from SPI to better select the onset areas. Furthermore, using different precipitation databases can improve the confidence in results. Finally, a prediction strategy can be developed using the statistical information obtained from the study.

Overall, this thesis has provided valuable strategies and frameworks to enhance our understanding of drought events by considering multiple characteristics while keeping the results simple and accessible for decision-makers. By bridging the gap between science and management, this research has contributed to improving our knowledge of drought events and our capacity to cope with future droughts.

REFERENCES

AAS, K.; CZADO, C.; FRIGESSI, A. Pair-copula constructions of multiple dependence Projektpartner Pair-copula constructions of multiple dependence. **Insurance: Mathematics and Economics**, v. 44, p. 182–198, 2009. Disponível em: <https://mediatum.ub.tum.de/doc/1083600/file.pdf>. Acesso em: 7 fev. 2023.

AGNEW, C. Using the SPI to identify drought. **Drought Networks News**, v. 12, n. 1, p. 5–12, 2000. Disponível em: <http://digitalcommons.unl.edu/droughtnetnews/1/>. Acesso em: 7 fev. 2023.

ALIDOOST, F.; SU, Z.; STEIN, A. Evaluating the effects of climate extremes on crop yield, production and price using multivariate distributions: A new copula application. **Weather and Climate Extremes**, v. 26, n. July, p. 100227, 2019. Disponível em: <https://doi.org/10.1016/j.wace.2019.100227>. Acesso em: 7 fev. 2023.

ANDREADIS, K. M.; CLARK, E. A.; WOOD, A. W.; HAMLET, A. F.; LETTENMAIER, D. P. Twentieth-century drought in the conterminous United States. **Journal of Hydrometeorology**, v. 6, n. 6, p. 985–1001, 2005.

ANDREOLI, R. V.; KAYANO, M. T. ENSO-related rainfall anomalies in South America and associated circulation features during warm and cold Pacific decadal oscillation regimes. **International Journal of Climatology**, v. 25, n. 15, p. 2017–2030, 2005.

AWANGE, J. L.; MPELASOKA, F.; GONCALVES, R. M. When every drop counts: Analysis of Droughts in Brazil for the 1901-2013 period. **Science of the Total Environment**, v. 566–567, p. 1472–1488, 2016. Disponível em: <http://dx.doi.org/10.1016/j.scitotenv.2016.06.031>. Acesso em: 7 fev. 2023.

AYANTOBO, O. O.; LI, Y.; SONG, S. Multivariate Drought Frequency Analysis using Four-Variate Symmetric and Asymmetric Archimedean Copula Functions. **Water Resources Management**, v. 33, n. 1, p. 103–127, 2019.

AYANTOBO, O. O.; LI, Y.; SONG, S.; JAVED, T.; YAO, N. Probabilistic modelling of drought events in China via 2-dimensional joint copula. **Journal of Hydrology**, v. 559, p. 373–391, abr. 2018. Disponível em: <https://linkinghub.elsevier.com/retrieve/pii/S0022169418300969>. Acesso em: 7 fev. 2023.

BEVACQUA, E.; MARAUN, D.; HOBÆK HAFF, I.; WIDMANN, M.; VRAC, M. Multivariate statistical modelling of compound events via pair-copula constructions: Analysis of floods in Ravenna (Italy). **Hydrology and Earth System Sciences**, v. 21, n. 6, p. 2701–2723, 2017.

BRECHMANN, E. C.; SCHEPSMEIER, U. Modeling Dependence with C- and D-Vine Copulas: The *R* Package **CDVine**. **Journal of Statistical Software**, v. 52, n. 3, 2013. Disponível em: <http://www.jstatsoft.org/v52/i03/>. Acesso em: 7 fev. 2023.

BRITO, S. S. B.; CUNHA, A. P. M. A.; CUNNINGHAM, C. C.; ALVALÁ, R. C.; MARENGO, J. A.; CARVALHO, M. A. Frequency, duration and severity of drought in the Semiarid Northeast Brazil region. **International Journal of Climatology**, v. 38, n. 2, p. 517–

529, 2018.

CAMPOS, J. N. B. Paradigms and Public Policies on Drought in Northeast Brazil: A Historical Perspective. **Environmental Management**, v. 55, n. 5, p. 1052–1063, 2015.

CEARÁ, E. Decreto no 23.068, de 11 de fevereiro de 1994. [s.d.]

CHANG, J.; LI, Y.; WANG, Y.; YUAN, M. Copula-based drought risk assessment combined with an integrated index in the Wei River Basin, China. **Journal of Hydrology**, v. 540, p. 824–834, 2016. Disponível em: <http://dx.doi.org/10.1016/j.jhydrol.2016.06.064>. Acesso em: 7 fev. 2023.

CHEN, L.; SINGH, V. P.; GUO, S.; MISHRA, A. K.; GUO, J. Drought Analysis Using Copulas. **Journal of Hydrologic Engineering**, v. 18, n. 7, p. 797–808, 2013. Disponível em: <http://ascelibrary.org/doi/10.1061/%28ASCE%29HE.1943-5584.0000697>. Acesso em: 7 fev. 2023.

CHEN, X.; LI, F.; LI, J.; FENG, P. Three-dimensional identification of hydrological drought and multivariate drought risk probability assessment in the Luanhe River basin , China. 2019.

CORTESI, N.; GONZALEZ-HIDALGO, J. C.; TRIGO, R. M.; RAMOS, A. M. Weather types and spatial variability of precipitation in the Iberian Peninsula. **International Journal of Climatology**, v. 34, n. 8, p. 2661–2677, 2014.

COSTA, D. D.; UVO, C. B.; ROLIM DA PAZ, A.; DE OLIVEIRA CARVALHO, F.; FRAGOSO, C. R. Long-term relationships between climate oscillation and basin-scale hydrological variability during rainy season in eastern Northeast Brazil. **Hydrological Sciences Journal**, v. 63, n. 11, p. 1636–1652, 2018.

CUNHA, A. P. M. A.; TOMASELLA, J.; RIBEIRO-NETO, G. G.; BROWN, M.; GARCIA, S. R.; BRITO, S. B.; CARVALHO, M. A. Changes in the spatial–temporal patterns of droughts in the Brazilian Northeast. **Atmospheric Science Letters**, v. 19, n. 10, p. 1–8, 2018.

CUNHA, A. P. M.; ALVALÁ, R. C.; NOBRE, C. A.; CARVALHO, M. A. Monitoring vegetative drought dynamics in the Brazilian semiarid region. **Agricultural and Forest Meteorology**, v. 214–215, p. 494–505, 2015. Disponível em: <http://dx.doi.org/10.1016/j.agrformet.2015.09.010>. Acesso em: 7 fev. 2023.

DE AZEVEDO, S. C.; CARDIM, G. P.; PUGA, F.; SINGH, R. P.; DA SILVA, E. A. Analysis of the 2012-2016 drought in the northeast Brazil and its impacts on the Sobradinho water reservoir. **Remote Sensing Letters**, v. 9, n. 5, p. 438–446, 2018. Disponível em: <https://doi.org/10.1080/2150704X.2018.1437290>. Acesso em: 7 fev. 2023.

DE BRITO, Y. M. A.; RUFINO, I. A. A.; BRAGA, C. F. C.; MULLIGAN, K. The Brazilian drought monitoring in a multi-annual perspective. **Environmental Monitoring and Assessment**, v. 193, n. 1, 1 jan. 2021.

DELGADO, J. M.; VOSS, S.; BÜRGER, G.; VORMOOR, K.; MURAWSKI, A.; PEREIRA, J. M. R.; MARTINS, E.; VASCONCELOS JÚNIOR, F.; FRANCKE, T. Seasonal drought prediction for semiarid northeastern Brazil: Verification of six hydro-meteorological forecast products. **Hydrology and Earth System Sciences**, v. 22, n. 9, p. 5041–5056, 2018.

DIAZ, V.; CORZO PEREZ, G. A.; VAN LANEN, H. A. J.; SOLOMATINE, D.; VAROUCHAKIS, E. A. Characterisation of the dynamics of past droughts. **Science of the Total Environment**, n. xxxx, p. 134588, 2019. Disponível em: <https://doi.org/10.1016/j.scitotenv.2019.134588>. Acesso em: 7 fev. 2023.

DIAZ, V.; PEREZ, G. A. C.; LANEN, H. A. J. Van; SOLOMATINE, D.; VAROUCHAKIS, E. A.; VAROUCHAKIS, E. A. **An approach to characterise spatio-temporal drought dynamics**. [s.l.] Elsevier Ltd, 2020. 103512 p.

DRACUP, J. A.; LEE, K. S.; PAULSON, E. G. On the definition of droughts. **Water Resources Research**, v. 16, n. 2, p. 297–302, abr. 1980. Disponível em: <http://doi.wiley.com/10.1029/WR016i002p00297>. Acesso em: 7 fev. 2023.

EM-DAT. **EM-DAT**. Disponível em: <https://www.emdat.be/>. Acesso em: 2 fev. 2023.

ENFIELD, D. B.; MESTAS-NUÑEZ, A. M.; TRIMBLE, P. J. The Atlantic multidecadal oscillation and its relation to rainfall and river flows in the continental U.S. **Geophysical Research Letters**, v. 28, n. 10, p. 2077–2080, 2001.

ESPINOSA, L. A.; PORTELA, M. M.; PONTES FILHO, J. D..; ZELENAKOVA, M. Bivariate Modelling of a Teleconnection Index and Extreme Rainfall in a Small North Atlantic Island. **Climate**, v. 9, n. 86, p. 1–21, 2021.

ESPINOSA, L. A.; PORTELA, M. M.; PONTES FILHO, J. D.; STUDART, T. M. de C.; SANTOS, J. F.; RODRIGUES, R. Jointly modeling drought characteristics with smoothed regionalized SPI series for a small island. **Water (Switzerland)**, v. 11, n. 12, p. 1–27, 2019.

EUROPEAN COMMISSION. **Report on the Review of the European Water Scarcity and Droughts Policy**. Brussels, 2012.

FORMIGA-JOHNSSON, R. M.; KEMPER, K. E. **Institutional and Policy Analysis of River Basin Management**. Rochester, NY: 3649, World Bank Policy Research Working Paper, 2005. 1–40 p.

GENEST, C.; FAVRE, A.-C. Everything You Always Wanted to Know about Copula Modeling but Were Afraid to Ask. **Journal of Hydrologic Engineering**, v. 12, n. 4, p. 347–368, jul. 2007. Disponível em: <http://ascelibrary.org/doi/10.1061/%28ASCE%291084-0699%282007%2912%3A4%28347%29>. Acesso em: 7 fev. 2023.

GENEST, C.; GHOUDI, K.; RIVEST, L. p. A semiparametric estimation procedure of dependence parameters in multivariate families of distributions. **Biometrika**, v. 82, n. 3, p. 543–552, 1995.

GIMENO, L.; NIETO, R.; TRIGO, R. M.; VICENTE-SERRANO, S. M.; LÓPEZ-MORENO, J. I. Where Does the Iberian Peninsula Moisture Come From? An Answer Based on a Lagrangian Approach. **Journal of Hydrometeorology**, v. 11, n. 2, p. 421–436, abr. 2010. Disponível em: <http://journals.ametsoc.org/doi/abs/10.1175/2009JHM1182.1>. Acesso em: 7 fev. 2023.

GOMES, H. B.; AMBRIZZI, T.; HERDIES, D. L.; HODGES, K.; PONTES DA SILVA, B. F. Easterly wave disturbances over Northeast Brazil: An observational analysis. **Advances in Meteorology**, v. 2015, 2015.

GUTIÉRREZ, A. P. A.; ENGLE, N. L.; DE NYS, E.; MOLEJÓN, C.; MARTINS, E. S. Drought preparedness in Brazil. **Weather and Climate Extremes**, v. 3, p. 95–106, 2014. Disponível em: <http://dx.doi.org/10.1016/j.wace.2013.12.001>. Acesso em: 7 fev. 2023.

GUTTMAN, N. B. Accepting the standardized precipitation index: A calculation algorithm. **Journal of the American Water Resources Association**, v. 35, n. 2, p. 311–322, 1999.

HAAN, C. T. **Statistical Methods in Hydrology**. [s.l.] Press, The Iowa State, 2002.

HAO, Z.; HAO, F.; SINGH, V. P.; OUYANG, W.; CHENG, H. An integrated package for drought monitoring, prediction and analysis to aid drought modeling and assessment. **Environmental Modelling and Software**, v. 91, p. 199–209, 2017. Disponível em: <http://dx.doi.org/10.1016/j.envsoft.2017.02.008>. Acesso em: 7 fev. 2023.

HAO, Z.; HAO, F.; SINGH, V. P.; ZHANG, X. Statistical prediction of the severity of compound dry-hot events based on El Niño-Southern Oscillation. **Journal of Hydrology**, 2019. Disponível em: <https://doi.org/10.1016/j.jhydrol.2019.03.001>. Acesso em: 7 fev. 2023.

HAO, Z.; SINGH, V. P. Review of dependence modeling in hydrology and water resources. **Progress in Physical Geography**, v. 40, n. 4, p. 549–578, 2016.

HAO, Z.; SINGH, V. P.; ASCE, F. Compound Events under Global Warming : A Dependence Perspective. v. 25, n. 9, p. 1–12, 2020.

HAO, Z.; SINGH, V. P.; HAO, F. Compound Extremes in Hydroclimatology : A Review. **water**, p. 16–21, 2018.

HARRIS, I.; OSBORN, T. J.; JONES, P.; LISTER, D. Version 4 of the CRU TS monthly high-resolution gridded multivariate climate dataset. **Scientific Data**, v. 7, n. 1, p. 1–18, 2020.

HASTENRATH, S. Exploring the climate problems of Brazil's Nordeste: A review. **Climatic Change**, v. 112, n. 2, p. 243–251, 2012.

HASTENRATH, S.; HELLER, L. Dynamics of climatic hazards in northeast Brazil. **Quarterly Journal of the Royal Meteorological Society**, v. 103, n. 435, p. 77–92, 1977.

HAYES, M. J.; ALVORD, C.; LOWREY, J. Drought Indices 2007. **Intermountain West Climate Summary**, n. July, p. 1–5, 2007.

HEIM, R. R. A review of twentieth-century drought indices used in the United States. Bulletin. **Bulletin of the American Meteorological Society.**, v. 83 (8), n. August, p. 1149–1165, 2002.

HERRERA-ESTRADA, J. E.; DIFFENBAUGH, N. S. Landfalling Droughts: Global Tracking of Moisture Deficits From the Oceans Onto Land. **Water Resources Research**, v. 56, n. 9, 2020.

HERRERA-ESTRADA, J. E.; SATOH, Y.; SHEFFIELD, J. Spatiotemporal dynamics of global drought. **Geophysical Research Letters**, v. 44, n. 5, p. 2254–2263, 2017.

HOUNSOU-GBO, G. A.; SERVAIN, J.; ARAUJO, M.; CANIAUX, G.; BOURLÈS, B.;

FONTENELE, D.; MARTINS, E. S. P. R. SST indexes in the tropical South Atlantic for forecasting rainy seasons in Northeast Brazil. **Atmosphere**, v. 10, n. 6, 2019.

HOUNSOU-GBO, G. A.; SERVAIN, J.; ARAUJO, M.; MARTINS, E. S.; BOURLÈS, B.; CANIAUX, G. Oceanic Indices for Forecasting Seasonal Rainfall over the Northern Part of Brazilian Northeast. **American Journal of Climate Change**, v. 05, n. 02, p. 261–274, 2016.

JOE, H. **Multivariate Models and Dependence Concepts**. London: Chapman & Hall, 1997.

JONES, C.; CARVALHO, L. M. V. The influence of the Atlantic multidecadal oscillation on the eastern Andes low-level jet and precipitation in South America. **npj Climate and Atmospheric Science**, v. 1, n. 1, p. 1–7, 2018. Disponível em: <http://dx.doi.org/10.1038/s41612-018-0050-8>. Acesso em: 7 fev. 2023.

KAO, S. C.; GOVINDARAJU, R. S. A copula-based joint deficit index for droughts. **Journal of Hydrology**, v. 380, n. 1–2, p. 121–134, 2010a. Disponível em: <http://dx.doi.org/10.1016/j.jhydrol.2009.10.029>. Acesso em: 7 fev. 2023.

KAO, S.; GOVINDARAJU, R. S. A copula-based joint deficit index for droughts. **Journal of Hydrology**, v. 380, n. 1–2, p. 121–134, 2010b. Disponível em: <http://dx.doi.org/10.1016/j.jhydrol.2009.10.029>. Acesso em: 7 fev. 2023.

KAYANO, M. T.; ANDREOLI, R. V. Decadal variability of northern northeast Brazil rainfall and its relation to tropical sea surface temperature and global sea level pressure anomalies. **Journal of Geophysical Research: Oceans**, v. 109, n. 11, p. 1–8, 2004.

KAYANO, M. T.; ANDREOLI, R. V.; GARCIA, S. R.; DE SOUZA, R. A. F. How the two nodes of the tropical Atlantic sea surface temperature dipole relate the climate of the surrounding regions during austral autumn. **International Journal of Climatology**, v. 38, n. 10, p. 3927–3941, 2018.

KAYANO, M. T.; CAPISTRANO, V. B. How the Atlantic multidecadal oscillation (AMO) modifies the ENSO influence on the South American rainfall. **International Journal of Climatology**, v. 34, n. 1, p. 162–178, 2014.

KERR, R. A. A North Atlantic Climate Pacemaker for the Centuries. **Science**, v. 288, n. 5473, p. 1984–1985, 16 jun. 2000. Disponível em: <http://www.sciencemag.org/cgi/doi/10.1126/science.288.5473.1984>. Acesso em: 7 fev. 2023.

KEYANTASH, J.; DRACUP, J. A. The quantification of drought: An evaluation of drought indices. **Bulletin of the American Meteorological Society**, v. 83, n. 8, p. 1167–1180, 2002.

KIM; YOO; CHUNG; KIM. Hydrologic Risk Assessment of Future Extreme Drought in South Korea Using Bivariate Frequency Analysis. **Water**, v. 11, n. 10, p. 2052, 30 set. 2019. Disponível em: <https://www.mdpi.com/2073-4441/11/10/2052>. Acesso em: 7 fev. 2023.

KLEIN, B.; MEISSNER, D.; KOBIALKA, H.-U.; REGGIANI, P. Predictive Uncertainty Estimation of Hydrological Multi-Model Ensembles Using Pair-Copula Construction. **Water**, v. 8, n. 4, p. 125, 31 mar. 2016. Disponível em: <http://www.mdpi.com/2073-4441/8/4/125>. Acesso em: 7 fev. 2023.

KNIGHT, J. R.; FOLLAND, C. K.; SCAIFE, A. A. Climate impacts of the Atlantic multidecadal oscillation. **Geophysical Research Letters**, v. 33, n. 17, p. 2–5, 2006.

KRISHNAMURTHY R, P. K.; FISHER, J. B.; SCHIMEL, D. S.; KAREIVA, P. M. Applying Tipping Point Theory to Remote Sensing Science to Improve Early Warning Drought Signals for Food Security. **Earth's Future**, v. 8, n. 3, 1 mar. 2020.

KWON, H.-H.; LALL, U. A copula-based nonstationary frequency analysis for the 2012-2015 drought in California. **Water Resources Research**, v. 52, n. 7, p. 5662–5675, jul. 2016. Disponível em: <http://doi.wiley.com/10.1002/2016WR018959>. Acesso em: 7 fev. 2023.

LAZOGLOU, G.; ANAGNOSTOPOULOU, C. Joint distribution of temperature and precipitation in the Mediterranean, using the Copula method. **Theoretical and Applied Climatology**, p. 1–13, 2018.

LI, J.; WANG, Z.; WU, X.; XU, C. Y.; GUO, S.; CHEN, X. Toward monitoring short-term droughts using a novel daily scale, standardized antecedent precipitation evapotranspiration index. **Journal of Hydrometeorology**, v. 21, n. 5, p. 891–908, 2020.

LIU, B.; LIANG, M.; HUANG, Z.; TAN, X. Duration–severity–area characteristics of drought events in eastern China determined using a three-dimensional clustering method. **International Journal of Climatology**, 2020.

LIU, X.; PAN, Y.; ZHU, X.; YANG, T.; BAI, J.; SUN, Z. Drought evolution and its impact on the crop yield in the North China Plain. **Journal of Hydrology**, 2018. Disponível em: <https://doi.org/10.1016/j.jhydrol.2018.07.077>. Acesso em: 7 fev. 2023.

LIU, Y.; ZHU, Y.; REN, L.; SINGH, V. P.; YONG, B.; JIANG, S.; YUAN, F.; YANG, X. Understanding the Spatiotemporal Links Between Meteorological and Hydrological Droughts From a Three-Dimensional Perspective. **Journal of Geophysical Research: Atmospheres**, v. 124, n. 6, p. 3090–3109, 27 mar. 2019a. Disponível em: <https://onlinelibrary.wiley.com/doi/abs/10.1029/2018JD028947>. Acesso em: 7 fev. 2023.

LIU, Y.; ZHU, Y.; REN, L.; YONG, B.; SINGH, V. P.; YUAN, F.; JIANG, S.; YANG, X. On the mechanisms of two composite methods for construction of multivariate drought indices. **Science of The Total Environment**, v. 647, p. 981–991, jan. 2019b. Disponível em: <https://doi.org/10.1016/j.scitotenv.2018.07.273>. Acesso em: 7 fev. 2023.

LLOYD-HUGHES, B. A spatio-temporal structure-based approach to drought characterisation. v. 418, n. January 2011, p. 406–418, 2012.

LUCENA, D. B.; SERVAIN, J.; FILHO, M. F. G. Rainfall response in Northeast Brazil from ocean climate variability during the second half of the twentieth century. **Journal of Climate**, v. 24, n. 23, p. 6174–6184, 2011.

LUO, M.; LAU, N. C.; LIU, Z.; WU, S.; WANG, X. An Observational Investigation of Spatiotemporally Contiguous Heatwaves in China From a 3D Perspective. **Geophysical Research Letters**, v. 49, n. 6, 28 mar. 2022.

MANN, H. B. Nonparametric Tests Against Trend. **The Econometric Society**, v. 13, n. 3, p. 245–259, 1945.

MARENGO, J. A.; ALVES, L. M.; ALVALA, R. C. .; CUNHA, A. P.; BRITO, S.; MORAES, O. L. L. Climatic characteristics of the 2010-2016 drought in the semiarid Northeast Brazil region. **Anais da Academia Brasileira de Ciências**, v. 90, n. 2 suppl 1, p. 1973–1985, 14 ago. 2017. Disponível em: <http://www.scielo.br/scielo.php?script=sci_arttext&pid=S0001-37652018000501973&lng=en&tlng=en>. Acesso em: 7 fev. 2023.

MARENGO, J. A.; ALVES, L. M.; SOARES, W. R.; RODRIGUEZ, D. A.; CAMARGO, H.; RIVEROS, M. P.; PABLÓ, A. D. Two Contrasting Severe Seasonal Extremes in Tropical South America in 2012: Flood in Amazonia and Drought in Northeast Brazil. **Journal of Climate**, v. 26, n. 22, p. 9137–9154, nov. 2013. Disponível em: <http://journals.ametsoc.org/doi/abs/10.1175/JCLI-D-12-00642.1>. Acesso em: 7 fev. 2023.

MARENGO, J. A.; CUNHA, A. P.; ALVES, L. M. A seca de 2012-15 no semiárido do Nordeste do Brasil no contexto histórico. **Revista Climanálise**, v. 4, n. 1, p. 49–54, 2016. Disponível em: <https://ods.ibge.gov.br/>. Acesso em: 7 fev. 2023.

MARENGO, J. A.; TORRES, R. R.; ALVES, L. M. Drought in Northeast Brazil—past, present, and future. **Theoretical and Applied Climatology**, v. 129, n. 3–4, p. 1189–1200, 2017. Disponível em: <http://dx.doi.org/10.1007/s00704-016-1840-8>. Acesso em: 7 fev. 2023.

MARTINS, E. S. P. R. .; DE NYS, E. .; MOLEJÓN, C. .; BIAZETO, B. .; VIEIRA, R. F. .; ENGLE, N. L. Search a new paradigm for drought management in Northeast: drought monitor. *In*: WORLD BANK. **Água Brasil Series no 10**. [s.l: s.n.]p. 128.

MARTINS, E. S. P. R.; COELHO, C. A. S.; HAARSMA, R.; OTTO, F. E. L.; KING, A. D.; JAN VAN OLDENBORGH, G.; KEW, S.; PHILIP, S.; VASCONCELOS JÚNIOR, F. C.; CULLEN, H. A Multimethod Attribution Analysis of the Prolonged Northeast Brazil Hydrometeorological Drought (2012–16). **Bulletin of the American Meteorological Society**, v. 99, n. 1, p. S65–S69, jan. 2018. Disponível em: <http://journals.ametsoc.org/doi/10.1175/BAMS-D-17-0102.1>. Acesso em: 7 fev. 2023.

MARTINS, E. S. P. R.; MAGALHÃES, A. R.; FONTENELE, D. A seca plurianual de 2010-2017 no Nordeste e seus impactos. **Parcerias Estratégicas**, v. 22, n. 44, p. 17–40, 2017. Disponível em: <http://seer.cgee.org.br/index.php/parcerias_estrategicas/article/viewFile/844/772>. Acesso em: 7 fev. 2023.

KENDALL, M. G. **Rank correlation methods**. 4th Edition, Charles Griffin, London, 1975.

MCKEE, T. B.; DOESKEN, N. J.; KLEIST, J. The relationship of drought frequency and duration to time scales. **AMS 8th Conference on Applied Climatology**, n. January, p. 179–184, 1993. Disponível em: <http://ccc.atmos.colostate.edu/relationshipofdroughtfrequency.pdf>. Acesso em: 7 fev. 2023.

MISHRA, A. K.; SINGH, V. P. A review of drought concepts. **Journal of Hydrology**, v. 391, n. 1–2, p. 202–216, 2010. Disponível em: <http://dx.doi.org/10.1016/j.jhydrol.2010.07.012>. Acesso em: 7 fev. 2023.

MONTASERI, M.; AMIRATAEE, B.; REZAIE, H. New approach in bivariate drought duration and severity analysis. **Journal of Hydrology**, 2018.

MOURA, A. D.; SHUKLA, J. On the Dynamics of Droughts in Northeast Brazil: Observations, Theory and Numerical Experiments with a General Circulation Model. **Journal of the Atmospheric Sciences**, v. 38, n. 12, p. 2653–2675, 1981.

NELSEN, R. B. **An Introduction to Copulas**. [s.l.] Springer, 2006. 1–656 p.

NIAZ, R.; ALMAZAH, M. M. A.; HUSSAIN, I.; FILHO, J. D. P. A new framework to substantiate the prevalence of drought intensities. **Theoretical and Applied Climatology**, v. 147, n. 3–4, p. 1079–1090, fev. 2022a. Disponível em: <https://link.springer.com/10.1007/s00704-021-03876-7>. Acesso em: 7 fev. 2023.

NIAZ, R.; ALMAZAH, M. M. A.; HUSSAIN, I.; FILHO, J. D. P.; AL-ANSARI, N.; SH SAMMEN, S. Assessing the Probability of Drought Severity in a Homogeneous Region. **Complexity**, v. 2022, p. 1–8, 29 jan. 2022b. Disponível em: <https://www.hindawi.com/journals/complexity/2022/3139870/>. Acesso em: 7 fev. 2023.

NOBRE, C. A.; MARENGO, J. A.; SELUCHI, M. E.; CUARTAS, L. A.; ALVES, L. M. Some Characteristics and Impacts of the Drought and Water Crisis in Southeastern Brazil during 2014 and 2015. **Journal of Water Resource and Protection**, v. 08, n. 02, p. 252–262, 2016.

NOBRE, P.; SHUKLA, J. Variatons of Sea Surface Temperature, Wind Stress, and Rainfall Over the Tropical Atlantic and South America. **Journal of Climate**, v. 9, n. 2464, 1996.

OJEDA, M. M. del V. G.-V. **Climate-change Projections in the Iberian Peninsula : a Study on the Hydrological Impacts**. 2018. Universidad de Granada, 2018.

PALMER, W. C. **Meteorological Drought**. U.S. Weather Bureau, Res. Pap. No. 45, 1965. Disponível em: <https://www.ncdc.noaa.gov/temp-and-precip/drought/docs/palmer.pdf>. Acesso em: 7 fev. 2023.

PAN, T.; CHEN, J.; LIU, Y. Spatial and Temporal Pattern of Drought Hazard under Different RCP Scenarios for China in the 21st century. **Natural Hazards and Earth System Sciences Discussions**, n. October, p. 1–18, 2018.

PIEPER, P. **meteorological drought universal monitoring and reliable seasonal prediction with the standardized precipitation index**. 2020. 2020. Disponível em: <https://www.ncdc.noaa.gov/temp-and-precip/drought/docs/palmer.pdf>. Acesso em: 7 fev. 2023.

PONTES FILHO, J. D.; PORTELA, M. M.; MARINHO DE CARVALHO STUDART, T.; SOUZA FILHO, F. de A. A Continuous Drought Probability Monitoring System, CDPMS, Based on Copulas. **Water**, v. 11, n. 9, p. 1925, 14 set. 2019. Disponível em: <https://www.mdpi.com/2073-4441/11/9/1925>. Acesso em: 7 fev. 2023.

PORTELA, M. M.; DOS SANTOS, J. F.; SILVA, A. T.; BENITEZ, J. B.; FRANK, C.; REICHERT, J. M. Drought analysis in southern Paraguay, Brazil and northern Argentina: regionalization, occurrence rate and rainfall thresholds. **Hydrology Research**, v. 46, n. 5, p. 792–810, 2015a.

PORTELA, M. M.; SANTOS, J. F. F. dos; NAGHETTINI, M.; MATOS, J. P.; SILVA, A. T. Superfícies de limiares de precipitação para identificação de secas em Portugal continental:

uma aplicação complementar do Índice de Precipitação Padronizada, SPI. **Revista Recursos Hídricos**, v. 33, n. 2, p. 5–23, 2012. Disponível em: <http://www.aprh.pt/rh/v33n2-1.html>. Acesso em: 7 fev. 2023.

PORTELA, M. M.; ZELEŇÁKOVÁ, M.; SANTOS, J. F.; PURCZ, P.; SILVA, A. T.; HLAVATÁ, H. A comprehensive drought analysis in Slovakia using SPI. **European Water**, v. 51, p. 15–31, 2015b.

PORTELE, T. C.; LORENZ, C.; DIBRANI, B.; LAUX, P.; BLIEFERNICHT, J.; KUNSTMANN, H. Seasonal forecasts offer economic benefit for hydrological decision making in semi-arid regions. **Scientific Reports**, v. 11, n. 1, 1 dez. 2021.

RIBEIRO, A. F. S.; RUSSO, A.; GOUVEIA, C. M.; PÁSCOA, P. Copula-based agricultural drought risk of rainfed cropping systems. **Agricultural Water Management**, v. 223, n. July, p. 105689, 2019a. Disponível em: <https://doi.org/10.1016/j.agwat.2019.105689>. Acesso em: 7 fev. 2023.

RIBEIRO, A. F. S.; RUSSO, A.; GOUVEIA, C. M.; PASCOA, P.; PIRES, C. A. L. Probabilistic modelling of the dependence between rainfed crops and drought hazard. **Natural Hazards and Earth System Sciences**, v. 19, n. 12, p. 2795–2809, 2019b.

RIBEIRO, A. F. S.; RUSSO, A.; GOUVEIA, C. M.; PÁSCOA, P.; ZSCHEISCHLER, J. Risk of crop failure due to compound dry and hot extremes estimated with nested copulas. **Biogeosciences Discussions**, n. April, p. 1–21, 2020.

ROCHA, R. V.; SOUZA FILHO, F. de A. de; SILVA, S. M. O. da. Análise da Relação entre a Precipitação Média do Reservatório Orós, Brasil - Ceará, e os índices PDO e AMO Através da Análise de Changepoints e Transformada de Ondeletas. **Revista Brasileira de Meteorologia**, v. 34, n. 1, p. 139–149, 2019.

RODRIGUES, R. R.; MCPHADEN, M. J. Why did the 2011-2012 La Niña cause a severe drought in the Brazilian Northeast? **Geophysical Research Letters**, v. 41, n. 3, p. 1012–1018, 16 fev. 2014. Disponível em: <http://doi.wiley.com/10.1002/2013GL058703>. Acesso em: 7 fev. 2023.

RUSSO, A. C.; GOUVEIA, C. M.; TRIGO, R. M.; LIBERATO, M. L. R.; DACAMARA, C. C. The influence of circulation weather patterns at different spatial scales on drought variability in the Iberian Peninsula. **Frontiers in Environmental Science**, v. 3, n. February, p. 1–15, 2015.

SANKARASUBRAMANIAN, A.; LALL, U.; SOUZA FILHO, F. A.; SHARMA, A. Improved water allocation utilizing probabilistic climate forecasts: Short-term water contracts in a risk management framework. **Water Resources Research**, v. 45, n. 11, p. 1–18, 2009.

SANTOS, J. F. F. dos. **Drought analysis in mainland Portugal: spatial distribution, frequency and hindcasting**. 2012. Instituto Superior Técnico, 2012.

SANTOS, J. A.; MARINS, R. V.; AGUIAR, J. E.; CHALAR, G.; SILVA, F. A. T. F.; LACERDA, L. D. Hydrochemistry and trophic state change in a large reservoir in the Brazilian northeast region under intense drought conditions. **Journal of Limnology**, v. 76, n. 1, p. 41–51, 2017.

SANTOS, J. F.; PORTELA, M. M. F. dos; NAGHETTINI, M.; MATOS, J. P.; SILVA, A. T. Precipitation thresholds for drought recognition: a complementary use of the standardized precipitation index, SPI. **River Basin Management**, 2013.

SANTOS, J. F.; PORTELA, M. M.; PULIDO-CALVO, I. Spring drought prediction based on winter NAO and global SST in Portugal. **Hydrological Processes**, v. 28, n. 3, p. 1009–1024, 2014.

SANTOS, J. F.; PULIDO-CALVO, I.; PORTELA, M. M. Spatial and temporal variability of droughts in Portugal. **Water Resources Research**, v. 46, n. 3, p. 1–13, 2010.

SHARIFI, E.; SAGHAFIAN, B.; STEINACKER, R. Copula-based stochastic uncertainty analysis of satellite precipitation products. **Journal of Hydrology**, v. 570, n. January, p. 739–754, 2019. Disponível em: <https://linkinghub.elsevier.com/retrieve/pii/S0022169419301027>. Acesso em: 7 fev. 2023.

SHEFFIELD, J.; WOOD, E. F. Characteristics of global and regional drought, 1950-2000: Analysis of soil moisture data from off-line simulation of the terrestrial hydrologic cycle. **Journal of Geophysical Research Atmospheres**, v. 112, n. 17, p. 1–21, 2007.

SHIAU, J.-T.; SHEN, H. W. Recurrence Analysis of Hydrologic Droughts of Differing Severity. **Journal of Water Resources Planning and Management**, v. 127, n. 1, p. 30–40, fev. 2001. Disponível em: <http://ascelibrary.org/doi/10.1061/%28ASCE%290733-9496%282001%29127%3A1%2830%29>. Acesso em: 7 fev. 2023.

SHIAU, J. T. Return period of bivariate distributed extreme hydrological events. **Stochastic Environmental Research and Risk Assessment**, v. 17, n. 1–2, p. 42–57, 2003.

SHIAU, J. T. Fitting drought duration and severity with two-dimensional copulas. **Water Resources Management**, v. 20, n. 5, p. 795–815, 2006.

SHIN, J. Y.; CHEN, S.; LEE, J.-H.; KIM, T.-W. Investigation of drought propagation in South Korea using drought index and conditional probability. **Terrestrial, Atmospheric and Oceanic Sciences**, v. 29, n. 2, p. 231–241, 2018. Disponível em: <http://tao.cgu.org.tw/index.php/articles/archive/hydrology/item/1565>. Acesso em: 7 fev. 2023.

SILVA, B. K. N.; AMORIM, A. C. B.; SILVA, C. M. S.; LUCIO, P. S.; BARBOSA, L. M. Rainfall-related natural disasters in the Northeast of Brazil as a response to ocean-atmosphere interaction. **Theoretical and Applied Climatology**, n. 2010, 2019.

SILVA, S. M. O. da; SOUZA FILHO, F. de A. de; ARAÚJO JÚNIOR, L. M. de. Mecanismo financeiro projetado com índices de seca como instrumento de gestão de risco em recursos hídricos. **Revista Brasileira de Recursos Hídricos**, v. 20, n. 2, p. 320–330, 2015. Disponível em: <http://www.abrh.org.br/SGCv3/index.php?PUB=1&ID=157&SUMARIO=5057>. Acesso em: 7 fev. 2023.

SINGH, V. P.; ZHANG, L. IDF Curves Using the Frank Archimedean Copula. **Journal of Hydrologic Engineering**, v. 12, n. 6, p. 651–662, 2007.

SONG, S.; SINGH, V. P. Meta-elliptical copulas for drought frequency analysis of periodic hydrologic data. **Stochastic Environmental Research and Risk Assessment**, v. 24, n. 3, p.

425–444, 17 mar. 2010. Disponível em: <http://link.springer.com/10.1007/s00477-009-0331-1>. Acesso em: 7 fev. 2023.

SONG, Z.; XIA, J.; SHE, D.; LI, L.; HU, C.; HONG, S. Assessment of meteorological drought change in the 21st century based on CMIP6 multi-model ensemble projections over mainland China. **Journal of Hydrology**, v. 601, 1 out. 2021.

SOUZA FILHO, F. A.; LALL, U. Seasonal to interannual ensemble streamflow forecasts for Ceara, Brazil: Applications of a multivariate, semiparametric algorithm. **Water Resources Research**, v. 39, n. 11, p. 1–13, 2003.

STAHL, K.; KOHN, I.; BLAUHUT, V.; URQUIJO, J.; DE STEFANO, L.; ACÁCIO, V.; DIAS, S.; STAGGE, J. H.; TALLAKSEN, L. M.; KAMPRAGOU, E.; VAN LOON, A. F.; BARKER, L. J.; MELSEN, L. A.; BIFULCO, C.; MUSOLINO, D.; DE CARLI, A.; MASSARUTTO, A.; ASSIMACOPOULOS, D.; VAN LANEN, H. A. J. Impacts of European drought events: Insights from an international database of text-based reports. **Natural Hazards and Earth System Sciences**, v. 16, n. 3, p. 801–819, 2016.

TIJDEMAN, E.; BLAUHUT, V.; STOELZLE, M.; MENZEL, L.; STAHL, K. Different drought types and the spatial variability in their hazard, impact, and propagation characteristics. **Natural Hazards and Earth System Sciences**, v. 22, n. 6, p. 2099–2116, 2022.

TOSUNOGLU, F.; CAN, I. Application of copulas for regional bivariate frequency analysis of meteorological droughts in Turkey. **Natural Hazards**, 2016.

TOSUNOGLU, F.; KISI, O. Joint modelling of annual maximum drought severity and corresponding duration. **Journal of Hydrology**, v. 543, n. October, p. 406–422, 2016. Disponível em: <http://dx.doi.org/10.1016/j.jhydrol.2016.10.018>. Acesso em: 7 fev. 2023.

TRIGO, R. M.; DACAMARA, C. C. Circulation weather types and their influence on the precipitation regime in Portugal. **International Journal of Climatology**, v. 20, p. 1559–1581, 2000.

TRIGO, R. M.; POZO-VÁZQUEZ, D.; OSBORN, T. J.; CASTRO-DÍEZ, Y.; GÁMIZ-FORTIS, S.; ESTEBAN-PARRA, M. J. North Atlantic oscillation influence on precipitation, river flow and water resources in the Iberian Peninsula. **International Journal of Climatology**, v. 24, n. 8, p. 925–944, 2004.

TRIGO, R. M.; VALENTE, M. A.; TRIGO, I. F.; MIRANDA, P. M. A.; RAMOS, A. M.; PAREDES, D.; GARCÍA-HERRERA, R. The impact of North Atlantic wind and cyclone trends on European precipitation and significant wave height in the Atlantic. **Annals of the New York Academy of Sciences**, v. 1146, p. 212–234, 2008.

TU, X.; SINGH, V. P.; CHEN, X.; MA, M.; ZHANG, Q.; ZHAO, Y. Uncertainty and variability in bivariate modeling of hydrological droughts. **Stochastic Environmental Research and Risk Assessment**, 2016.

UTIDA, G.; CRUZ, F. W.; ETOURNEAU, J.; BOULOUBASSI, I.; SCHEFUSS, E.; VUILLE, M.; NOVELLO, V. F.; PRADO, L. F.; SIFEDDINE, A.; KLEIN, V.; ZULAR, A.; VIANA, J. C. C.; TURCQ, B. Tropical South Atlantic influence on Northeastern Brazil precipitation and ITCZ displacement during the past 2300 years. **Scientific Reports**, v. 9, n.

1, p. 1–8, 2019.

UTSUNOMIYA, Y. T.; UTSUNOMIYA, A. T. H.; TORRECILHA, R. B. P.; PAULAN, S. de C.; MILANESI, M.; GARCIA, J. F. Growth Rate and Acceleration Analysis of the COVID-19 Pandemic Reveals the Effect of Public Health Measures in Real Time. **Frontiers in Medicine**, v. 7, n. May, p. 1–9, 2020.

UVO, C. B.; REPELLI, C. A.; ZEBIAK, S. E.; KUSHNIR, Y. The Relationships between Tropical Pacific and Atlantic SST andNortheast Brazil Monthly Precipitation. **Journal of Climate**, n. Kousky 1979, p. 551–562, 1998.

VAN LOON, A. F. **On the propagation of drought. How climate and catchment characteristics influence hydrological drought development and recovery**. 2013. 2013.

VAN LOON, A. F. Hydrological drought explained. **Wiley Interdisciplinary Reviews: Water**, v. 2, n. 4, p. 359–392, 2015.

VICENTE-SERRANO, S. M. Spatial and temporal analysis of droughts in the Iberian Peninsula (1910-2000). **Hydrological Sciences Journal**, v. 51, n. 1, p. 83–97, 2006.

VICENTE-SERRANO, S. M.; BEGUERÍA, S.; LÓPEZ-MORENO, J. I. A multiscalar drought index sensitive to global warming: The standardized precipitation evapotranspiration index. **Journal of Climate**, v. 23, n. 7, p. 1696–1718, 2010.

VICENTE-SERRANO, S. M.; GONZÁLEZ-HIDALGO, J. C.; DE LUIS, M.; RAVENTÓS, J. Drought patterns in the Mediterranean area: The Valencia region (eastern Spain). **Climate Research**, v. 26, n. 1, p. 5–15, 2004.

VIEIRA, R. M. S. P.; TOMASELLA, J.; ALVALÁ, R. C. S.; SESTINI, M. F.; AFFONSO, A. G.; RODRIGUEZ, D. A.; BARBOSA, A. A.; CUNHA, A. P. M. A.; VALLES, G. F.; CREPANI, E.; DE OLIVEIRA, S. B. P.; DE SOUZA, M. S. B.; CALIL, P. M.; DE CARVALHO, M. A.; VALERIANO, D. M.; CAMPELLO, F. C. B.; SANTANA, M. O. Identifying areas susceptible to desertification in the Brazilian northeast. **Solid Earth**, v. 6, n. 1, p. 347–360, 2015.

WEN, X.; TU, Y. hong; TAN, Q. feng; LI, W. yi; FANG, G. hua; DING, Z. yu; WANG, Z. ni. Construction of 3D drought structures of meteorological drought events and their spatio-temporal evolution characteristics. **Journal of Hydrology**, v. 590, p. 125539, 2020. Disponível em: <https://doi.org/10.1016/j.jhydrol.2020.125539>. Acesso em: 7 fev. 2023.

WILHITE, D. A. **Drought and Water Crises**. CRC Press, Boca Raton, 2005.

WILHITE, D. A. Breaking the hydro-illogical cycle: Changing the paradigm for drought management. **Earth**, v. 57, n. 7, p. 70–71, 2012.

WILHITE, D. A.; GLANTZ, M. H. Understanding: the Drought Phenomenon: The Role of Definitions. **Water International**, 1985. Disponível em: <http://www.tandfonline.com/action/journalInformation?journalCode=rwin20>. Acesso em: 7 fev. 2023.

WILHITE, D. A.; HAYES, M. J.; KNUTSON, C. L. Drought preparedness planning: Building institutional capacity. *In*: **Drought and Water Crises: Science, Technology, and**

Management Issues. CRC Press, 2005. p. 93–135.

WILHITE, D. a; SVOBODA, M. D. Drought early warning systems in the context of drought preparedness and mitigation. **Early warning systems for drought preparedness and drought management**, p. 1–21, 2000.

WILKS, D. S. **Statistical methods in the atmospheric sciences**. [s.l: s.n.]2–676 p.

WU, J.; CHEN, X.; YAO, H.; LIU, Z.; ZHANG, D. Hydrological Drought Instantaneous Propagation Speed Based on the Variable Motion Relationship of Speed-Time Process. **Water Resources Research**, v. 54, n. 11, p. 9549–9565, 2018.

WU, X.; HAO, Z.; HAO, F.; LI, C.; ZHANG, X. Spatial and temporal variations of compound droughts and hot extremes in China. **Atmosphere**, v. 10, n. 2, p. 5–8, 2019.

XU, K.; YANG, D.; XU, X.; LEI, H. Copula based drought frequency analysis considering the spatio-temporal variability in Southwest China. **Journal of Hydrology**, v. 527, p. 630–640, 2015a.

XU, K.; YANG, D.; YANG, H.; LI, Z.; QIN, Y.; SHEN, Y. Spatio-temporal variation of drought in China during 1961–2012: A climatic perspective. **Journal of Hydrology**, v. 526, p. 253–264, jul. 2015b. Disponível em: <http://dx.doi.org/10.1016/j.jhydrol.2014.09.047>. Acesso em: 7 fev. 2023.

YANG, T. H.; LIU, W. C. A general overview of the risk-reduction strategies for floods and droughts. **Sustainability (Switzerland)**, v. 12, n. 7, 1 abr. 2020.

YEVJEVICH V, I. J. **An objective approach to definitions and investigations of continental hydrologic droughts**. [s.l: s.n.]

ZHANG, Q.; XIAO, M.; SINGH, V. P. Uncertainty evaluation of copula analysis of hydrological droughts in the East River basin, China. **Global and Planetary Change**, 2015.

ZHOU, H.; LIU, Y.; LIU, Y. An Approach to Tracking Meteorological Drought Migration. **Water Resources Research**, v. 55, n. 4, p. 3266–3284, 2019.

ZHOU, K.; WANG, Y.; CHANG, J.; ZHOU, S.; GUO, A. Spatial and temporal evolution of drought characteristics across the Yellow River basin. **Ecological Indicators**, v. 131, p. 108207, 2021. Disponível em: <https://doi.org/10.1016/j.ecolind.2021.108207>. Acesso em: 7 fev. 2023.

ZHU, Y.; LIU, Y.; WANG, W.; SINGH, V. P.; MA, X.; YU, Z. Three dimensional characterization of meteorological and hydrological droughts and their probabilistic links. **Journal of Hydrology**, v. 578, n. July, p. 124016, 2019. Disponível em: <https://doi.org/10.1016/j.jhydrol.2019.124016>. Acesso em: 7 fev. 2023.

APPENDICE A – MAIN DROUGHT EVENTS CHARACTERITICS

In this section, figures of the main drought events detected by the spatio-temporal drought characterization algorithm are presented.

The five main events selected were the 1950-1956, 1957-1961, 1980-1984, 2012-2014, and 2015-2018 droughts. These events were selected for their temporal scope, all with more than two years duration, and spatial, and the severity of the events.

The growth curves, growth rate, and acceleration of the severity characteristic was brought in as an example for each of these events. In addition, the cumulative severity for each grid point and the path taken by the centroid are also shown to facilitate understanding of the displacement of drought in both time and space.

Figure A1: Growth curve, Growth rate and Acceleration of the severity characteristic of the 1950-1956 drought event in Northeast Brazil using SPI 12, threshold -1.

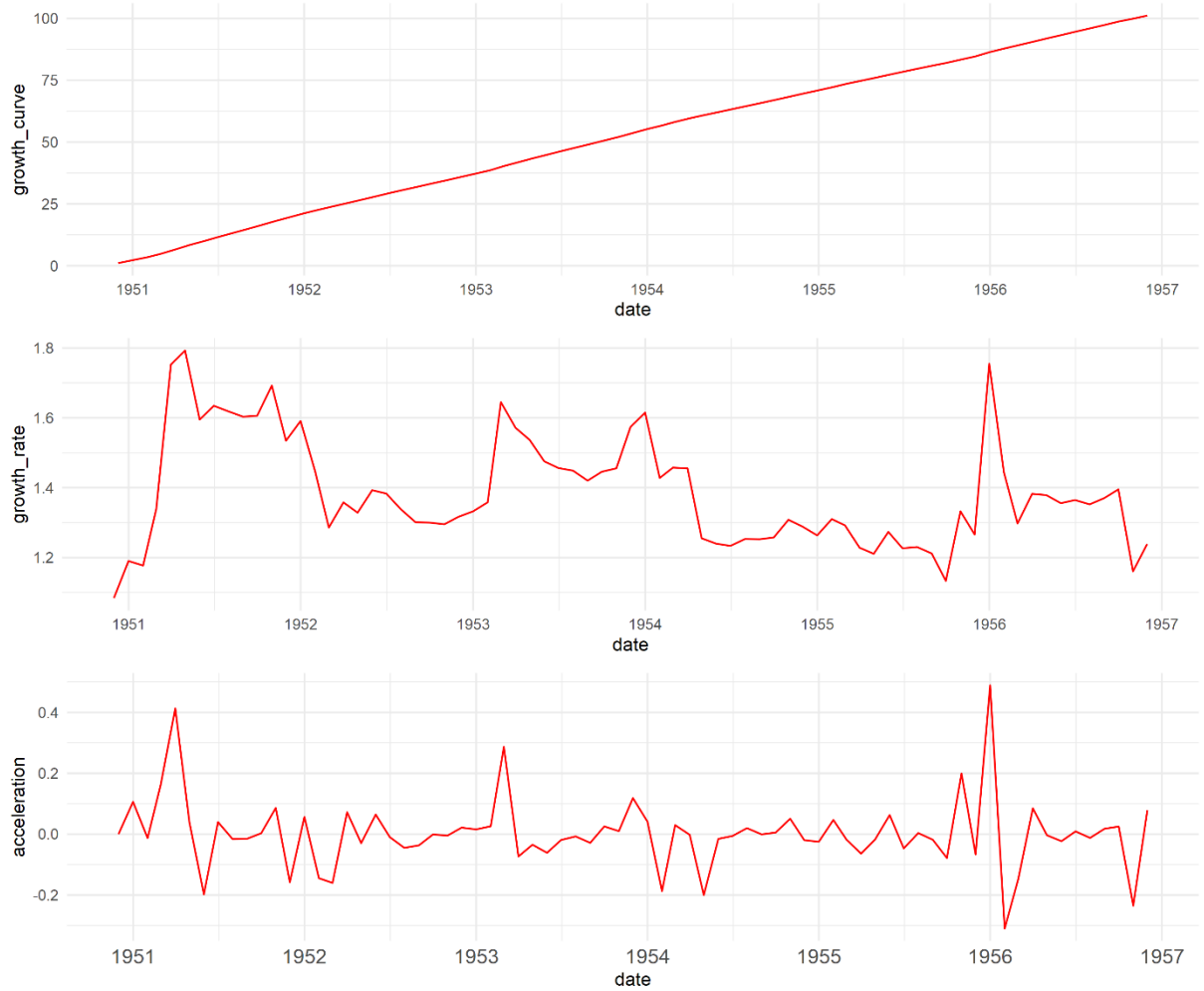

Figure A2: Aggregated severity for each grid cell and the centroid path (red is the onset and blue the offset of the drought event) for the 1950-1956 drought event.

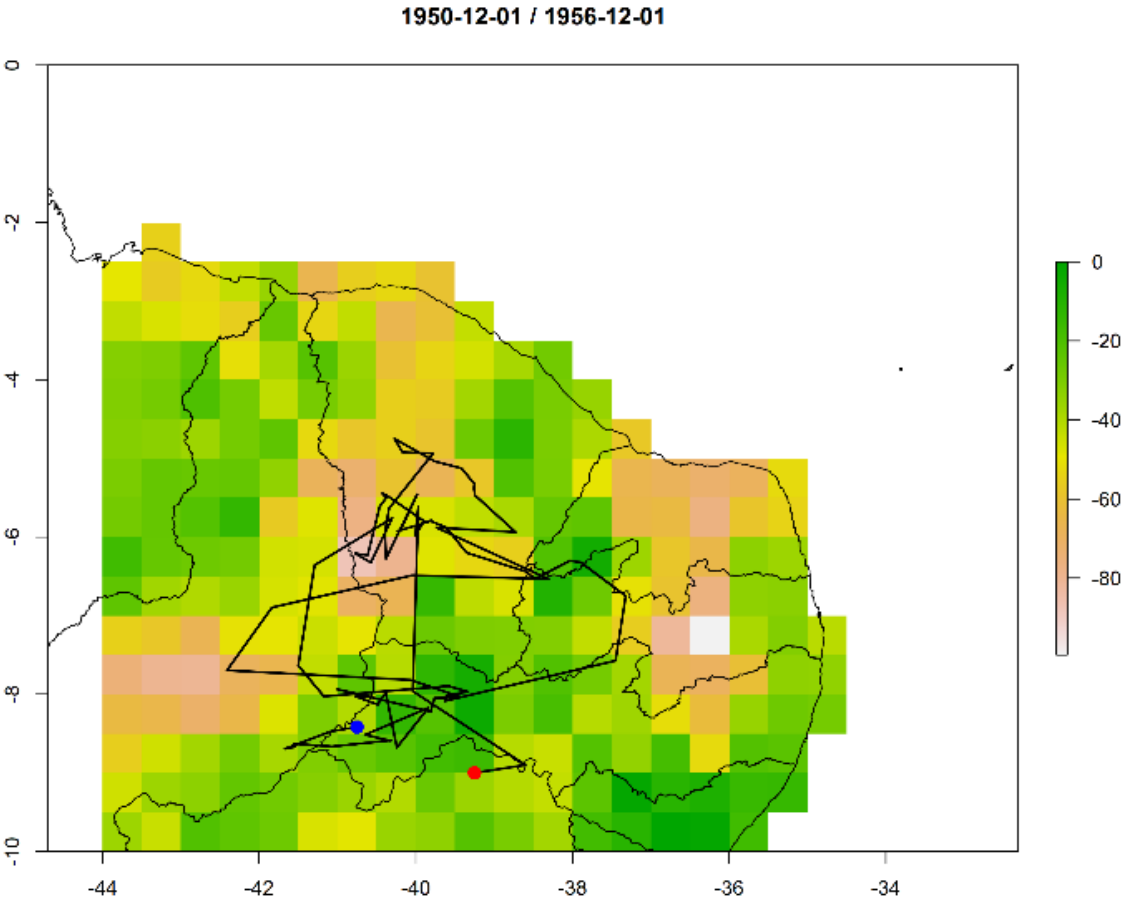

Figure A3: Growth curve, Growth rate and Acceleration of the severity characteristic of the 1957-1961 drought event in Northeast Brazil using SPI 12, threshold -1.

Figure A4: Aggregated severity for each grid cell and the centroid path (red is the onset and blue the offset of the drought event) for the 1957-1961 drought event.

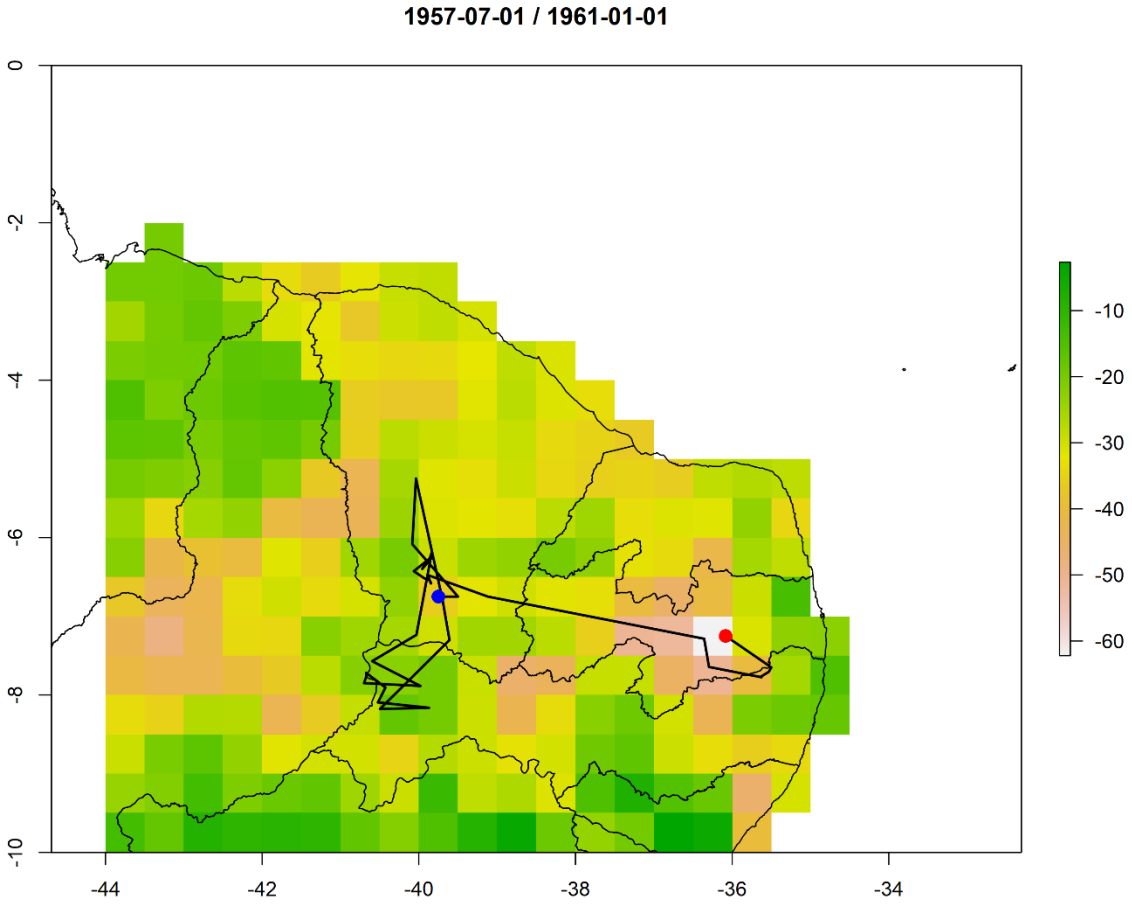

Figure A5: Growth curve, Growth rate and Acceleration of the severity characteristic of the 1980-1984 drought event in Northeast Brazil using SPI 12, threshold -1.

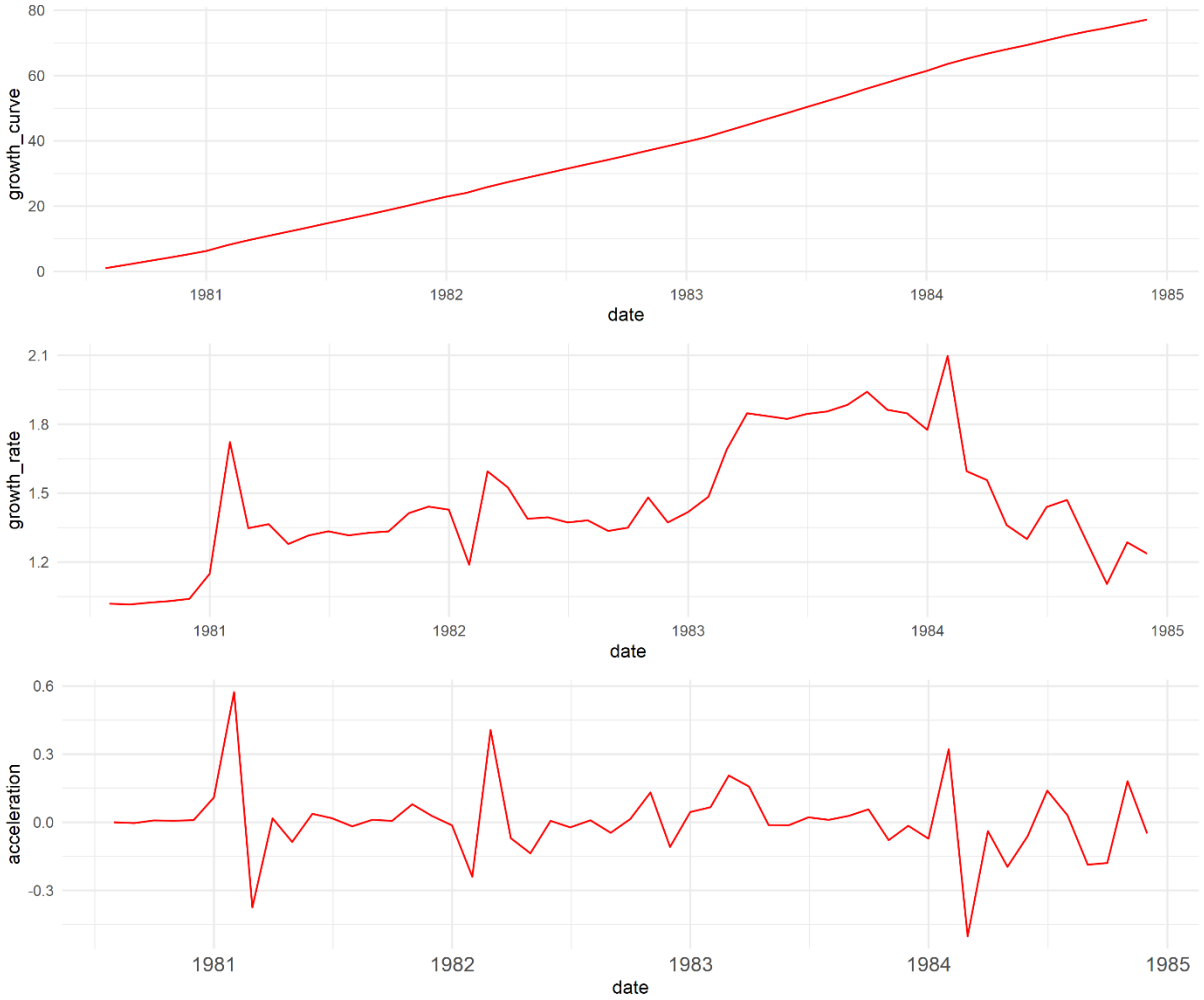

Figure A6: Aggregated severity for each grid cell and the centroid path (red is the onset and blue the offset of the drought event) for the 1980-1984 drought event.

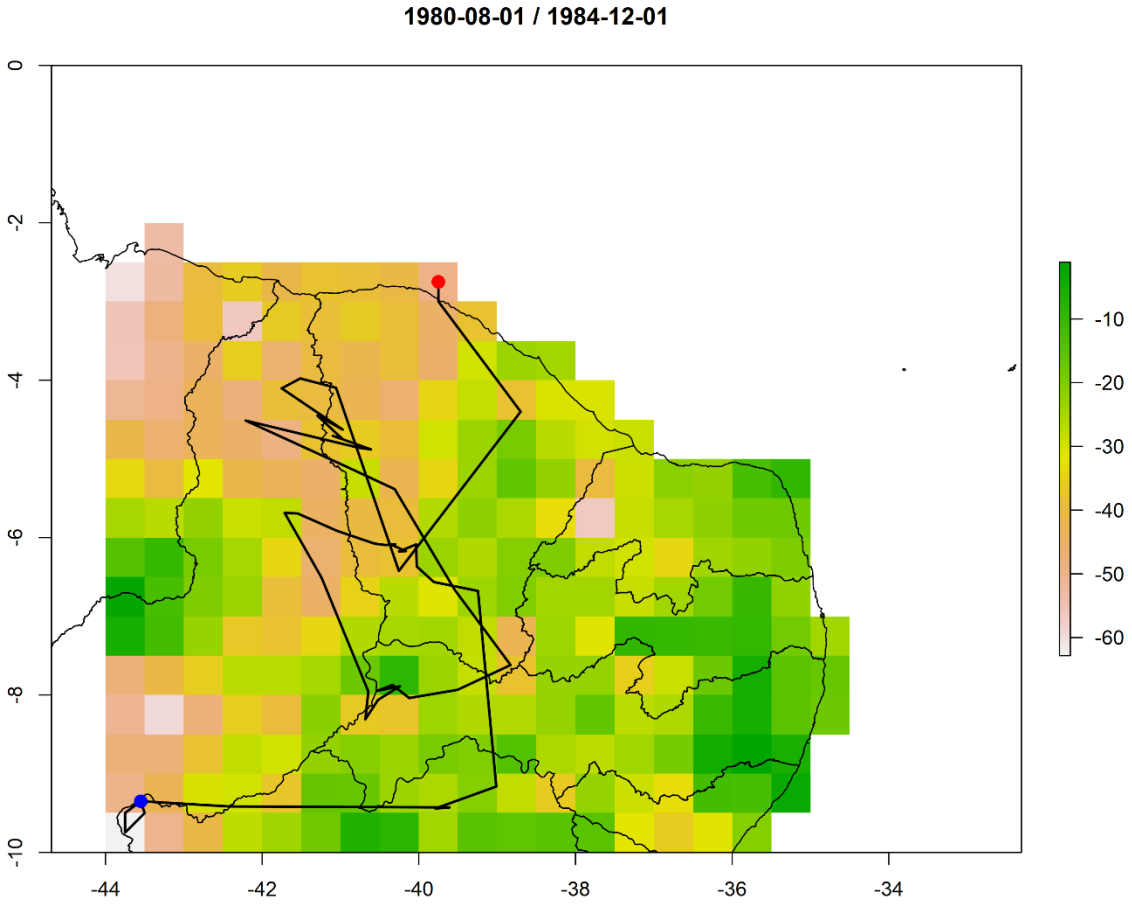

Figure A7: Growth curve, Growth rate and Acceleration of the severity characteristic of the 2012-2014 drought event in Northeast Brazil using SPI 12, threshold -1.

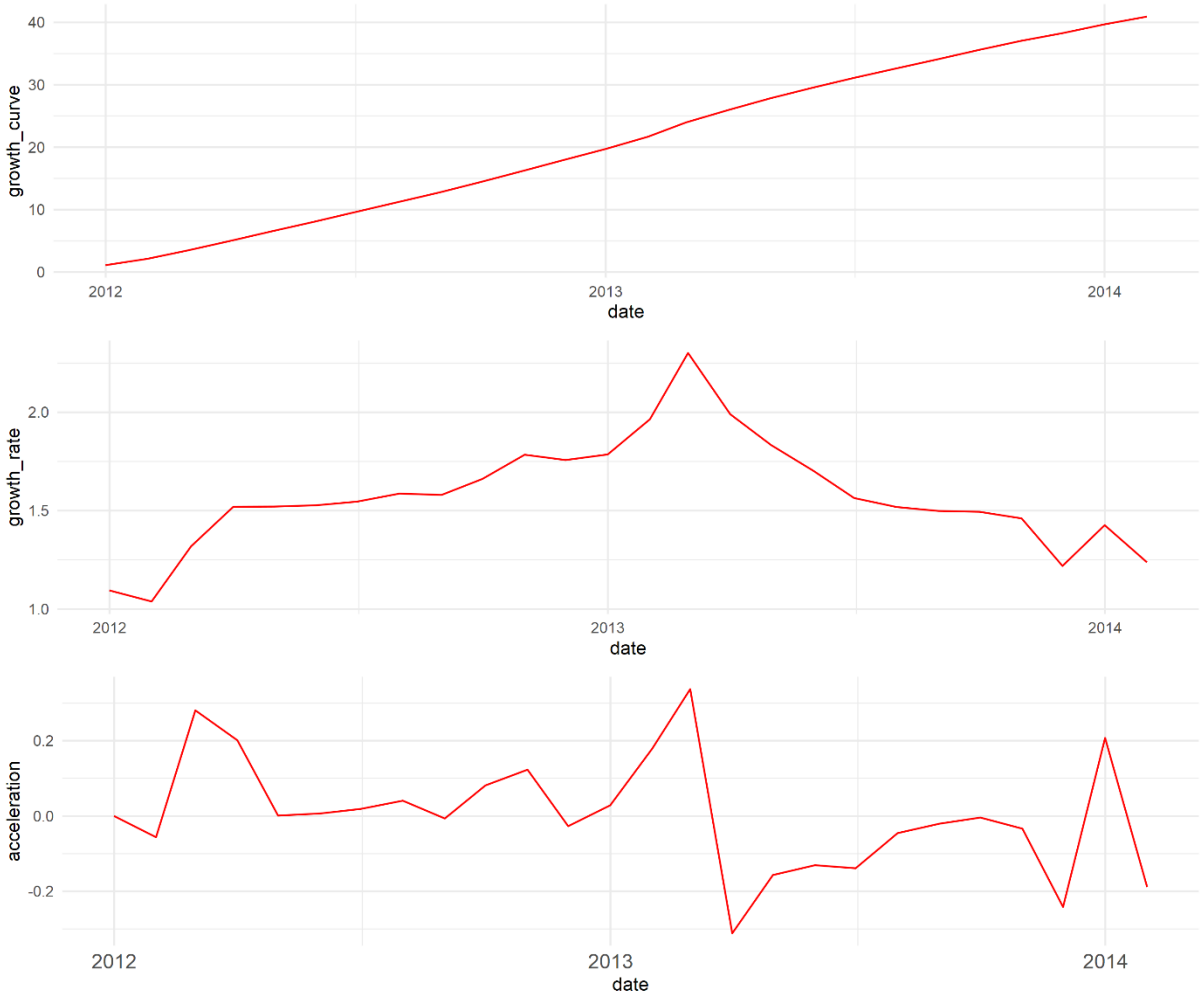

Figure A8: Aggregated severity for each grid cell and the centroid path (red is the onset and blue the offset of the drought event) for the 2012-2014 drought event.

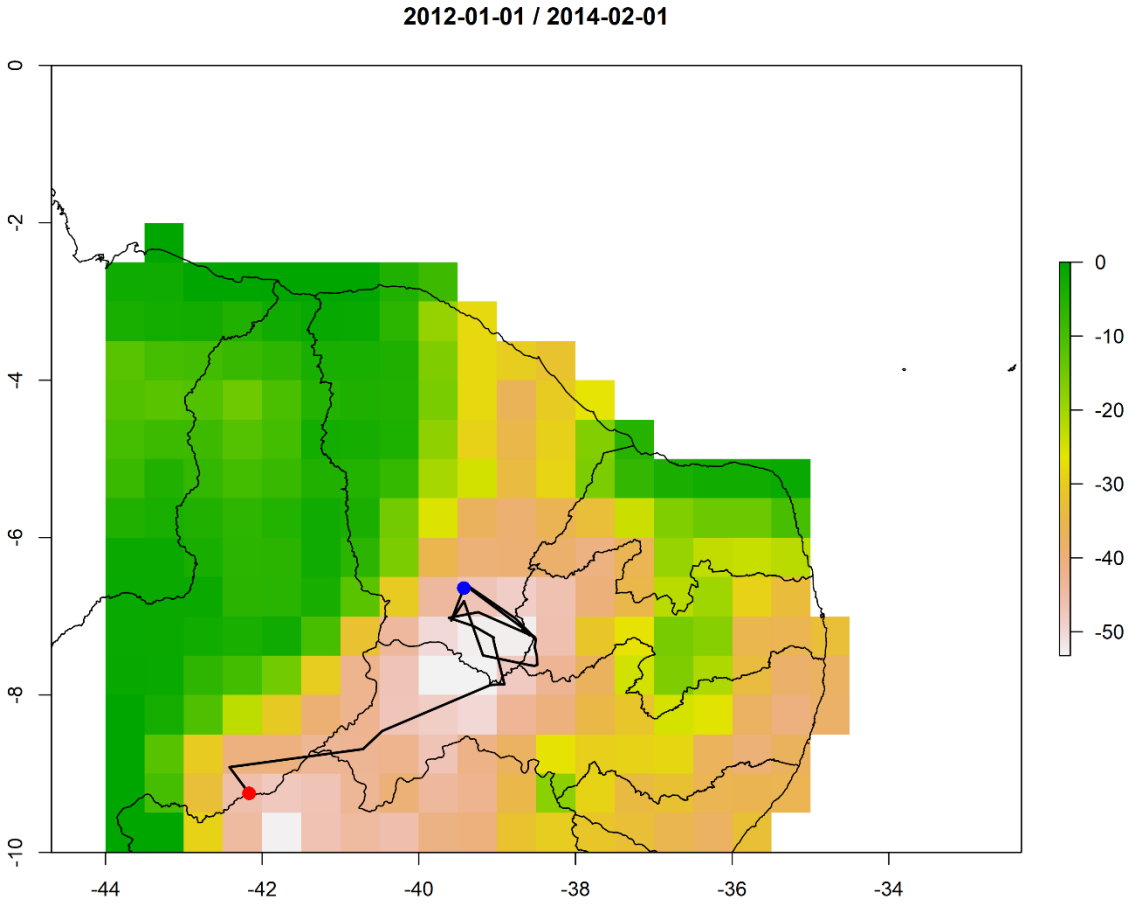

Figure A9: Growth curve, Growth rate and Acceleration of the severity characteristic of the 2015-2018 drought event in Northeast Brazil using SPI 12, threshold -1.

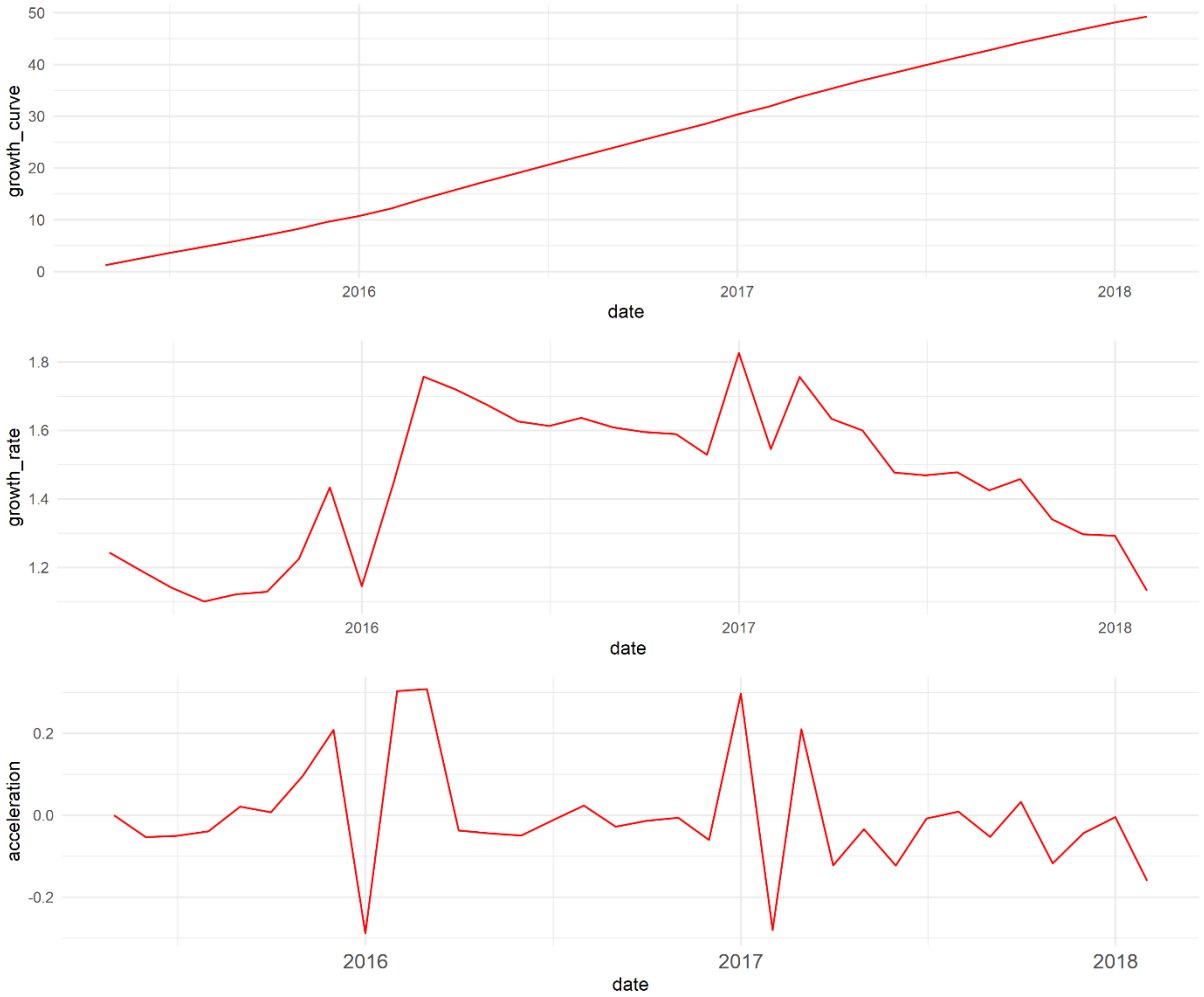

Figure A10: Aggregated severity for each grid cell and the centroid path (red is the onset and blue the offset of the drought event) for the 2015-2018 drought event.